TORSIONAL EFFECTS IN MASONRY STRUCTURES UNDER LATERAL LOADING

A Thesis Submitted for the Degree of
Doctor of Philosophy
of the
UNIVERSITY OF EDINBURGH

by

ÖZDEMİR KESKİN

Department of Civil Engineering
and Building Science.

July, 1974

ACKNOWLEDGEMENTS

I would firstly like to thank Professor A.W. Hendry for the opportunity to carry out this research programme and for assistance with helpful discussion.

I would like to express my sincere gratitude to Dr. S.R. Davies who gave great encouragement and assistance in overcoming the many hurdles which are so often encountered in a research programme.

I would like to extend my appreciation to: Dr. A.H.P. Maurenbrecher, Dr. B.P. Sinha, Dr. C.L. Khoo and Dr. M. Rostampour.

All the technical staff of the workshop and photographic unit.

Mrs. Avril Davies for typing the manuscript.

CONTENTS

PRINCIPAL NOTATION

A_{di} ..... Equivalent area of connecting beams for shear deformation

a, b ..... Overall structure dimensions

C_1, C_2, C_3 ..... Coefficients

c_{xi}, c_{yi} ..... Distance from the centre of the structure to the centroid of the element i, in X and Y direction, respectively.

d ..... Flange length of the cross section.

E ..... Modulus of elasticity

e ..... Distance of element centroid from flanges

e_B, e_C, e_D ..... Eccentricity of applied loads P_B , P_C , P_D, respectively

e_{xi}, e_{yi} ..... Distance from the centre of the structure to the Shear centre of the element i, in x and y directions, respectively

G ..... Shear modulus

H ..... Total height of structures

h ..... Storey height (spacing between centre lines of connecting beams)

I_{xi}, I_{yi} ..... Moment of inertia of element i about x and y axes, respectively

I^* ..... $= I_{xi}\, e_{xi}^2 + I_{yi}\, e_{yi}^2$

I_ω ..... $= \int_A \omega^2 dA$ sectorial moment of inertia

I_ω^* ..... $= I^* + I_\omega$

K_s ..... Coefficient defined by equation (33)

K_T ..... Saint Venant moment of inertia

l_i ..... Clear span of connecting beams

M_x, M_y ..... Bending moment in x and y directions

M_F ..... Torsional moment defined from shear forces

M_{sv} ..... Saint Venant torsional moment

M_s ..... Torsional moment resulting from distributed shear forces on the connecting media

M_ω ..... Warping torsional moment

M_T ..... Total external twisting moment

$m_{ci}, \bar{m}_{ci}$ ..... Coefficients defined for channel section by equations (53b) and (56)

$m_i, \bar{m}_i$ ..... Coefficients defined by equations (23, 24) and (28a)(28b).

P_A, P_B, P_C, P_D, ... Applied horizontal forces

Q_{xi}, Q_{yi}, Q_{Ti} ..... Shear forces and torques on element i
$\bar{Q}_{xi}, \bar{Q}_{yi}, \bar{Q}_{Ti}$

$\bar{Q}_{(z)i}$ ..... Axial shear forces along the cut

$q_{(z)_i}$ ..... Distributed shear forces in connecting media

S_ω ..... The sectorial statical moment

s ..... Coordinate along centre line of thin walled section

t ..... Thickness of cross section and slab

u , v ..... Deflection in x and y directions

Θ ..... Rotation of centre of structure

X, Y, Z ..... Overall system axes

x_i, y_i, z_i ..... Axes of element i

$\gamma_{1,2}$ ..... Coefficient defined by equation (36)

δ_{aj} ..... Relative vertical displacement due to horizontal deflection and rotation of element i

δ_{bj} ..... Vertical deflection due to the shear forces

Δ_{PA} , Δ_{PB} , Δ_{PC} , Δ_{PD} ..... Horizontal bending deformation at slab levels due to the axially applied load

Δ_{M_B} , Δ_{M_C}, Δ_{M_D} ... Horizontal deflection due to the flexural twisting moment

λ_i ..... Beam stiffness factor

$\sigma_{\omega(s)}$ ..... Warping stress

σ_w ..... Shearing stress

ω_I , ω_T ..... Sectorial area of element

ABSTRACT

The work presented in this thesis is concerned with the analysis of multi-storey masonry shear wall structures connected by floor slabs, under axial and various eccentric lateral loadings, producing bending and torsional deformations. For analysis, the problem is split into two parts, namely that due to direct lateral load and that due to twisting moment. The equivalent frame and wide column frame analogies are used for the determining of the bending effects and the finite element method is used for both the bending and the stress analyses. For torsion analysis, the governing equation is obtained by considering that the externally applied torque is equilibrated by the internal torques. The governing equation is derived for a system of third-degree linear non-homogeneous, differential equations with the unknown in the problem being the angle of twist.

The results obtained from various forms of the proposed theory are compared with results from tests on a five-storey 1/3rd scale concrete blockwork structure. For further comparison, the theory was modified for a symmetrical channel cross-section and the theoretical results compared with the experimental values taken from another worker's test on a four-storey, 1/6th scale brickwork structure.

When both structures are analysed by the proposed theory with and without warping, and with and without considering slab effect, the closest agreement with the experimental results is obtained when the slab effect is neglected. The rotation is underestimated when slab effect is included in the governing equations for both structures. Warping is shown to be of minor importance in the calculation of rotations and stresses. The stresses calculated using the theory,

including the slab effect compares closely with the experimental values which were obtained from the symmetrical channel cross-section. The axial deformations of the vertical elements were neglected in both the analyses.

The proposed theory can be applied to both symmetrical and unsymmetrical sections. The method of analysis yields results of sufficient accuracy for application to be made in engineering practice. It is also sufficiently simple that an explicit solution can be obtained using a slide rule or desk calculator and does not require the use of a computer.

CHAPTER I

1 - INTRODUCTION

The number of tall buildings is increasing rapidly in almost every country, the reason being a combination of shortage of available land, increase in land costs and the prestige value. When the buildings reach such a height that lateral wind or seismic loading becomes a major factor in the design, then greater strength and stiffness are required than are provided by a system of frames. Therefore, in taller buildings, certainly when above fifteen storeys, the bracing to counteract the lateral loads can be most effectively and economically obtained by a system of shear walls, or cross walls for the basic structure.

Shear walls are playing an increasingly important role in high rise building construction. The shear wall components may be a straight wall or walls combined to form a complex symmetrical or asymmetrical arrangement. The shear walls are primarily used to resist lateral forces but may also be load-bearing walls or act in combination with columns or form a complete structure. Also with careful planning they can not only be utilised for non-structural purposes of building and enclosing but may also provide acoustic insulating and fire resisting divisions between the units of the structure. When such a structure is subjected to lateral forces, the slabs, which are very stiff in their plane, act as deep beams and not

only transmit the horizontal forces to the vertical wall elements but they also interact with the walls to give a stiffer and stronger structure. Additionally floor slabs keep storey heights to a minimum. The exact analysis of the shear wall structures is complicated and so a number of approximate methods have been developed, which replaced the structure by a simple idealised form.

2 - REVIEW OF LITERATURE

The actual behaviour of the coupled shear wall structures bears little relationship to that predicted by the analytical methods due to the simplifying assumptions made in each theory.

A - Continuum Method

In recent years, the problem of the interaction between shear walls and floor slabs systems in tall buildings has been given more attention. The problem has frequently been tackled by assuming that the system of connections, formed by lintel beams or floor slabs can be replaced by a continuous connecting medium of the same stiffness. Also it is assumed that the walls deflect equally and the connecting beams deform with a fixed point of contraflexure. The behaviour of the structure may be expressed by a single second order differential equation which is solved to give shear, moments and deformations throughout the wall.

This continuum method was probably first applied to building frames by Chitty and Wan (1947) [15]* and to coupled shear walls with

*Figures in curved brackets represent year of publication.
Figures in square brackets refer to bibliography.

openings by Beck (1962) [2]. The technique has been extensively used and developed for the analysis of plane coupled shear walls subjected to lateral loading by many workers e.g. Rosman (1964) [44, 45], Burns (1965) [12], Coull and Chaudhury (1967) [16], Coull and Puri (1968) [17] and Coull and Irwin (1970) [20]. The method has the advantage that the accuracy of the solution increases with an increasing number of storeys.

B - Equivalent Frame Analogy

Analytical methods for analysis for shear wall and shear wall frame systems, using digital computers, are more accurate, more flexible and can consider more variables than the continuum approach Green (1952) [29] presented a simple treatment of the analysis of multi-storey coupled shear walls, with deep beams, in which he considered the structure as an "equivalent frame" with the point of contraflexure at the midpoint of the piers and spandrels. Amaratunga (1962) [1], in his analysis used the "equivalent frame" approach in which he replaced the shear-wall structure with columns having the same flexural rigidities as the walls. The beam lengths are equal to the distance between the centroidal axes of neighbouring columns and having the same stiffness as the actual beams or slabs. His deflection results, including shear and axial deformations, were overestimated when compared with results obtained from perspex model tests.

A method of equivalent frame analysis which was applicable to diverse shear wall structures was presented by Schaighofer and Microys (1969) [48]. The cross-sectorial characteristics of columns in the

equivalent frame were considered identical with those of the corresponding wall sections and the beams have the same cross-sectorial areas as the connecting beams of the shear wall structure. Good agreement with experimental data was provided by this method.

C - Wide Column Frame Analogy

A basically similar approach is the wide column frame technique. It considers a frame with beams which are assumed to be infinitely stiff from the centreline of the column to the edge of the actual opening and as a normal beam within the opening, as in the equivalent frame method. Macleod (1968) [38] using the "wide column frame" analogy analysed coupled shear walls by considering shear, axial and bending deformations in the members and assuming rigid connections at beam-wall joints. Sinha (1967) [50] tested a five storey one-sixth scale cross-wall structure in brickwork under lateral loading and compared the results with continuum and wide column frame analogy methods. Both methods underestimated deflection, later Maurenbrecher, Sinha and Hendry (1970) [41] presented a series of test results on a full-scale five storey brickwork shear-wall structure subjected to lateral loading. Sinha and Hendry (1973) [51] then compared these results, along with deflection results obtained by Sinha [50] and Kalita [37] with the deflection calculated by four different methods, namely continuum, wide column frame, equivalent frame and cantilever. The first two of these methods underestimate, and the cantilever method overestimates the deflection. The equivalent frame analogy gave the best agreement for deflection. Similar conclusions were presented by Rostampour (1973) [47]. In addition, he applied the method of

"finite element" to stress and deflection analysis. This method was suitable for stress analysis but underestimated deflection.

D - Finite Element Method

The finite element method is a commonly applied approach to plane wall analysis of multi-storey structures. In this method, the structure is sub-divided into a mesh of two dimensional elements of triangular or rectangular shape, Jenkins (1968) [36]. The accuracy depends on the fineness of the mesh used which in turn affects the computer running costs. Macleod (1969) [39] used the finite element method for analysis of coupled shear walls and later Macleod and Green (1973) [40] compared this approach with wide column frame analogy. They found the finite element analysis marginally more accurate but it was less efficient computationally.

E - Torsion Analysis

The deformations of coupled shear walls subjected to lateral loading, under many circumstances, are not restricted to their plane. The torsional effect cannot be neglected in most asymmetric structures and even for symmetric structures when the lateral load is non-uniformly distributed along the structure. Essentially torsion will occur if the centre of rigidity of the vertical resisting elements does not coincide with the line of action of the horizontal loading.

A thin-walled prismatic member of open cross-sectorial profile, characterised by high bending rigidity but extremely weak for torsion, was first studied by Timoshenko (1956) [55]. The most extensive early

study has been by Vlasov (1958) [58, 59] who postulated a theory on the effect of elastic warping of thin-walled beams. His method was based on the "sectorial properties" of a cross section of beams and shells. He treated the theory mathematically in great depth and it has been extended and proved in numerous experiments. Vlasov explained the behavioural differences between "thin-walled" and "thick-walled" beams under the same loading. The Saint-Venant (1855) [54] theory developed for the twisting moment acting on a thick-walled beam was inadequate to calculate the stresses and distortions of a thin-walled beam.

Benjamin (1959) [3] was one of the earlier workers to point out the torsional problems in the analysis of shear wall structure. The method of shear distribution provides a simple approach but was applied to one and two storey structures. Murthy (1964) [43] tested unsymmetrical three-storey model, cross-wall, brickwork structure under lateral loading and compared the experimental with the analytical results, calculated as suggested by Benjamin. Reasonable agreement was obtained with the theoretical rigidity at the first floor but the second and third floor analytical rigidities were found to be higher compared with the actual.

Seto (1967) [49] developed Benjamin's method in accordance with the fundamental principles of applied mechanics and strength of materials and suggested that the theory may be applied to the approximate analysis of multi-storey shear wall structures. Kalita (1970) [37] carried out tests on a multi-storey symmetrical channel section structure in one-sixth scale brickwork, under eccentrically applied

lateral loading. For analysis, the problem was split into two parts. The finite element method was used for solution due to bending. In the torsional analysis, he obtained the theory from combining the thin-walled section theory of Timoshenko with the theory developed by Seto [49]. The analytical and experimental results compared favourably but doubt can be cast on the reliability of this theory as an unacceptably low modulus of elasticity value was used in the calculations.

Jenkins and Harrison (1966) [35] analysed tall buildings with shear walls under bending and torsion. Bending was conveniently calculated using a stiffness matrix method involving the use of a digital computer, and for the torsion analysis the theorem of Minimum Potential Energy was used. The slab stiffness could be included in the finite element technique. The experimental results obtained from perspex models compared rather disappointingly with the analytical data.

Experimental results of Jenkins and Harrison [35] have been quoted by Taranath (1968) [53] for comparison with the theoretical results calculated from his theory. His own experiments were concerned with testing thin-walled members interconnected by internal or external slabs in perspex models. He recognised the inadequacy of St. Venant torsion theory and so applied the restrained torsion theory of Vlasov, which fully allows for warping of cross-sections. He showed theoretically and experimentally that the warping stiffness of floor slabs increases the strength and stiffness of the structures. Warping displacements for open sections and the corresponding warping

stiffness of floor slabs were solved by computer. Experimental results for the models were compared with the theoretical results, with and without warping and with and without floor slabs. Stafford Smith and Taranath (1973) [52] incorporated the slab warping stiffness of each floor into the analysis by adding it to the appropriate diagonal elements of the core stiffness matrix. They recommended the finite element method as the most convenient for analysis of the slab. Additionally, vertical stresses due to warping in core cross-section should be taken into account in the design of open cores, as they can be of the same magnitude as the bending stresses.

Rosman (1969) [46] developed an analytical method, based on the principle of minimum complementary energy, for perforated concrete shafts of tall buildings subjected to torsion. The use of dimensionless coefficients made it possible to find a general solution for different loadings. He recognised a complate mathematical analogy between the torsionally loaded shaft and the laterally loaded shear wall.

The analysis of interconnected structures of three dimensional open section prismatic members was approached by two methods by Harrison (1971) [30], both the Wagner-Kappus equation and a Ritz Energy approach were used.

The redistribution of lateral loads in buildings symmetrical in plan was considered by Clough et al (1964) [13] and a similar method for the analysis of buildings, unsymmetrical in plan, which have shear walls and frames, was presented by Winkour and Gluck (1968) [60]. They believed their matrix method to be a most effective approach for solving problems with many degrees of freedom, and the

solution could be obtained by computer in a few minutes.

Heidebrecht and Swift (1971) [32] described a matrix method based on Vlasov's thin-walled beams theory for analysing coupled asymmetrical shear walls. The method considers warping of the shear walls by floor beams and slabs. The solution can be simplified by considering the floor slabs as equivalent to beams. The analysis allows for varying storey height and varying wall thicknesses throughout the height of the buildings. Results obtained by this method compared reasonably with the experimental results previously obtained by Jenkins and Harrison [35] from a plexiglass model. However, the results obtained using the continuum method of Michael [42] compared more closely with the experimental data.

A simple method for torsional analysis of three dimensional core wall structures, consisting of two equal channels, has been presented by Michael (1969) [42]. The analysis makes use of the symmetrical nature of the structure. His governing equation was found by considering compatibility equations combined with the torque-rotation and the bending-moment curvature relationship. The method is similar to that for coupled shear walls where the continuous connecting technique is employed, but due to neglecting the warping restraint of the beams, the stiffness is underestimated. The vertical element displacements are also neglected in his calculations.

Research concerned with the analysis of shear wall systems, particularly those where vertical and horizontal plates act as walls and floor slabs and where few or no columns are present, has been presented by Irwin (1970) [33]. His theoretical solution was based on the continuous connection method for two and three dimensional

shear wall structures. Also Coull and Irwin (1968) [19] have discussed a method for analysis of multi-storey structures which consist essentially of parallel assemblies of coupled shear walls. The load deflection characteristics of individual shear elements were determined using the continuous connecting technique. The complete structure was analysed using compatability and equilibrium conditions and to give a convenient equation, a system of Macaulay's brackets was adopted. Coull and Irwin (1970) [20] developed the technique to more realistic conditions of bending and torsion. A method was presented for analysing structures which had discrete assemblies of wall units, even if the system of walls was complex. Agreement between experimental results, obtained from perspex models, and the thecretical results, was very satisfactory. A simple approximate method of analysis for coupled shear walls and core elements has been discussed by Coull and Irwin (1974) [21]. The same procedure as Michael [42] was followed for torsional analysis of core elements. The theory predicts the deflection accurately but the torsional stiffness is underestimated probably due to the neglecting of the warping restraint of the floor slabs and of the influence of the coupling of pairs of walls in line.

Jaeger et al (1972) [34] developed a theory based on the continuum approach, for the analysis of tall three dimensional multiple shear wall buildings. In the theory, the torsional rigidities of the shear walls were neglected and the torsion moment is equilibrated by the shear forces associated with bending of the shear walls. A good correlation was achieved between data obtained by the finite element method and experimental results obtained from a seven storey multiple shear wall model.

The continuous method has also been extended, by using Vlasov's theory of thin-walled beams by Gluck (1970) [24] who developed it to cover the bending and torsion analysis of more complex structures consisting of coupled shear walls and a frame arranged asymmetrically in floor plan. The total stiffness of the coupled wall system was considered to be equal to the sum of the stiffnesses of the shear walls and the elastic medium of known stiffness properties which replaced the connecting beams between the walls. The axial deformations of the shear walls were neglected and to derive the stiffness matrix of the elastic media, he considered the horizontal shear forces and torque on the coupled walls to act through the centre of gravity of each element. The influence of normal strains in frame column and shear walls was then included in the analysis (1972) [25] and further (1972) [26] a linear dynamic analysis of asymmetric multi-storey structures was presented. Both analyses included the axial deformations in vertical elements. Recently, (1974) [28] it was found necessary to include the axial deformations when the beam system was of significant stiffness compared to the walls.

Later Biswas and Tso (1970) [11] modified Gluck's [24] method and took the forces to act through the shear centre of the individual element. Furthermore, Tso and Biswas (1973) [56] presented a simple continuum approach for the three-dimensional analysis of non planar coupled shear walls, of arbitrary cross-sectional shape, subjected to lateral loading. The theory gives the torsional and flexural deformations of the structure. A comparison was made with calculations based on the theory, including and neglecting axial deformation with the experimental results obtained from tests on a flexiglas model.

Neglecting axial deformation produced an error but the theory including axial deformation compared favourably with experimental results. Later Tso and Biswas (1974) [57] reformulated the theory to consider symmetrical core wall structures. The governing equation was obtained by equilibrium consideration of internal torques and applied torques. They showed that the warping stress could be significant compared with the bending stresses and should be taken into account in design. The relative vertical displacement due to the axial forces were neglected as, due to the symmetry of the core wall structure, the terms cancelled each other out on summing the two compatibility equations.

Heidebrecht and Stafford Smith (1973) [31] presented a relatively simple method, suitable for sliderule or desk calculator, for the torsion analysis of asymmetric open section shear walls. For analysis lintel beams and floor slabs were replaced by an equivalent continuum. By consideration of the compatibility conditions at the envisaged cut along the mid-span of the beams and slabs, the restraining effect coefficients were calculated and included in the differential governing equations. The analytical results, with and without lintel beams compared closely with experimental results obtained from Stafford Smith and Taranath (1972) [52]. Coull and Stafford Smith (1973) [22] and later in greater detail Coull (1974) [18], presented a simple theory for the analysis of regular, symmetrical three-dimensional, cross-wall structures. The structure is replaced by an equivalent plane coupled shear wall-cantilever structure.

3 - SCOPE OF THIS THESIS

The aim of this thesis is to present a method of analysis of coupled shear wall multi-storey buildings, whose lateral load-bearing masonry structures consist of shear and cross walls. The structure is subjected to lateral point loading causing bending and torsion. Two methods were applied for bending analysis, namely equivalent frame and wide column frame analogies. The finite element technique was used for stress and bending analyses. The governing equations for the torsion moment was obtained by considering that the external torque is equilibrated by the shear forces associated with bending of the shear walls, and the internal torques, which are comprised of St. Venant torque, warping and contributions from the connecting media. The accuracy of the theoretical method was verified by comparison with tests carried out on a one-third scale model structure. Also, the theoretical results obtained by the method modified for symmetrical channel cross-sections, were compared with results calculated by other theories and with experimental data obtained by Kalita (1970) [37].

The method is suitable for calculation by sliderule or desk calculator and is useful for the designer who wishes to consider torsion effects on tall buildings at the start of the design process.

CHAPTER II

THEORETICAL INVESTIGATION OF THE BEHAVIOUR OF MULTI-STOREY STRUCTURES

1 - INTRODUCTION

If the resultant horizontal force due to lateral loading does not pass through the centre of twist of a structure, the application of this force will cause not only deformation but also twisting. The solution of this type of problem is simplified by replacing the lateral forces by a single statically equivalent force with a well defined line of action in the same plane. Any number of forces applied to various points of the structure can be replaced by parallel forces passing through the centre of twist together with a torsion moment. The forces transferred to the shear centre will cause bending deformations and stresses which are determined by the usual elementary theory of bending. The concentrated external torsional moment obtained by transferring the horizontal force to the twist centre gives rise to complementary sectorial stresses and torsional deformation. Therefore, by considering the principle of independent action of different forces, the deformation and stresses caused by eccentric loading can be obtained by the superposition of the two actions, pure bending plus flexural torsion.

In the solution of the torsion analysis the standard literatures of Timoshenko, Vlasov, Michael and Tso, mainly have been consulted for the basic equations and assumptions. The effect of the slabs was

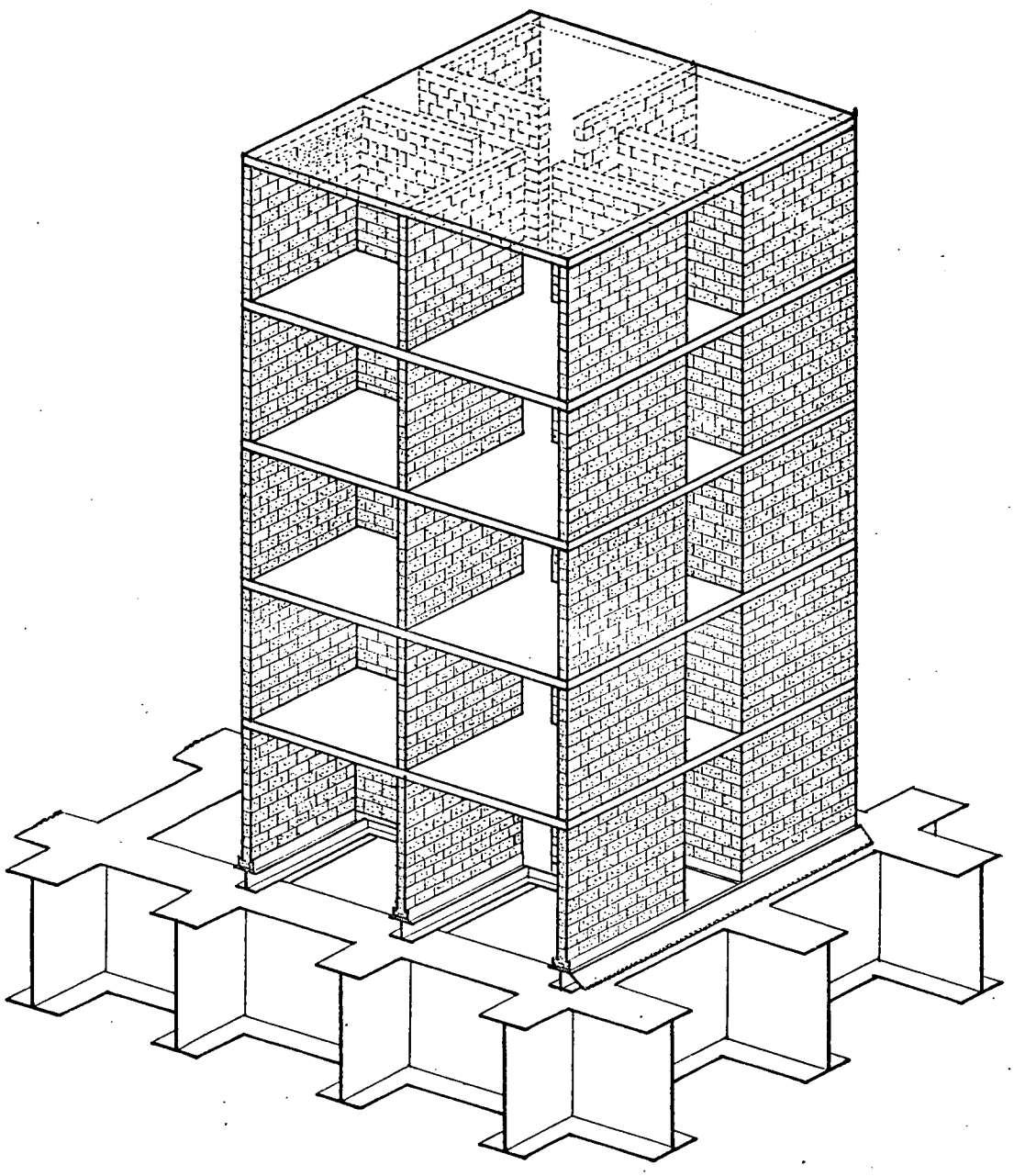

FIG 2.1 ISOMETRIC VIEW OF THE STRUCTURE

included in the analysis by applying the continuum medium approach and some different assumptions have been used to solve the structures. The theory was initially applied to a complex three dimensional coupled shear wall structure, and then modified for analysis of a symmetrical channel section.

A-FORMULATION OF PROBLEM

Figure (2.1) shows a view of a typical five storey structure, consisting of four equal angle sections and two single cross walls connected by floor slabs. The shear and cross walls are of uniform thickness over the entire height of the building, and the walls are rigidly tied to each other in the horizontal plane by the floor slabs. Therefore, it may be assumed for the sake of simplicity, that the floors are rigid horizontal diaphragms, and that these rotate as rigid bodies around the centre of twist of the structure. The axes of the walls are denoted by x, y, z which are the element axes and the overall system axes are denoted by X, Y, Z. GCi is the centre of gravity and CSi is the shear centre of the element i. The horizontal displacement of the shear centre along the x, y directions of the cross sections will be $u(z)i$ and $v(z)i$ respectively. The rotation $\theta(z)$ is about the Z axis which is assumed coincident with the torsional centre of the structure. The locations of the element centroid and shear centre are the distances from the centroids to the point O which is the system shear centre, the centre of gravity measured in the global direction is Cxi and Cyi and the distances from the point O to the element shear centre are denoted as e_{xi}, e_{yi} respectively, as shown in figure (2.2)(2.3). Due to the symmetry of

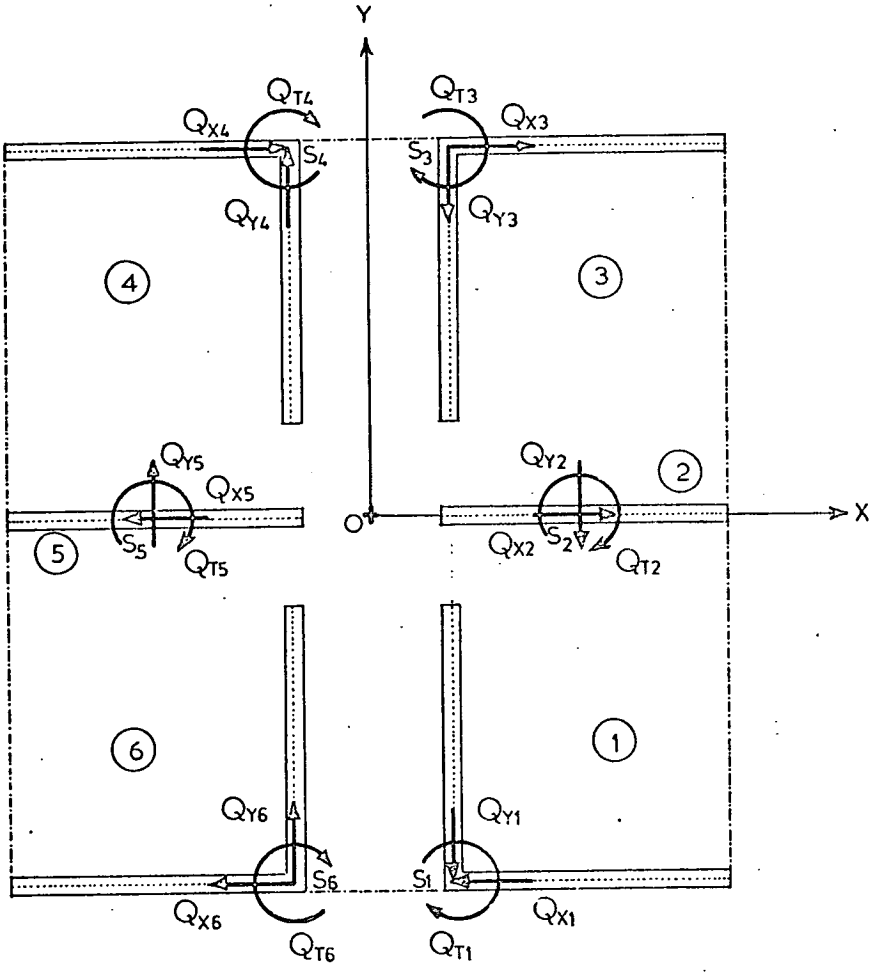

FIG 2.2 INTERNAL SHEAR FORCES AND TORQUES FROM INDIVIDUAL WALLS

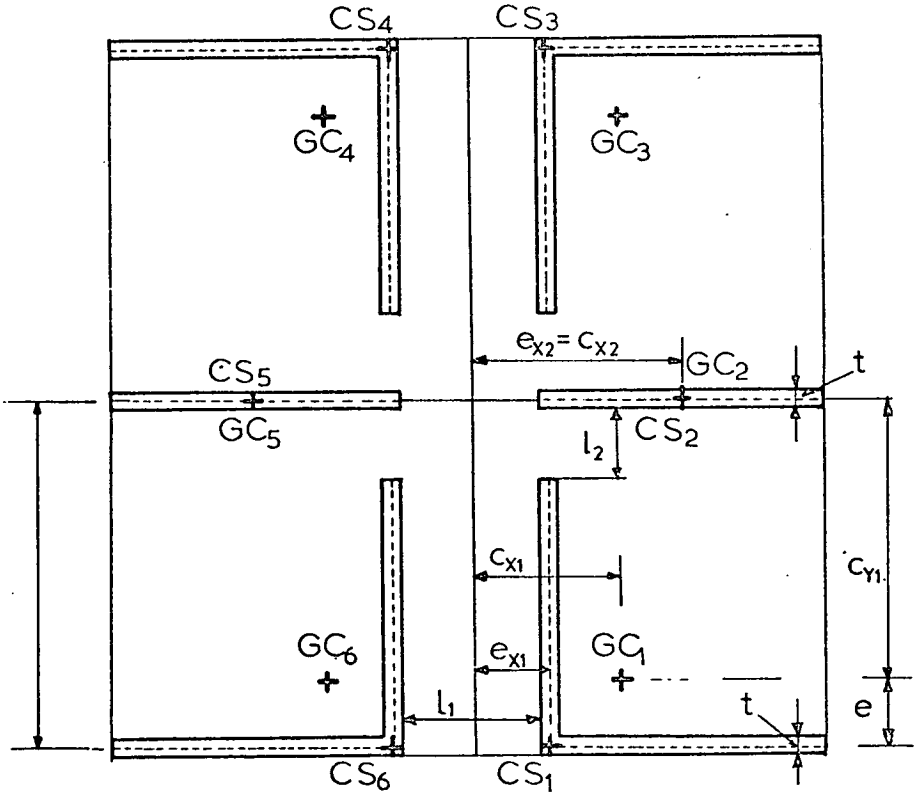

FIG 2.3 NOTATION OF PLAN

the individual elements the analysis is simplified by

$$J_{x1} = J_{x3} = J_{x4} = J_{x6} = J_{y1} = J_{y3} = J_{y4} = J_{y6} \quad \text{.....(1a)}$$

$$J_{x2} = J_{x5} \quad , \quad J_{y2} = J_{y5} \quad \text{.....(1b)}$$

and

$$e_{x1} = e_{x3} = e_{x4} = e_{x6} \quad \text{.....(1c)}$$

$$e_{y1} = e_{y3} = e_{y4} = e_{y6} \quad \text{.....(1d)}$$

and

$$e_{x2} = e_{x5} \quad , \quad e_{y2} = e_{y5} \quad \text{.....(1e)}$$

let the horizontal displacement of the system centre point O be $u(z)$ and $v(z)$ then, the displacements and rotations about the shear centres of the element i, can be related to the displacement and rotation $u(z)$, $v(z)$ and $\theta(z)$ from the simple geometric relationship, as

$$u_1 = -u_4 = -(u + \theta e_{y1}), \qquad v_1 = -v_4 = (v - \theta e_{x1}) \quad \text{.....(2a)}$$

$$u_3 = -u_6 = -(u + \theta e_{y3}), \qquad v_3 = -v_6 = (v - \theta e_{x3}) \quad \text{.....(2b)}$$

$$u_2 = u_5 \cong 0, \qquad v_2 = -v_5 = \theta e_{x2} \quad \text{.....(2c)}$$

Due to the symmetry of the structure U_2 and U_5 can be assumed equal to zero. Within the limitations of the simplifying assumptions an elementary analysis can be developed without complications.

a) Shear forces and internal torques

The internal torques and shear forces acting on an element's shear centre are shown in figure 2.2. The equation of the resultant torque for the whole structure about point O which is the axes origin, can be written as,

$$M_{T1} = \sum_{i=1}^{i=6} Q_{Ti} + \sum_{i=1}^{i=6} \left[Q_{xi} e_{yi} + Q_{yi} e_{xi} \right] \quad \ldots\ldots(3)$$

where, the clockwise rotations are positive. The internal torque which is contributed from the individual wall elements of the structure is a result of two combined actions, Saint Venant contribution (Msv) and the warping contribution (Mw), given by the formula

$$\sum_{i=1}^{i=6} Q_{Ti} = M_{SV} + M_W \quad \ldots\ldots(4)$$

Hence, from in the above equation the St. Venant torsion moment (M_{sv}) can be written as

$$M_{SV} = G K_T \frac{d\theta}{dz} \quad \ldots\ldots(5)$$

in which

$$K_T = \frac{1}{3} \sum_{i=1}^{i=6} s_i t_i^3 \quad \ldots\ldots(6)$$

The value K_T is called a torsion constant or St. Venant moment of inertia and GK_T is the St. Venant torsional rigidity; t_i is the thickness and s_i is the length of the wall elements.

The second term of equation (4), the warping torsional moment is

$$M_W = E I_\omega \frac{d^3\theta}{dz^3} \qquad \ldots\ldots(7)$$

where the term I_ω introduced by Vlasov, is the warping moment of inertia defined in the following expression.

$$I_\omega = \int_s \omega_{(s)}^2 t \, ds \qquad \ldots\ldots(8)$$

From equation (3) the terms Q_{x_i} and Q_{y_i} represent the respective shear forces acting on the individual shear centre of elements; e_{x_i} and e_{y_i} are the lever arms of the shear forces in OX and OY directions respectively. The accepted equations for the relationship between the shear forces and displacement are

$$Q_{x_i} = - E I_{y_i} \frac{d^3 u_i}{dz^3} \qquad \ldots\ldots(9a)$$

and

$$Q_{y_i} = - E I_{x_i} \frac{d^3 v_i}{dz^3} \qquad \ldots\ldots(9b)$$

from equation (2), differentiating u_i and v_i with respect to the variable z coordinate and substituting into equation (9a, 9b) and multiplying equation respectively by e_{x_i} and e_{y_i}, considering the symmetry of the building, we have,

$$\sum_{i=1}^{i=6} Q_{xi}\, e_{yi} = \left[EI_{y1}\frac{d^3u_1}{dz^3} - EI_{y3}\frac{d^3u_3}{dz^3} - EI_{y4}\frac{d^3u_4}{dz^3} + EI_{y6}\frac{d^3u_6}{dz^3} \right] e_{y1} \quad \text{.....(10a)}$$

and becomes

$$\sum_{i=1}^{i=6} Q_{xi}\, e_{yi} = -\,4EI_{y1}\, e_{y1}^2 \frac{d^3\theta}{dz^3} \quad \text{.....(10b)}$$

and

$$\sum_{i=1}^{i=6} Q_{yi}\, e_{xi} = \left[EI_{x1}\frac{d^3v_1}{dz^3} + EI_{x3}\frac{d^3v_3}{dz^3} - EI_{x4}\frac{d^3v_4}{dz^3} - EI_{x6}\frac{d^3v_4}{dz^3} - EI_{x5}\frac{d^3v_5}{dz^3} - EI_{x2}\frac{d^3v_2}{dz^3} \right] \quad \text{.....(11a)}$$

and becomes

$$\sum_{i=1}^{i=6} Q_{yi}\, e_{xi} = \left[4EI_{x1}\, e_{x1}^2 + 2EI_{x2}\, e_{x2}^2 \right] \frac{d^3\theta}{dz^3} \quad \text{.....(11b)}$$

Therefore the equations (10b) and (11b) are substituted into the shear force term of equation (3) and the resulting equation we denote by M_F, thus

$$M_F = -\left[4EI_{x1}\, e_{x1}^2 + 2EI_{x2}\, e_{x2}^2 + 4EI_{y1}\, e_{y1}^2 \right] \frac{d^3\theta}{dz^3} \quad \text{.....(12a)}$$

in which

$$I^* = 4I_{x1}\, e_{x1}^2 + 2I_{x2}\, e_{x2}^2 + 4I_{y1}\, e_{y1}^2 \quad \text{.....(12b)}$$

$$M_F = - E I^* \frac{d^3\theta}{dz^3} \quad \ldots\ldots (12c)$$

finally, equation (3) becomes

$$M_{T1} = M_{SV} + M_F + M_W \quad \ldots\ldots (13)$$

Substituting equations (5), (7) and (12c) into the above equation

$$M_{T1} = G K_T \frac{d\theta}{dz} - E I^* \frac{d^3\theta}{dz^3} - E I_\omega \frac{d^3\theta}{dz^3} \quad \ldots\ldots (14)$$

b) Slab effect

The torsional behaviour of such structures may be derived using an analysis which is comparable to the continuous medium technique widely used for plane walls with openings (19, 24, 42, 44, 56). The further assumption is that it is considered that the connecting media deform only in the vertical plane (XZ, YZ). These deformations can be obtained by cutting the structure at midspan and reapplying the vertical shear forces $\bar{Q}_{(z)j}$ and are written

$$\bar{Q}_{(z)j} = \int_z^H q_j \, d\bar{z} \quad \ldots\ldots (15)$$

In this case the midpoint of the connecting media is coincident with the contraflexure point and so there is zero bending moment and also their net axial force is zero. In a cut at this section as shown in figure (2.5) these applied shear forces $\bar{Q}_{(z)j}$ are transformed into an

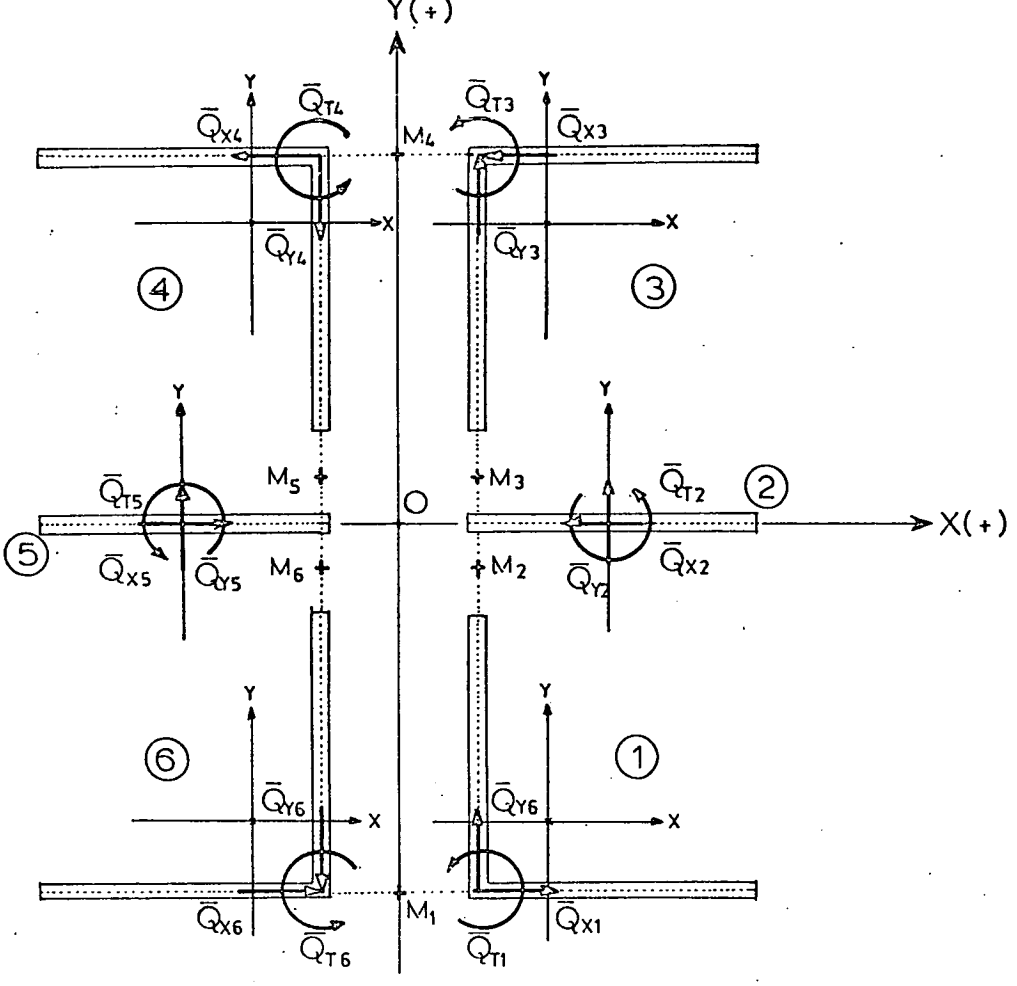

FIG 2.4 SHEAR FORCES AND TORQUES DUE TO DISTRIBUTED SHEAR $q_i(z)$ ON INDIVIDUAL WALL

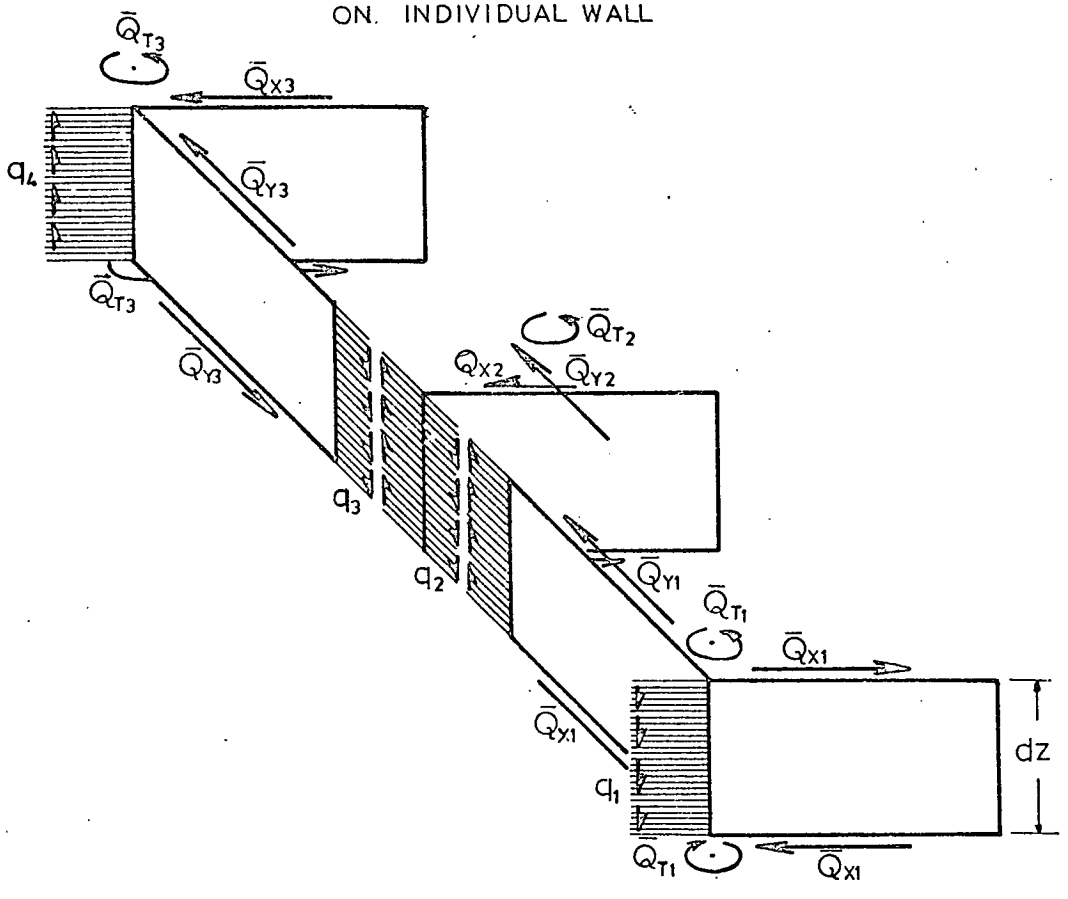

FIG 2.5 SHEAR FORCES AND TORQUES DUE TO DISTRIBUTED SHEAR q_i

equivalent distributed shear force acting on the continuous media with flexural rigidity EI_d and may be replaced by an equivalent connecting medium with flexural rigidity $\frac{EI_d}{h}$ per unit height, where h is the storey height, as shown in figure (2.5). Finally the walls can be considered as open thin-walled beam so that Vlasov's theory for thin-walled beams can be easily applied (23, 58, 59).

Secondly, additional forces and torques are developed in the connecting media due to the shear forces $q_{(z)j}$ as shown in figures (2.4) (2.5). The resultant torque (M_S) produced by these forces and torques, for the whole structure about point O can be written as,

$$M_S = \sum_{i=1}^{i=6} \left[\bar{Q}_{xi} e_{y_i} + \bar{Q}_{y_i} e_{xi} \right] + \sum_{i=1}^{i=6} \bar{Q}_{Ti} \qquad \text{.....(16)}$$

From equation (16) the shear forces $\bar{Q}_{x_i}$ and $\bar{Q}_{y_i}$ can be obtained by considering the static equilibrium of each element and by taking the total moments about the x_i and y_i axes as being equal to zero. Thus the following relationships can be written.

$$\sum M_{x_1} = 0 \qquad \text{.....(17a)}$$

$$-\bar{Q}_{y_1} dz + q_1 dz (e_{y_1} - c_{y_1}) + q_2 dz \left[c_{y_1} - \frac{l_2 + t}{2} \right] = 0 \qquad \text{.....(17b)}$$

$$\bar{Q}_{y_1} = q_1 (e_{y_1} - c_{y_1}) + q_2 \left[c_{y_1} - \frac{l_2 + t}{2} \right] \qquad \text{.....(17c)}$$

and

$$\sum M_{y_1} = 0 \qquad \text{.....(18a)}$$

$$\bar{Q}_{x1}\,dz - q_1\,dz\,c_{x1} + q_2\,dz\left[c_{x1} - e_{x1}\right] = 0 \qquad \text{(18b)}$$

$$\bar{Q}_{x1} = q_1 c_{x1} - q_2\left[c_{x1} - e_{x1}\right] \qquad \text{(18c)}$$

For second element

$$\sum M_{x2} = 0 \qquad \text{(19a)}$$

$$-\bar{Q}_{y2}\,dz + q_2\,dz\left[l_2 + t\right] = 0 \qquad \text{(19b)}$$

$$\bar{Q}_{y2} = q_2\left[l_2 + t\right] \qquad \text{(19c)}$$

and

$$\sum M_{y2} = 0 \qquad \text{(20a)}$$

$$\bar{Q}_{x2} = 0 \qquad \text{(20b)}$$

From the second term of equation (16) the torques of the individual elements about their own shear centre which are produced by the shear forces $q_{(z)i}$, act along the midpoints of the laminae. These torques are equal to the shear forces $q_{(z)i}$ times the sectorial area $\omega_{(s)j}$ appendix (I). It can be written

$$\bar{Q}_{Ti} = q_{(z)i}\,\omega_{(s)j} \qquad \text{(21)}$$

Hence, by substituting equations (17c), (18c), (19c), (20b) and (21) into equation (16) considering the symmetry, the result can be obtained as follows.

$$M_s = -\left[4\bar{Q}_{x1}e_{y_1} + 4\bar{Q}_{y_1}e_{x1} + 2\bar{Q}_{y_2}e_{x2} + 4\bar{Q}_{Ti} + 2\bar{Q}_{T2}\right] \quad \text{(22a)}$$

$$= -\Big\{4\left[q_1c_{x1} - q_2(c_{x1} - e_{x1})\right]e_{y_1} + 4\left[q_1\left(e_{y_1} - c_{y_1}\right) \quad q_2\left(c_{y_1} - \frac{l_2+t}{2}\right)\right]$$

$$+ 2q_2(l_2+t)e_{x2} + 4\left[\omega_{11}q_1 + \omega_{21}q_2\right] + 4\omega_{22}q_2\Big\} \quad \text{(22b)}$$

$$= -\Big\{q_2\left[e_{x1}\left(c_{y_1} - \frac{l_2+t}{2}\right) - e_{y_1}\left(c_{x1} - e_{x1}\right) + e_{x2}\frac{l_2+t}{2} + \omega_{21} + \omega_{22}\right]$$

$$+ q_1\left[c_{x1}e_{y_1} + e_{x1}\left(e_{y_1} - c_{y_1}\right) + \omega_{11}\right]\Big\}4 \quad \text{(22c)}$$

$$M_s = -\left[q_1m_1 + q_2m_2\right] \quad \text{(22d)}$$

In which m_1 and m_2 are denoted by

$$m_1 = 4\left[c_{x1}e_{y_1} + e_{x1}\left(e_{y_1} - c_{y_1}\right) + \omega_{11}\right] \quad \text{(23)}$$

$$m_2 = 4\left[e_{x1}\left(c_{y_1} - \frac{l_2+t}{2}\right) - e_{y_1}\left(c_{x1} - e_{x1}\right) + e_{x2}\frac{l_2+t}{2} + \omega_{21} + \omega_{22}\right] \quad \text{(24)}$$

In equation (22) the shear forces q_1 and q_2 are unknown variables. These two values can be obtained from consideration of compatibility along the cuts of the laminae. As mentioned earlier shear forces

applied along the cut on the wall elements of the structure. The walls deform independently and the connecting media are only allowed to displace in the longitudinal direction. The relative vertical displacement, due to the horizontal deflections and rotations along the cut, can be calculated by means of considering the theory of thin-walled beams, and can be written as

$$\delta_{aj} = \delta_{jx} + \delta_{jy} + \delta_{je} \qquad \text{.....(25)}$$

From equation (25) the deflections δ_{jx} and δ_{jy} arise as a result of bending in the xz and yz planes respectively. In such a deformation those elements that remain in plane rotate (3, 58, 59) about x and y axes as shown in figures (2.6) and (2.7). Now the third term of the equation determines the part of the displacement which arises due to torsion. Longitudinal displacement along the cut is equal to the product of the torsional warping $\frac{d\theta_i}{dz}$ times the sectorial area $\omega(s)j$. The displacements of point M_j for element number -1- in figures (2.4), (2.6) and (2.7) are as follows.

$$\delta_{a1} = c_{x1}\frac{du_1}{dz} + \left(e_{y1} - c_{y1}\right)\frac{dv_1}{dz} + \omega_{11}\frac{d\theta}{dz} \qquad \text{.....(26a)}$$

for the point M_j and elements, number 1 and 2 are

$$\delta_{a2} = \left(c_{x1} - e_{x1}\right)\frac{du_1}{dz} - \left(c_{y1} - \frac{l_2 + t}{2}\right)\frac{dv_1}{dz} + \omega_{21}\frac{d\theta}{dz} \qquad \text{.....(26b)}$$

Substituting the expression of equation (2) into equations (26a, 26b) and abbreviating, considering the symmetry of structure we obtain

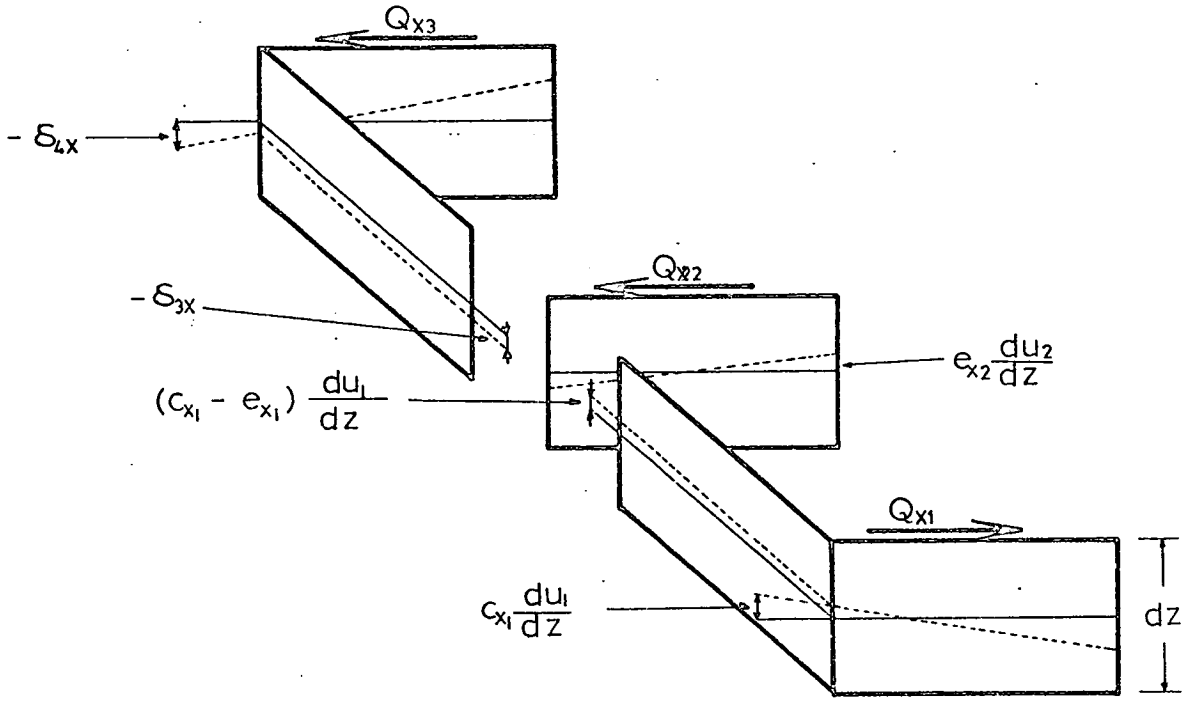

FIG 2.6 DUE TO DISPLACEMENT IN X DIRECTION ONLY

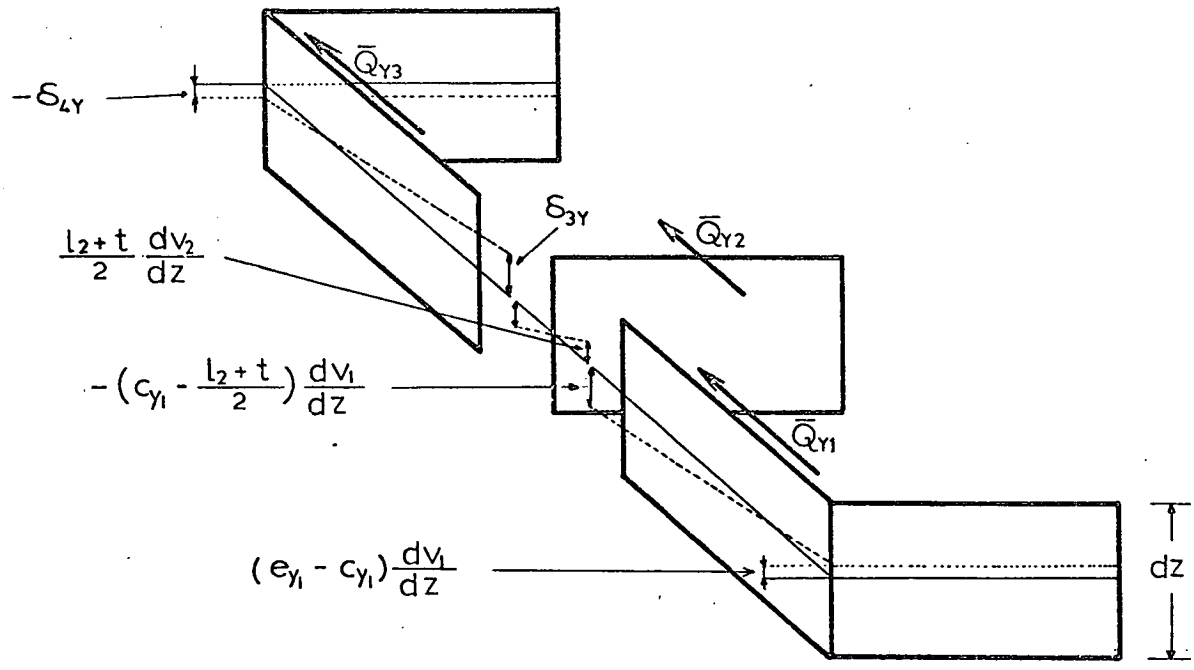

FIG 2.7 DUE TO DISPLACEMENT IN Y DIRECTION ONLY

In equation (30) A_{dj} is the effective area of the connecting laminae and I_{dj} its moment of inertia. ($j = 1,2$). These deflections δ_{a_1} and δ_{a_2} are equal in magnitude and opposite to the deflection δ_{b_1} and δ_{b_2} respectively (21, 42, 58, 59). Assuming that axial deformation of the walls under axial load $\bar{Q}_{(z)j}$, are negligible. Thus using equation (27a), (27b), (19a) and (29b) to eliminate δ_{aj} and δ_{bj} we get

$$q_1 = - \lambda_1 \bar{m}_1 E \frac{d\theta}{dz} \qquad \text{.....(31a)}$$

and

$$q_2 = - \lambda_2 \bar{m} E \frac{d\theta}{dz} \qquad \text{.....(31b)}$$

Substituting equations (31a) and (31b) into equation (22) the final equation becomes

$$M_s = E K_s \frac{d\theta}{dz} \qquad \text{.....(32)}$$

in which

$$K_s = \lambda_1 m_1 \bar{m}_1 + \lambda_2 m_2 \bar{m}_2 \qquad \text{.....(33)}$$

Finally by combining the moments M_{T1} and M_s, equating with the external twisting moment, which becomes

$$M_T = M_{SV} + M_s + M_F + M_W \qquad \text{.....(34)}$$

Further, by substituting the equations for the four terms into the above equation, the governing equation becomes

$$M_T = \left[G K_T + E K_S\right]\frac{d\theta}{dz} - \left[E I^* + E I_\omega\right]\frac{d^3\theta}{dz^3} \quad \ldots\ldots(35)$$

Dividing this equation by the coefficient of $-E(I^* + I_\omega)$ and introducing the notation

$$\gamma^2 = \frac{G K_T + E K_S}{E I^* + E I_\omega} \quad \ldots\ldots(36)$$

and

$$I^*_\omega = I^* + I_\omega \quad \ldots\ldots(37)$$

The equation (35) is simplified

$$\frac{d^3\theta}{dz^3} - \gamma^2 \frac{d\theta}{dz} = -\frac{M_T}{E I^*_\omega} \quad \ldots\ldots(38)$$

This differential equation formulates the relation between the angle of twist of the structure and the external load. The general solution of the equation (38) can be written when concentrated torque is applied, as (20)

$$\theta = C_1 + C_2\cosh(\gamma z) + C_3\sinh(\gamma z) + \frac{M_T z}{\gamma^2 E I^*_\omega} \quad \ldots\ldots(39)$$

The coefficients C_1, C_2 and C_3 are constants of integration and determined from the boundary conditions of the structure which are: if the structure is entirely built in at the base no rotation and no warping is developed, also at the top of the structure warping is not restrained. These boundary conditions can be expressed as,

at $z = 0$ $\quad \Theta(z) = 0$ .....(40a)

$$\frac{d\Theta}{dz} = 0 \quad \text{.....(40b)}$$

at $z = H$ $\quad \frac{d^2\Theta}{dz^2} = 0$ .....(40c)

with these boundary conditions equation (39) can be solved as (20)

$$\Theta = \left[\gamma z - \sinh(\gamma z) + \tanh(\gamma H)\left[\cosh(\gamma z) - 1\right]\right] \frac{M_T}{\gamma^3 E I_\omega^*} \quad \text{.....(41)}$$

Additionally, the differential equation for a distributed torque (m_t) can be found by differentiating equation (35) with respect to z axis such that,

$$-m_t = \left[GK_T + EK_s\right] \frac{d^2\Theta}{dz^2} - \left[EI^* + EI_\omega\right] \frac{d^4\Theta}{dz^4} \quad \text{.....(42)}$$

The differential equation is solved (20), and given as

$$\Theta = \left\{\left[\tanh(\gamma H) + \frac{1}{\lambda H}\operatorname{sech}(\gamma H)\right]\left[\cosh(\gamma z) - 1\right] + \gamma z - \frac{\gamma z^2}{2H} - \sinh(\gamma z)\right\} \frac{m_t H}{\gamma^3 E I_\omega^*} \quad \text{.....(43)}$$

The deformation of the building can be obtained by substituting the angle of twist into equation (2). Similarly, the vertical shear forces per unit height can be found from equations (31a) and (31b). We can easily determine the complementary warping stress and shearing stress in

the walls due to torsion, which can be obtained considering the thin-walled beams theory by the formulation,

$$\sigma_{\omega(s)} = E\,\omega(s)\,\frac{d^2\theta}{dz^2} \qquad \ldots\ldots(44)$$

$$\sigma_w = \frac{E\,S_\omega}{t}\,\frac{d^3\theta}{dz^3} \qquad \ldots\ldots(45)$$

In which $\omega(s)$ is the sectorial area and S_ω is the sectorial statical moment of the sections, both with respect to the individual element shear centre.

2 - MODIFICATION OF THE THEORY FOR CHANNEL SECTION

2.1 - INTRODUCTION

In this section a method is presented for the analysis of symmetrical channel sections connected by floor slabs. Previous workers [21, 24, 37, 42, 46, 55, 56] used channel core sections for development of their theories. For this reason, it was desirable to compare the analytical results obtained by the thesis theory and the analytical results obtained by the other workers, using their own theory, with the experimental data available for the symmetrical channel cross-section in figure (2.8) (2.9). In the experimental structure, the magnitude of the warping effect is not taken into consideration as the structure is comprised of an angle and single cross section. Therefore in the theoretical formula the warping torsional properties become zero. In other typical structures such as the channel section this is not the case and so additional equations have to be considered to take into account the warping torsional properties. Also this provides the opportunity to

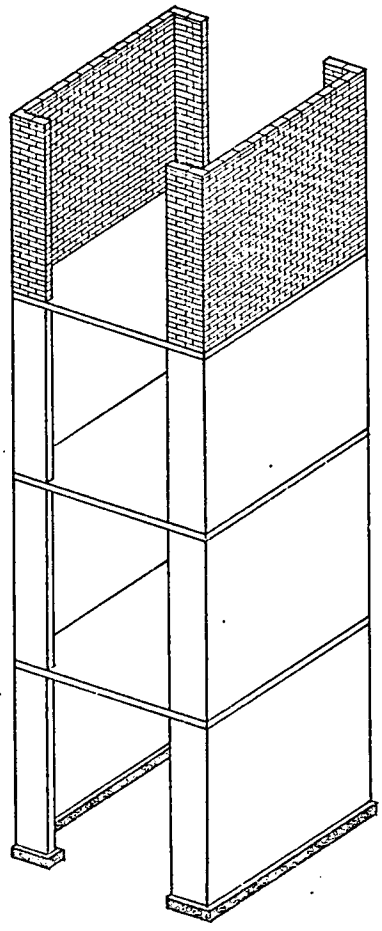

FIG 2.8 ISOMETRIC VIEW OF STRUCTURE

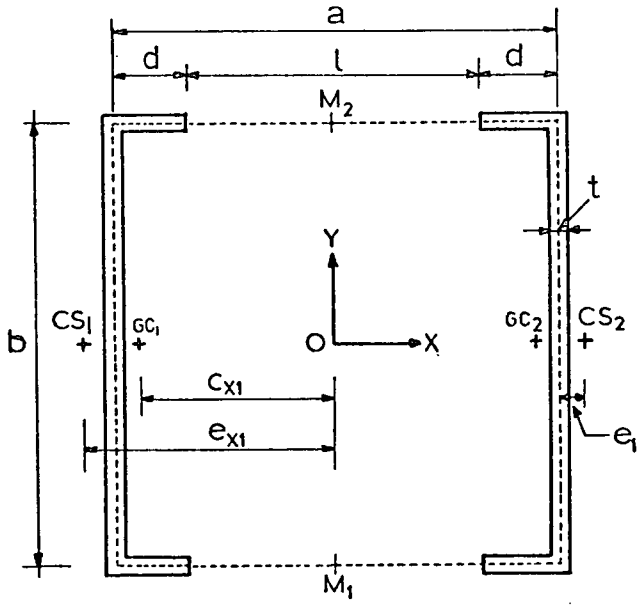

FIG 2.9 PLAN OF CORE WALL STRUCTURE

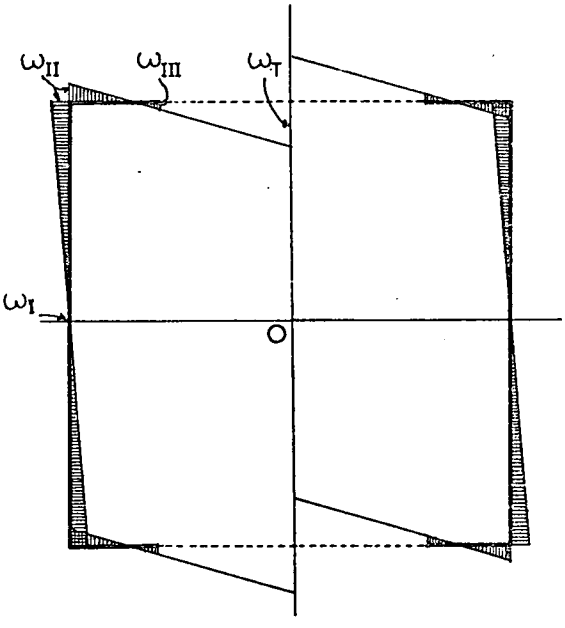

FIG 2.10 DIAGRAM OF THE SECTORIAL COORDINATE

compare the analytical and the experimental results in an example with warping and one without warping.

A - Warping Torsional Properties

Using the thin-walled beams theory, warping torsional properties of the channel cross section may easily be found as follows.

The figure (2.10) shows the diagram of the sectorial coordinate $\omega(s)$ in $[in^2, cm^2]$ with respect to the individual elements shear centre. Using the notations in Fig. (2.9) and according to the general formula, appendix (1)

$$\omega_I = 0 \qquad \text{.....(46a)}$$

$$\omega_{II} = \int_0^{b/2} e\,ds = -e\frac{b}{2} \qquad \text{.....(46b)}$$

$$\omega_{III} = \omega_{II} + \int_0^{d} \frac{b}{2}\,ds = \frac{b}{2}[d - e] \qquad \text{.....(46c)}$$

$$\omega_I \quad \omega_{III} + \int^{l/2} \frac{b}{2}\,ds = \frac{b}{4}[a - 2e] \qquad \text{.....(46d)}$$

The sectorial statical moment of the section with respect to the shear centre, according to the general formula (appendix I) for the points II and I, can be found.

$$S_{\omega II} = \int_0^{d} \left[\frac{\omega_{II} + \omega_{III}}{d}\right].t.s\,ds = \frac{bdt}{4}[d - 2e] \qquad \text{.....(47a)}$$

$$S_{\omega I} = S_{\omega II} - \int_0^{b/2} \frac{2\omega_{II}}{b}.t.s\,ds$$

$$= \frac{bt}{8}\left[2d(d - 2e) - be\right] \qquad \text{.....(47b)}$$

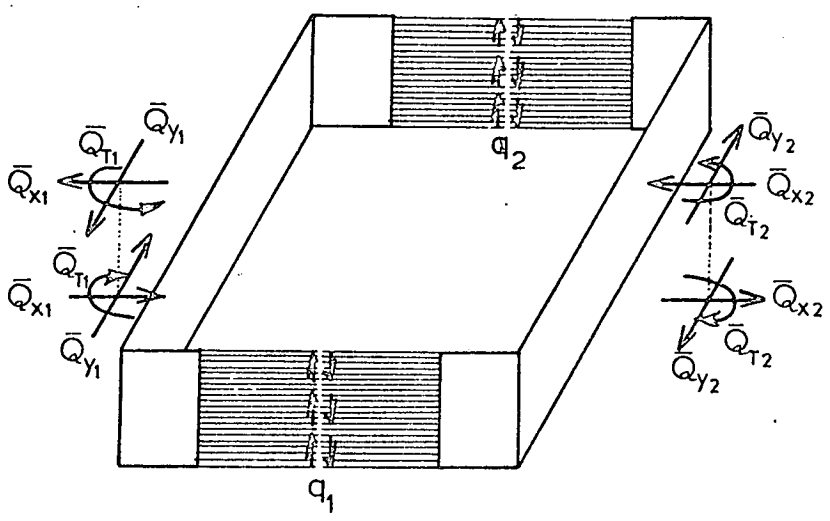

FIG. 2.11 INTERNAL SHEAR FORCES AND TORQUES FROM INDIVIDUAL WALLS DUE TO DISTRIBUTED SHEAR FORCES

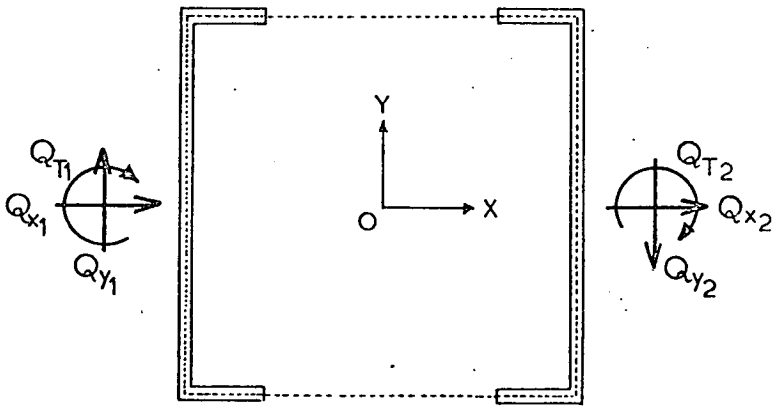

FIG. 2.12 SHEAR FORCES AND TORQUES FROM WALLS

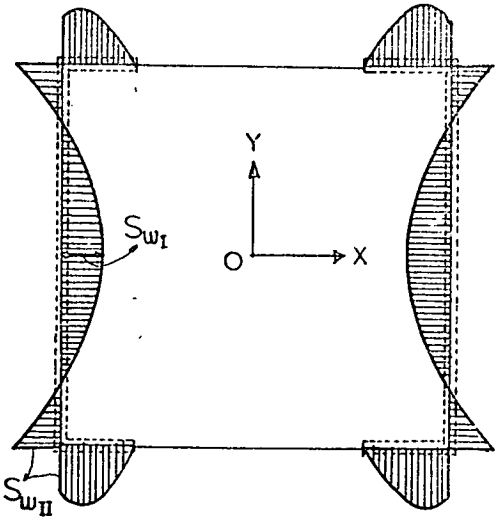

FIG 2.13 DIAGRAM OF THE SECTORIAL STATIC MOMENT

Figure (2.13) shows the diagram of the sectorial statical moment in (in^4 , cm^4).

B - Application of Theory

The Saint Venant Torsional moment (M_{SV}), the warping torsional moment M_W and M_F which is derived from shear forces of the individual elements, are already defined in the previous section. Their related stiffness properties are calculated below.

a) The channel cross-section is of constant thickness t_i and length $s_i(b,d)$. The St. Venant moment of inertia can be written ($i = 1,2$) as

$$K_T = \frac{2}{3}\left[b - 2d \right] t^3 \qquad (48)$$

b) Warping moment of inertia for channel cross-section is obtained according to the general formula appendix (I).

$$I_\omega = 2\int_0^{b/2} (es)^2 t \, ds + 2\int_0^{d} \left[\frac{b}{2} s - \frac{b}{2}(d - e)\right] t \, ds \qquad (49a)$$

$$I_\omega = \frac{b^2 t}{2}\left[\frac{b}{6} e^2 - de(d - e) + \frac{d^3}{3}\right] \qquad (49b)$$

c) Bending stiffness

$$I^* = 2 I_x e_x^2 \qquad (50)$$

d) The moment M_S, from equation (14), developed in the connecting media from the shear forces and torques, as shown in figures (2.12) can be written in the form to fit the channel section, ($i = 1,2$) as

$$M_s = 2\left(\bar{Q}_y e_x + \bar{Q}_T\right) \quad \text{.....(51)}$$

The horizontal shear forces and torques $\bar{Q}_{xi}$, $\bar{Q}_{yi}$ and $\bar{Q}_{Ti}$ can be related to the vertical shear forces $q_{(z)j}$ from consideration of the equilibrium conditions of the individual elements, as presented in figure [2.11].

Thus $\bar{Q}_{xi} = 0$ .....(52a)

$$\bar{Q}_{yi} = b\, q_1 \quad \text{.....(52b)}$$

and

$$\bar{Q}_T = \omega_T\, q_1 \quad \text{.....(52c)}$$

Equations 52(b,c) are substituted into equation (51) given by

$$M = m_{c1}\, q_1 \quad \text{.....(52a)}$$

In which

$$m_{c1} = b\left(be_y + \omega_T\right) \quad \text{.....(53b)}$$

The relative vertical displacement in the xz and yz planes due to deflection and rotation of the walls, as presented in figure [2.14] can be obtained by applying the equation (25) are derived previously is

$$\delta_{a1} = c_{x1}\frac{du_1}{dz} + \frac{b}{2}\frac{dv_1}{dz} + \omega_T\frac{d\theta}{dz} \quad \text{.....(54)}$$

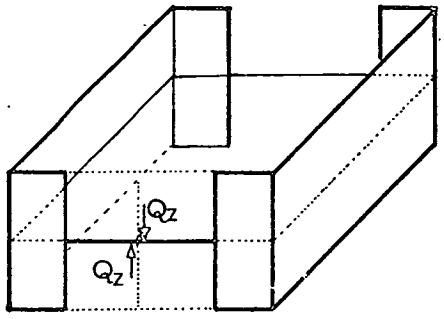

Applied shear force

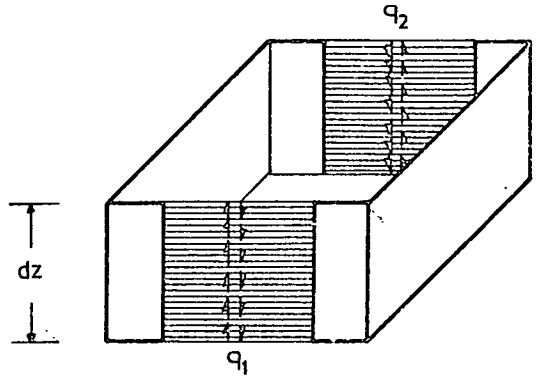

Distributed shear forces.

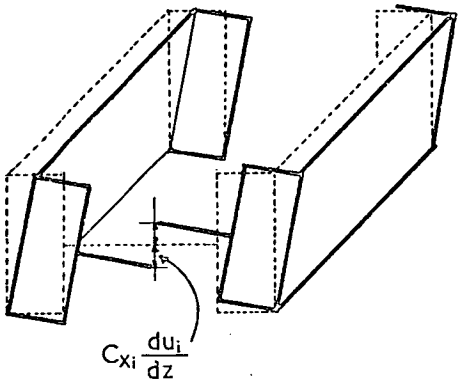

Due to displacement in X direction only.

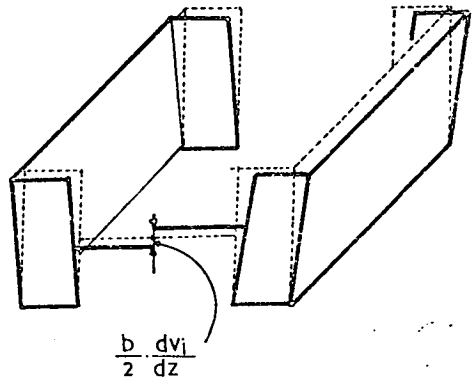

Due to displacement in Y direction only.

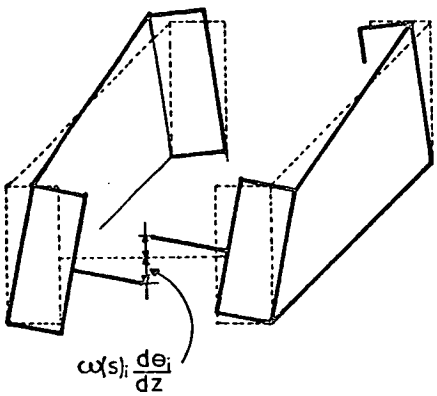

Due to warping only.

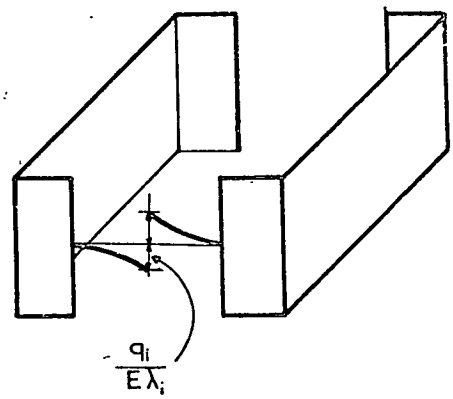

Due to shear and bending deformation of the connecting media.

FIG 2.14 NOTATION AND GEOMETRY OF DISPLACEMENT OF CROSS SECTION.

By substituting ω_T by equation (46d) into the above equation and considering the relationship between the deflection (u_1, v_1) and rotation (θ), the equation becomes

$$\delta_{a_1} = \bar{m}_{c1} \frac{d\theta}{dz} \qquad \text{.....(55)}$$

where

$$\bar{m}_{c1} = \frac{b}{2} \left[c_{x1} + a - e \right] \qquad \text{.....(56)}$$

The relative vertical displacement due to bending and shear of the connecting laminae is

$$\delta_{b1} = \frac{q_{(z)1}}{\lambda_1 E} \qquad \text{.....(57)}$$

From equations (55) and (57) the shear force $q_{(z)}$ can be derived and substituted into equation (52). Thus the final form of the moment is

$$M_s = \lambda_1 m_{c1} \bar{m}_{c1} E \frac{d\theta}{dz} \qquad \text{.....(58)}$$

where

$$K_s = \lambda_1 m_{c1} \bar{m}_{c1} \qquad \text{.....(59)}$$

Therefore, the coefficients thus derived can be substituted into the governing equation and by using the angle of twist relationship of the structure the related equations as detailed in section I can be solved to give,

a) The deflections on the structure

b) Shear forces along the cut

c) Complementary warping stress and shearing stress.

Furthermore, for the calculation of stresses, the structure can be analysed by Vlasov's thin-walled beams theory. The longitudinal stresses caused by axial, shear forces and bending moment are additive algebraically and can be calculated from the general formula as given

$$\sigma(s) = \frac{P}{A} + M_{xx}\frac{y(s)}{I_x} + M_{yy}\frac{x(s)}{I_y} + B\frac{\omega(s)}{I_\omega} \quad \text{.....(60)}$$

and

$$\sigma(s) = Q_x\frac{S_x(s)}{I_x} + Q_y\frac{S_y(s)}{I_y} + M_T\frac{S_\omega(s)}{t\,I_\omega} \quad \text{.....(61)}$$

Where Q_x and Q_y are the shear forces in the section acting in the X and Y direction. $S_x(s)$ and $S_y(s)$ are the static moments of inertia, $S_\omega(s)$ is the sectorial statical moment of inertia and t is the thickness of the cross-section.

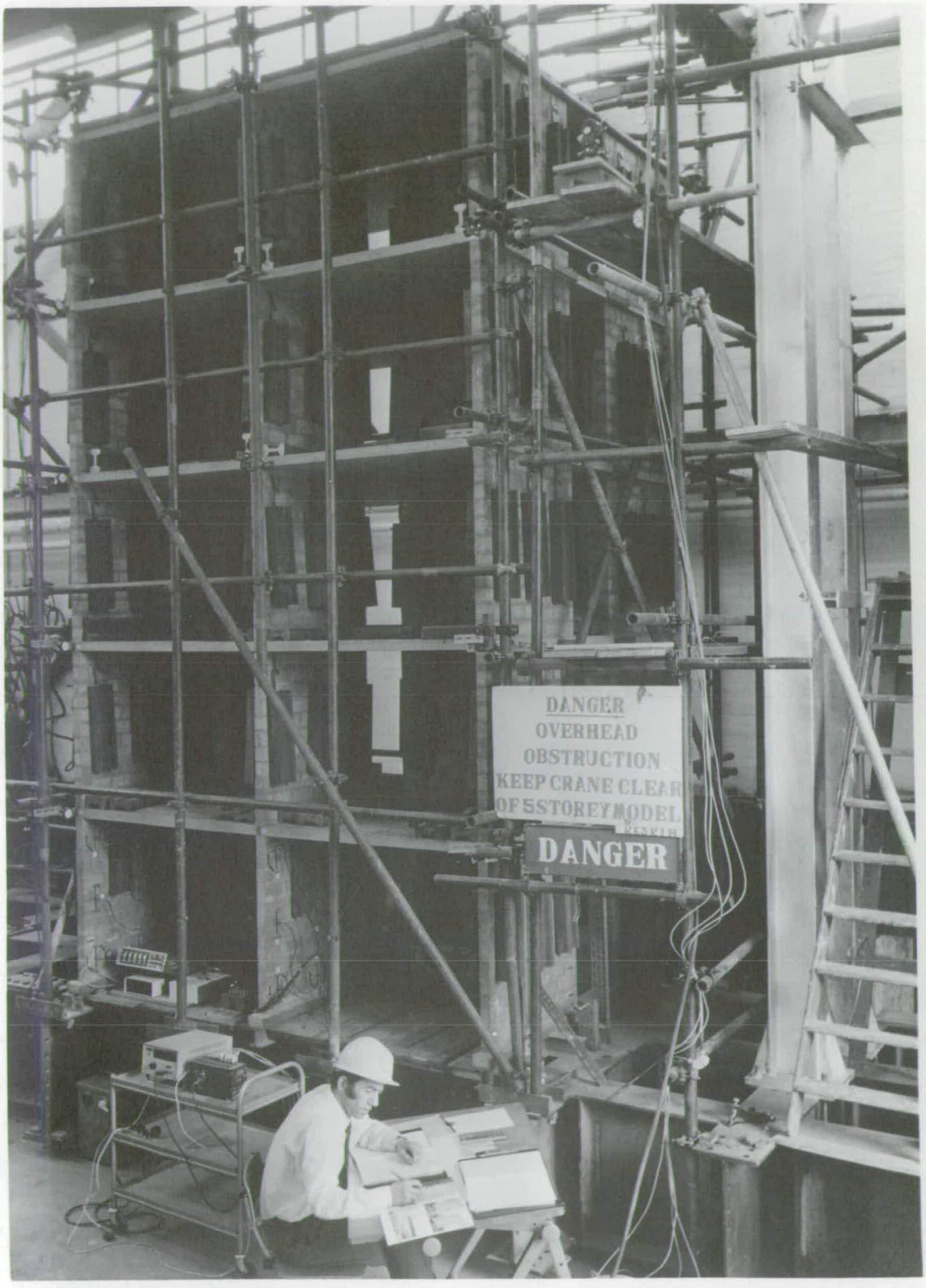

PLATE(3.1) ONE-THIRD SCALE BLOCKWORK MODEL STRUCTURE WITH LOADING AND DIAL GAUGES FRAMES

CHAPTER III

-III- EXPERIMENTAL INVESTIGATION OF THE BEHAVIOUR OF A MULTI-STOREY SHEAR WALLED STRUCTURE IN BLOCKWORK UNDER BENDING AND TORSION LOADING.

1 - INTRODUCTION

Load bearing masonry wall system, in recent years have received new attention as a structural system. This is evident from the number of articles published. The masonry walls can be made of any of several types of materials. One which is becoming increasingly used and from which the test structure is constructed is that of the concrete block. Concrete block is a versatile building material widely used throughout the world in different climatic conditions. The blocks have high thermal and sound insulation. Also, as well as being economical, they can be successfully handled by unskilled workers. Block production can either be in a large central factory or at the site as the demand arises. It is largely for these reasons that concrete blocks offer a unique opportunity in the construction program of underdeveloped countries which suffer from an acute shortage of industrial resources. But the future development of the concrete block is by no means limited to the underdeveloped countries. The advantages and disadvantage of concrete blocks have been extensively discussed by Rostampour (1973) [47].

With the increasing use of such blocks a greater knowledge of the behaviour of this type of structure is required. As buildings increase in height it becomes more important to ensure adequate lateral stiffness. In recent years this has been obtained by providing shear walls. They

can be walls of repeating unitsfigure 3.1 or are often grouped together to form a core which is utilised to form lift and service shafts. It is presently accepted that reinforced and unreinforced masonry shear wall structures which are designed to act jointly with floor slabs participating as horizontal diaphrams are effective in resisting gravity load, (dead and live weight) and the large lateral forces produced by wind, earthquake and other actions. Wind load is a major criterion in designing a tall building. The structural engineer must be sure the design is structurally safe and sufficient support systems are provided. Subsequently more attention is being paid to the adequacy of the design of buildings with regard to the lateral loads.

This investigation was to examine and analyse the lateral load (axial and eccentric) resistance of the structure (see typical plan figure 3.4). This type of structure may be used in current tall buildings for both commercial and residential purposes, partly as it has the advantage of being capable of carrying more lateral load along its axes than any other similar unit systems.

In this work, an experimental investigation was carried out to examine the behaviour of a structure and to test the accuracy of the theoretical analysis. For this purpose, a one-third scale five storey shear wall structure made up of "Aglite" blocks with opening was tested under lateral point loads. The loads were applied axially, through the shear centre of system and eccentrically at the top slab level of the structure.

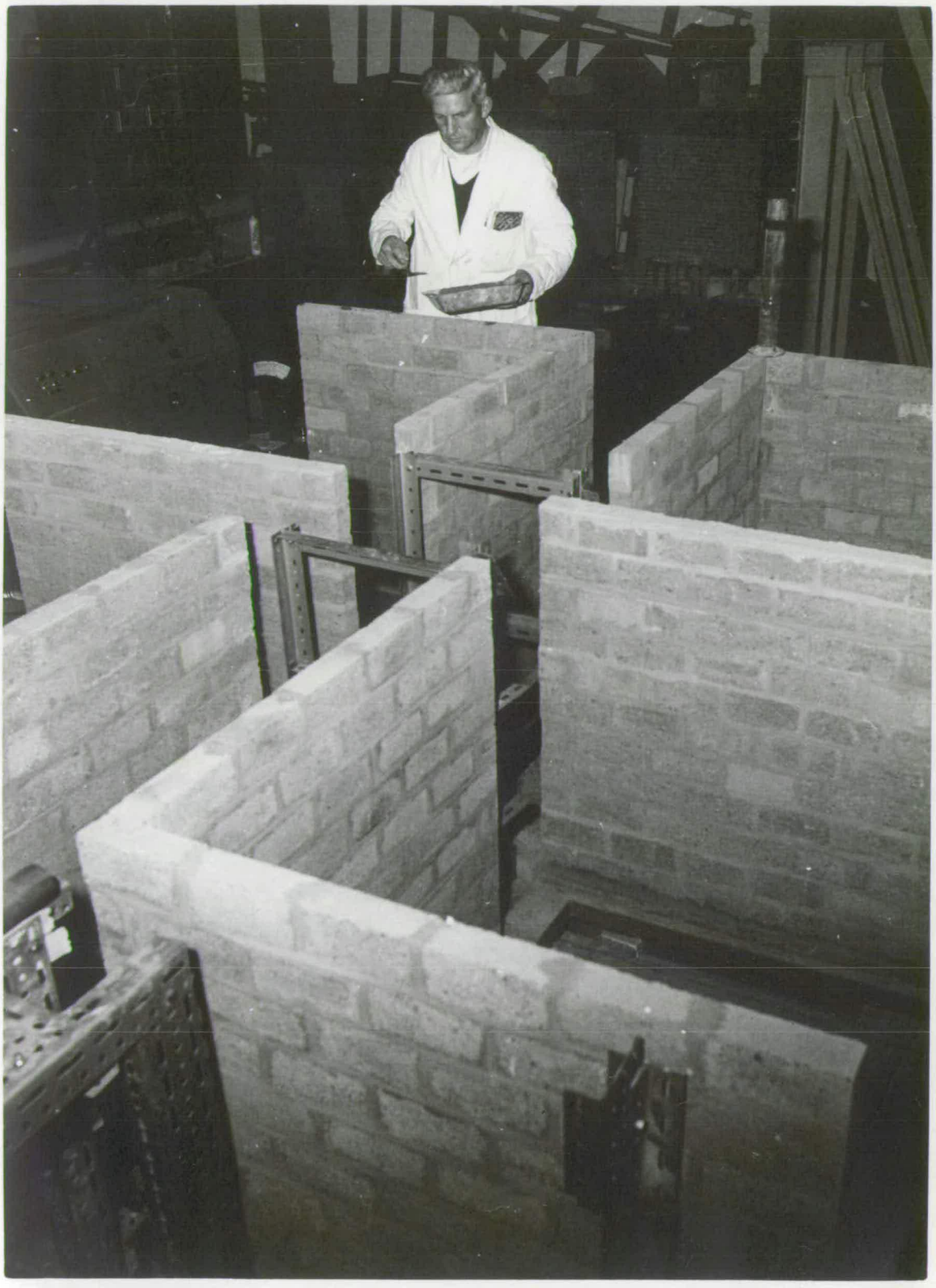

PLATE(3.2) IN SITU CONSTRUCTION OF SHEAR WALLS

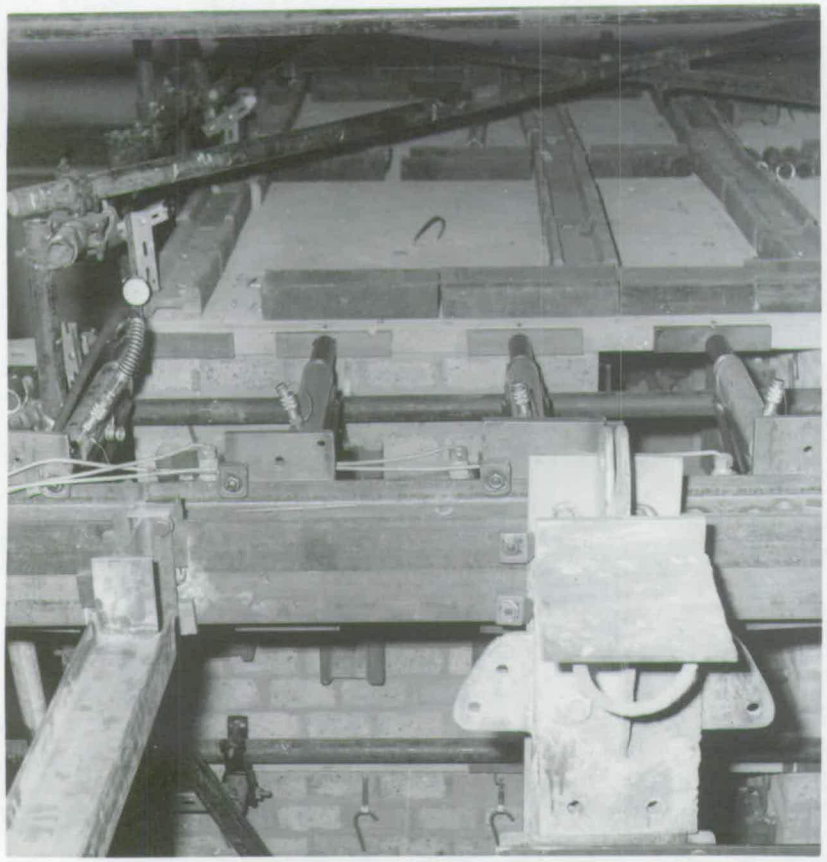

(3.3a)

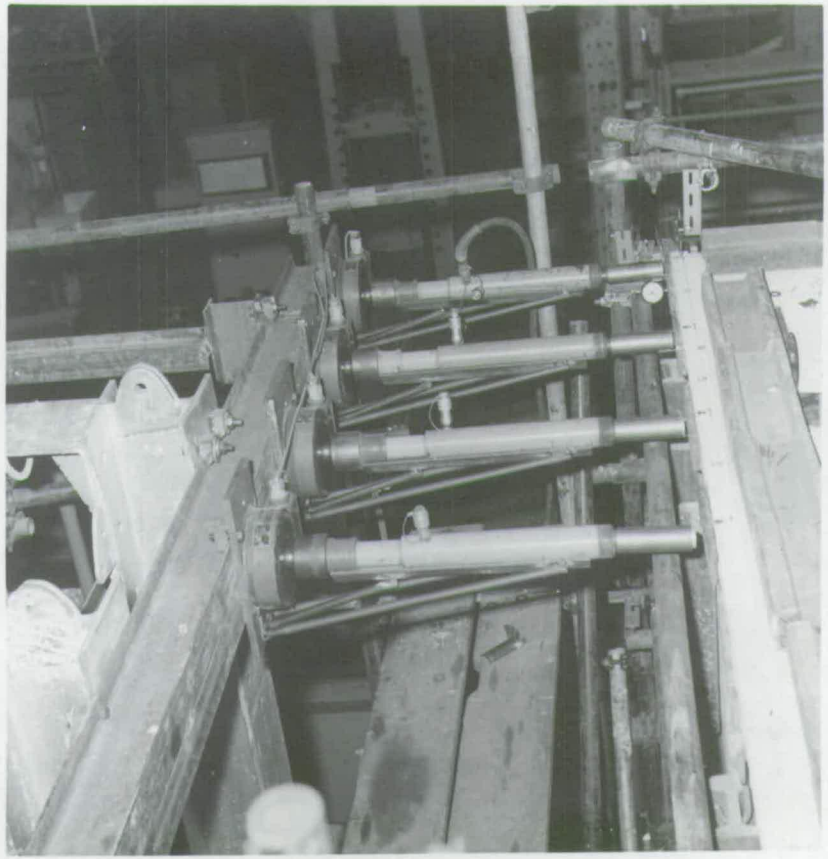

(3.3b)

PLATES (3.3a) AND (3.3b) SHOWING HYDRAULIC JACKS AND LOADING ARRANGEMENTS

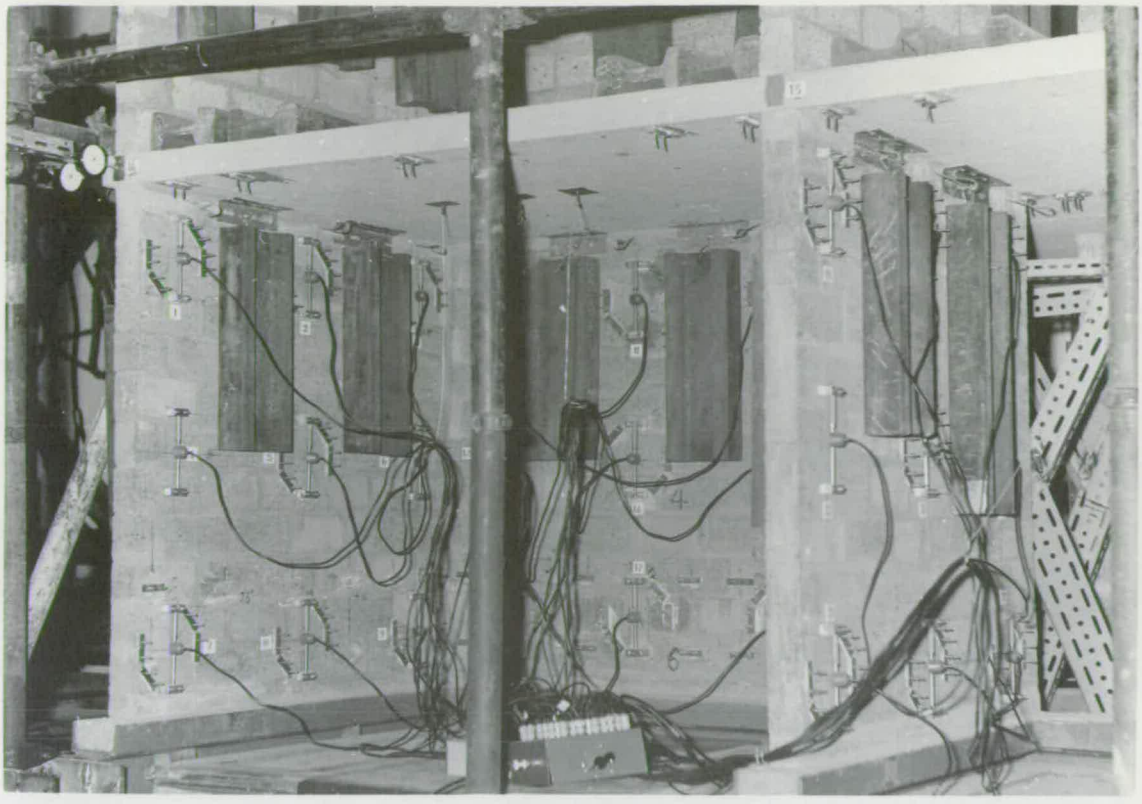

(3.4a)

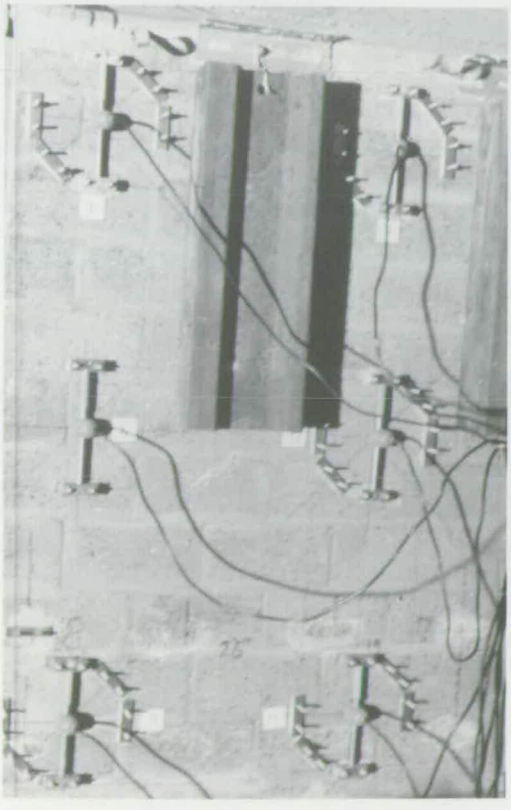

(3.4b)

PLATES (3.4a) AND (3.4b) SHOWING VIBRATING WIRE GAUGES FOR MEASURING THE PRINCIPAL STRAINS IN THE SHEAR AND CROSS WALLS

2 - MATERIALS

A - BLOCKS

One-third scale "Aglite" blocks measuring (152.4 x 76.2 x 50.8)mm were used for the walls. The blocks came from two different batches with mean crushing strengths of 9900 kN/m^2 and 13016 kN/m^2 according to BS 2028 [4] and the mean density was 1138.9 kg/m^3.

B - SAND

Locally available building sand was used for blockwork construction. The sand conformed with the limits of B.S. 1198 (1963) [5] and its grading is given in the table below.

Table 3.1 Sieve analysis of ordinary sand used in construction of building and beams.

B.S. Sieve No:	% passing by weight	% retained
3.18 mm	98.5	1.5
2.14 mm	98.0	0.5
1.20 mm	96.7	1.3
600 microns	92.9	3.8
300 microns	63.4	9.5
150 microns	17.4	46.1

B.S. 1198

C - CEMENT

"Ferrocrete" a rapid hardening Portland Cement was used to conform with B.S. 12 (1971) [6].

D - LIME

Hydrated lime class "A" was used to conform with B.S. 890 (1972) (7).

E - MORTAR

The mortar was Cement, Lime and Sand in of $1:\frac{1}{4}:3$ by volume. After conversion, all proportioning was done by weight B.S. 12 (1971) [6].

3 - CONSTRUCTIONAL DETAILS

The structure has five storeys, each consisting of four equal angle sections and two single cross sections, all having the same dimensions as showing in figure (3.3) plate (3.2) shows a photograph, and figure (3.1) (3.2) and (2.1), (3.2), (3.3) and (3.4) show the isometric view, front and side elevations and plan of the model structure.

The foundations of the structure consisted of (6.4 x 6.4) cm steel I sections welded to a steel base grillage (43.5 x 16.1) cm. The bottom course of the building was embedded in concrete in (6.4 x 3.2) cm steel channels which in turn was welded to the I sections. Additionally a steel plate was welded, one each side of the structure, between the top of the I section and the grill in an attempt to stop rotation at the base of the structure during the lateral loading.

All walls were constructed in situ by technicians, see plate (3.2) and after a curing period the floor slabs were lifted by crane on to mortar beds, then settled by tapping with hammer. The mortar joint was keyed in by a pointing tool. Each floor slab was precast in

reinforced concrete mix in the ratio of 1:1:2 by weight and was reinforced by a mesh of 1/8" (3.2 mm) diameter steel.

4 - SIMULATION OF DEAD LOAD STRESSES

It was necessary to increase the dead weight stresses by a factor of two to simulate the effect of gravity as the structure was of one-third scale. Weights were hung from hooks on the walls and placed on the floor slabs. See plates (3.1) to (3.5). The estimated precompressions were (345, 276, 207, 138, 69) kN/m^2 at the 1st, 2nd, 3rd, 4th, 5th floors respectively.

5 - TESTING EQUIPMENT

A - Loading Frame

A portal frame of two steel columns (203.2 mm x 203.2 mm x 15.9 kg) war bolted to the base grillage and secured in posi-tion by jointing with four I beam cross braces (152.4 mm x 114.3 mm x 9.2 kg) to a previously built compression rig.

B - Load Measuring Apparatus

The load was applied at various points on the top slab level by a three ton hydraulic jack, pumped by a "Losenhausen" testing machine. Before loading, the apparatus was calibrated in an "Avery Universal" testing machine and the calibration curves are shown in figure (3.31). The applied load was taken from a previously calibrated digital voltmeter, "Solatron type LM 1450" to an accuracy of about + 0.05%

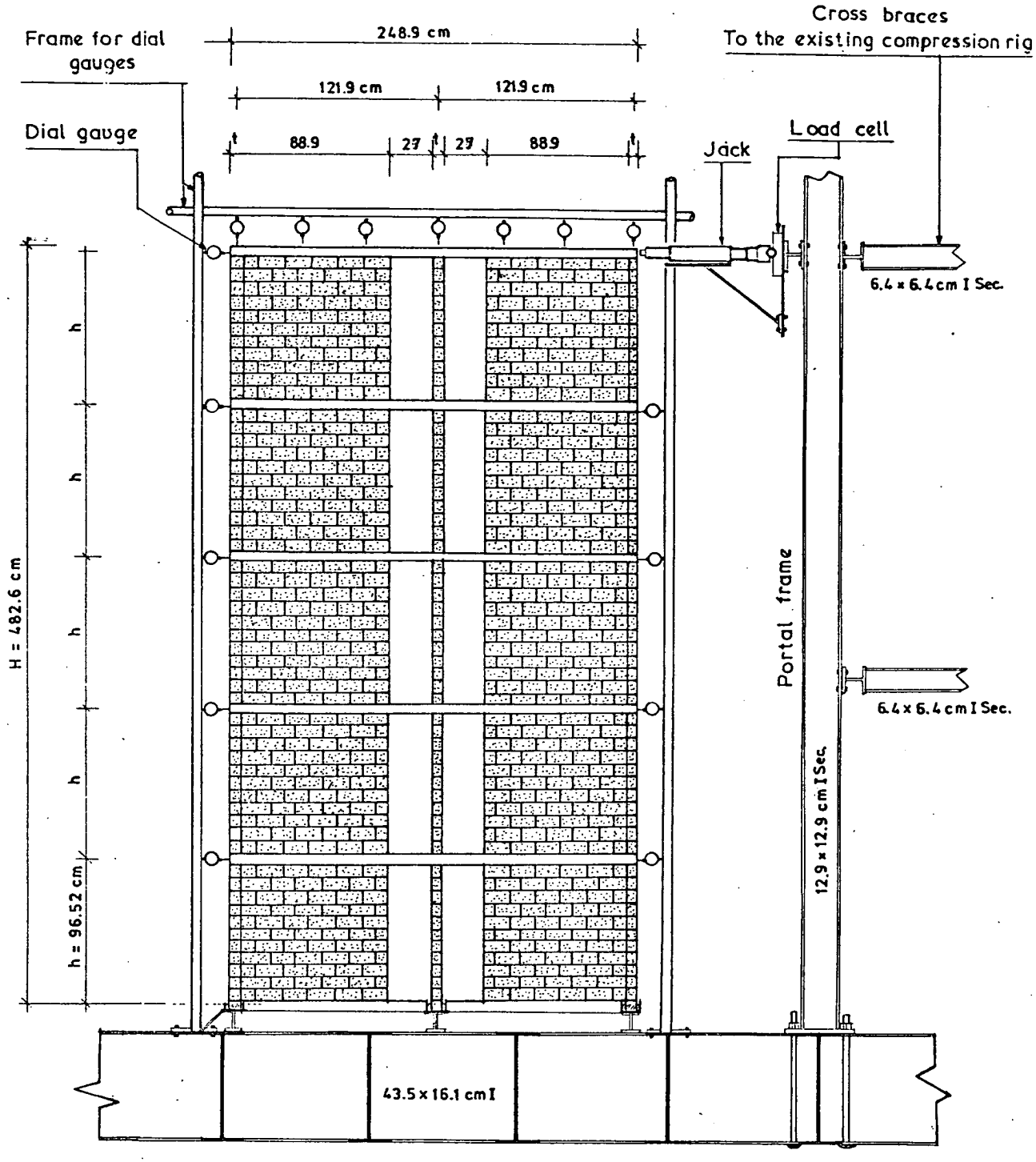

FIG 3.1 FRONT ELEVATION OF THE MODEL STRUCTURE SHOWING LOADING AND DIAL GAUGE FRAMES

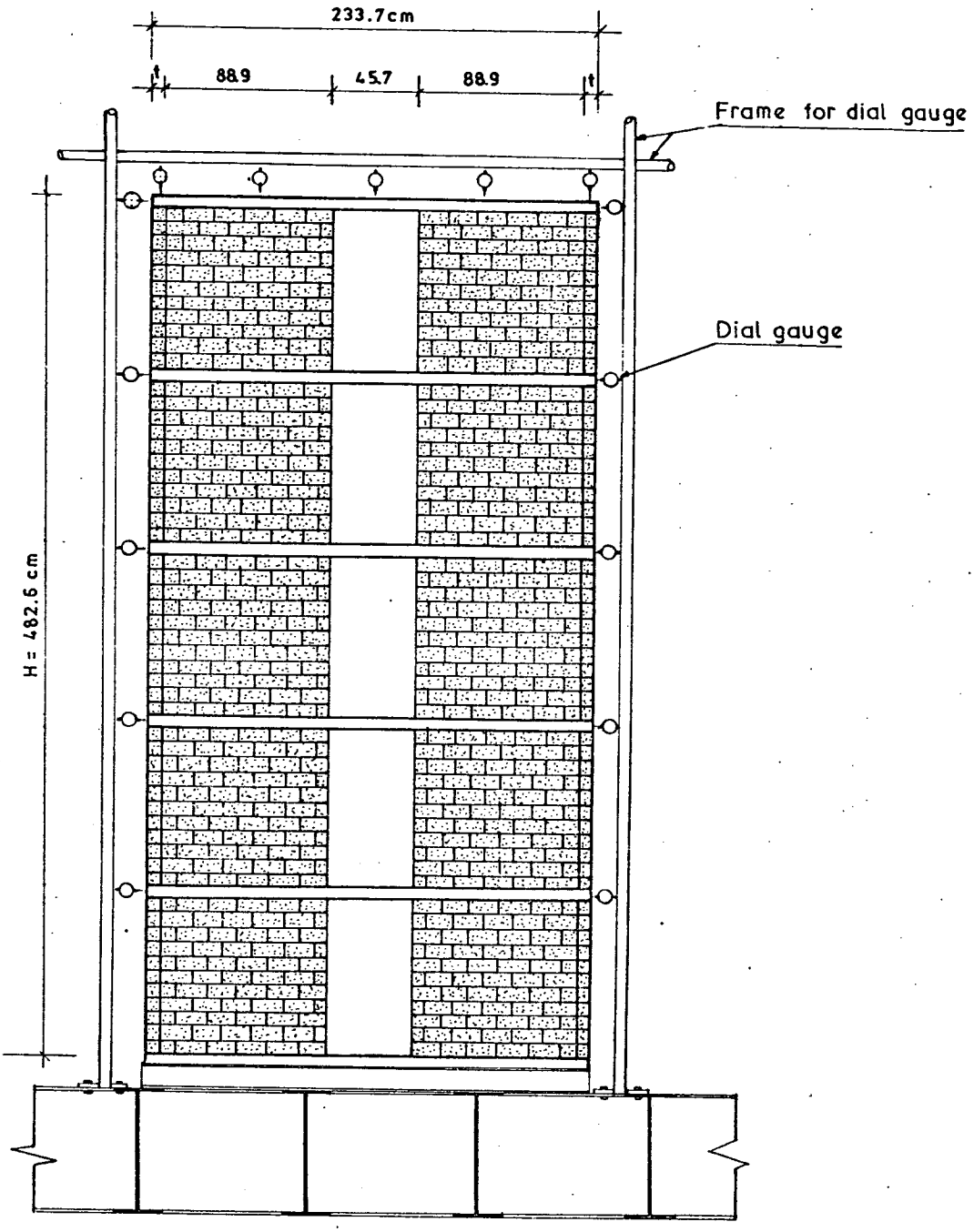

FIG 3,2 SIDE ELEVATION OF THE MODEL STRUCTURE

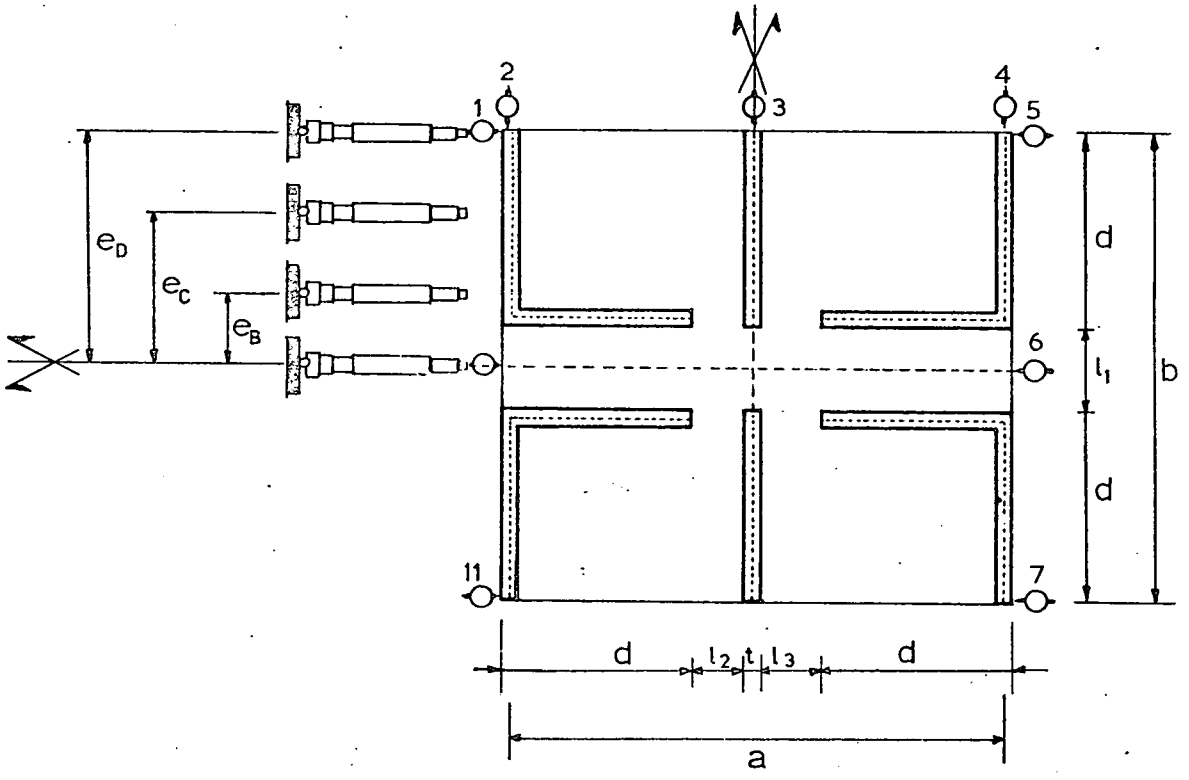

FIG 3.3 PLAN AND DETAILS OF THE LOADING ARRANGEMENT AND DIAL GAUGES POSITION

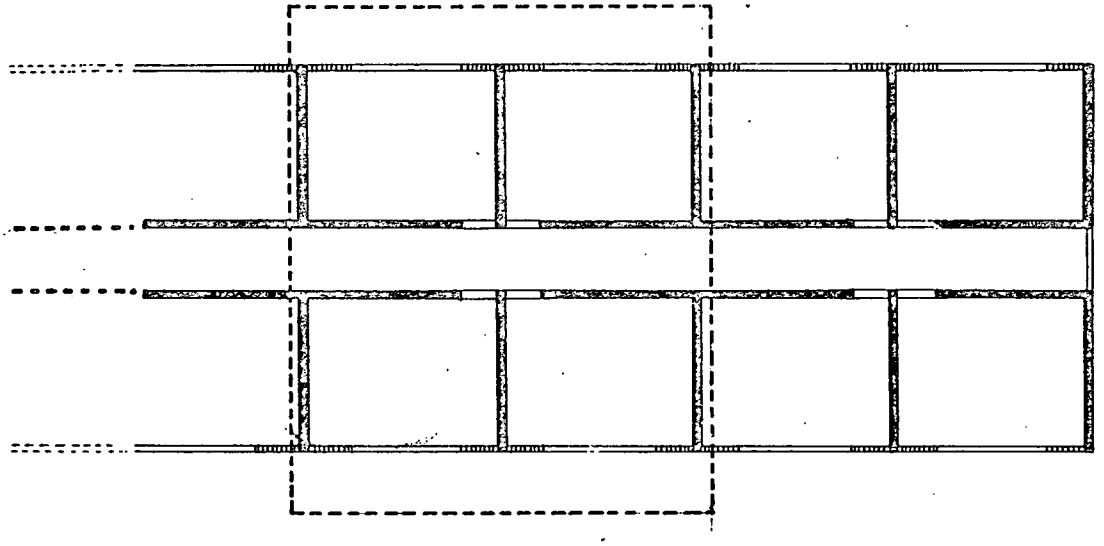

FIG 3.4 TYPICAL FLOOR PLAN

C - Dial Gauge Frame

The dial gauge frame was a system of scaffolding. The vertical poles were bolted to the foundation grillage and horizontal and diagonal members made the whole system stiff and rigid. Care was taken to ensure that the frame did not come in contact with the structure and loading frame.

D - Dial Gauges

Dial gauges, with a range of 0.01 mm, were bolted by "Dexion" scotted steel angle sections to their frame. The horizontal deflections X and Y directions were measured by gauges positioned near the corners (232 cm) apart on the side wall and (247 cm) apart on the front wall and in the middle of the walls, at all slab levels and the vertical deformation was measured by gauges positioned at the top of the building as shown in plates and figures (3.5) and (3.2), (3.3) and (3.4). A total of fifty gauges were fitted on the frame.

E - Strain Gauges

For measuring the strain distribution in the shear and cross walls, vibrating wire strain gauges were used. The strain gauges were of (5.5 in) 14 cm gauge length and the strain range measuring capacity of about 3000 microstrain. The strains were recoreded using a portable digital unit type GT 1169 and a 100 channel data logger type GT 1172, shown in plate (3.7).

6 - SOURCES OF EXPERIMENTAL ERROR

Measurement of deflection	±	0.01 mm
Measurement of load	±	0.05 kN
Measurement of strain	±	3 microstrains

When the lateral load is applied the structure will tend to overturn. The base of the structure rotated under the applied loading. Therefore, a large part of the error is coming from incomplete fixity of foundations.

7 - EXPERIMENTAL TECHNIQUES AND RESULTS

The dial gauges were bolted to the frame and lined up against the metal contact plates on the walls and slabs. Care was taken to ensure each gauge was plumbed to the wall and slabs. For positioning of the strain gauges, a metal plate was fixed by "Cataloy" to the wall and the gauge securely screwed to the plate. After all the gauges were checked, and the pre-loading gauge reading recorded, loading was commenced.

The first set of tests was carried out during the day, but when the results were plotted, the line did not pass through the origin and the curve was very irregular. It was decided that the sources of error were from the vibrations caused by the movement of the other workers and from temperature fluctuations at the top of the building, caused by the sunlight coming through the translucent roof. Therefore, all future tests and the tests presented, were carried out in the evening and at night. The time lapse between loading and reading the

gauges was between 5 to 8 minutes, to allow the building to stabilise. There was a further 5 to 8 minute time lapse before the gauges were read after the load was removed. The dial gauges were read by theodolite and always in the same order, to reduce the reading error. Each load test was repeated between 12 to 24 times.

a) Test - 1 Axial Loading

Forces of 1.0 to 5.0 kN were applied axially to the structure. No rotation occurred and the plots of load against deflection and storey against deflection are shown in Figures (3.5) and (3.6). The vertical strain distribution in the first floor shear walls, flanges and centre wall at cross section A-A was calculated and plotted in Figure (4.9a). The magnitude and direction of the principal strains in the ground floor shear and cross walls were calculated [Appendix 3] from test results, and are shown in Figure (4.6)(4.9).

b) Test - 2 Eccentric Loading e_B = 38.1 cm (15")

Forces of 0.75 to 4.53 kN were applied eccentrically to the structure. The plots of load against deflection and storey against deflection for individual dial gauges are shown in Figures (3.7 to 3.11). The load against rotation and storey against rotation data calculated from side and front readings are plotted in Figures (3.12) and (3.13). The strains in the first floor at section A-A are plotted in Figure (4.9). The magnitude and direction of the principal strain in the ground floor shear walls, flanges and central cross wall were calculated (Appendix 3) from test results and are shown in Figure (4.8).

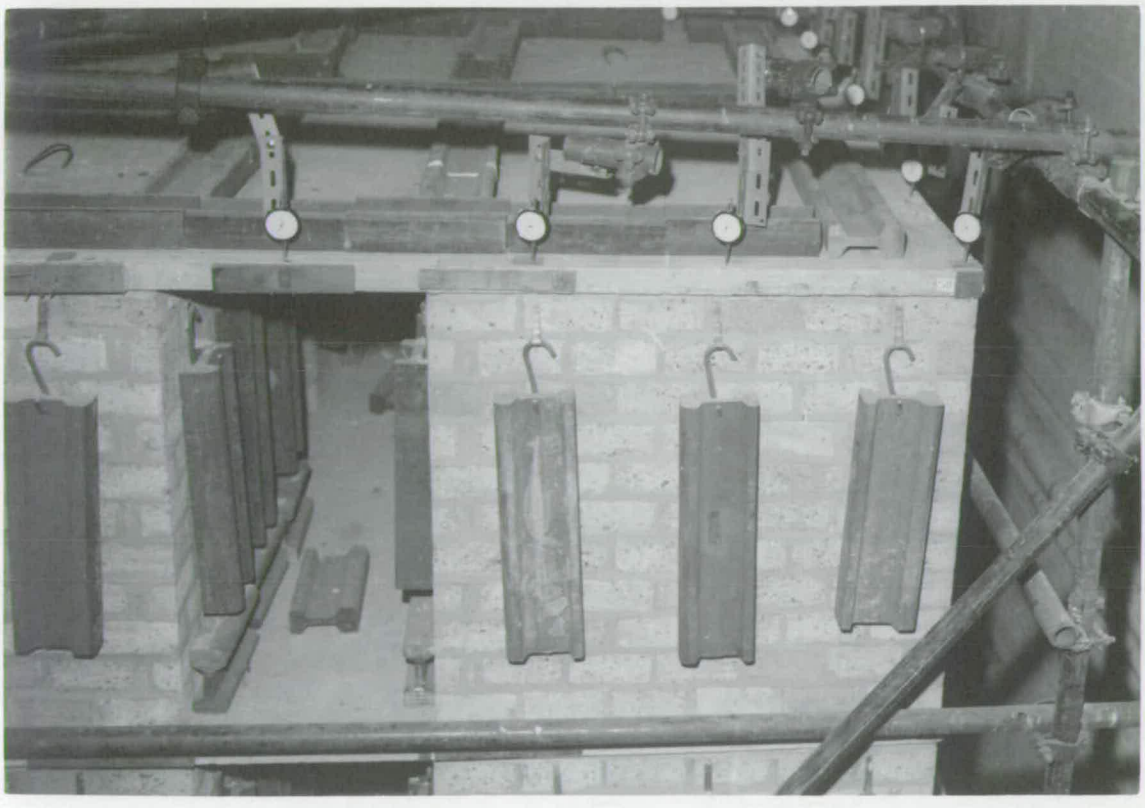

PLATE (3.5) DIAL GAUGES FOR MEASURING VERTICAL DEFLECTION OF THE BUILDING

c) Test - 3 Eccentric Loading e_C = 76.2 cm (30")

Forces of 0.58 to 3.08 kN were applied eccentrically to the structure. The plots of load against deflection and storey against deflection for individual dial gauges are shown in Figures (3.14 to 3.17). The load against rotation and storey against rotation data calculated from side and front reading are plotted in Figures (3.18) and (3.19).

d) Test - 4 Eccentric Loading e_D = 116.8 cm (46")

Finally forces of 0.38 to 2.88 kN were applied eccentrically to the structure. Plots of load against deflection and storey against deflection for individual dial gauges are shown in Figures (3.20 to 3.26). The load against rotation and storey against rotation data, calculated from side and front readings are also plotted in Figures (3.27 to 3.30).

The vertical deformation under the various loading measured in the Y-Y direction at the top of the structure, are plotted in the figure below.

In all the above tests, the experimental data presented was the average values from between 12 to 24 separate testings.

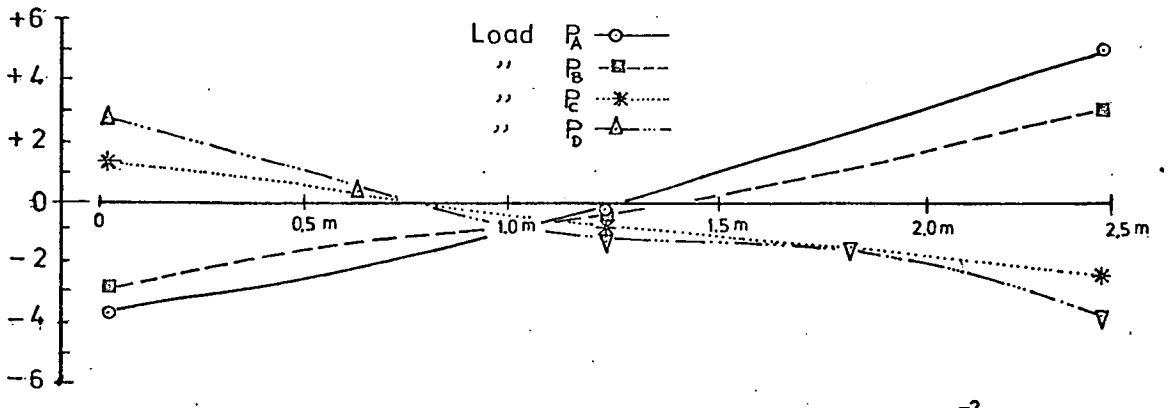

Distortions top slab of the structure Def. [mmx 10^{-2}]

$P_{A,B,C,D.}$ = 3.0 kN

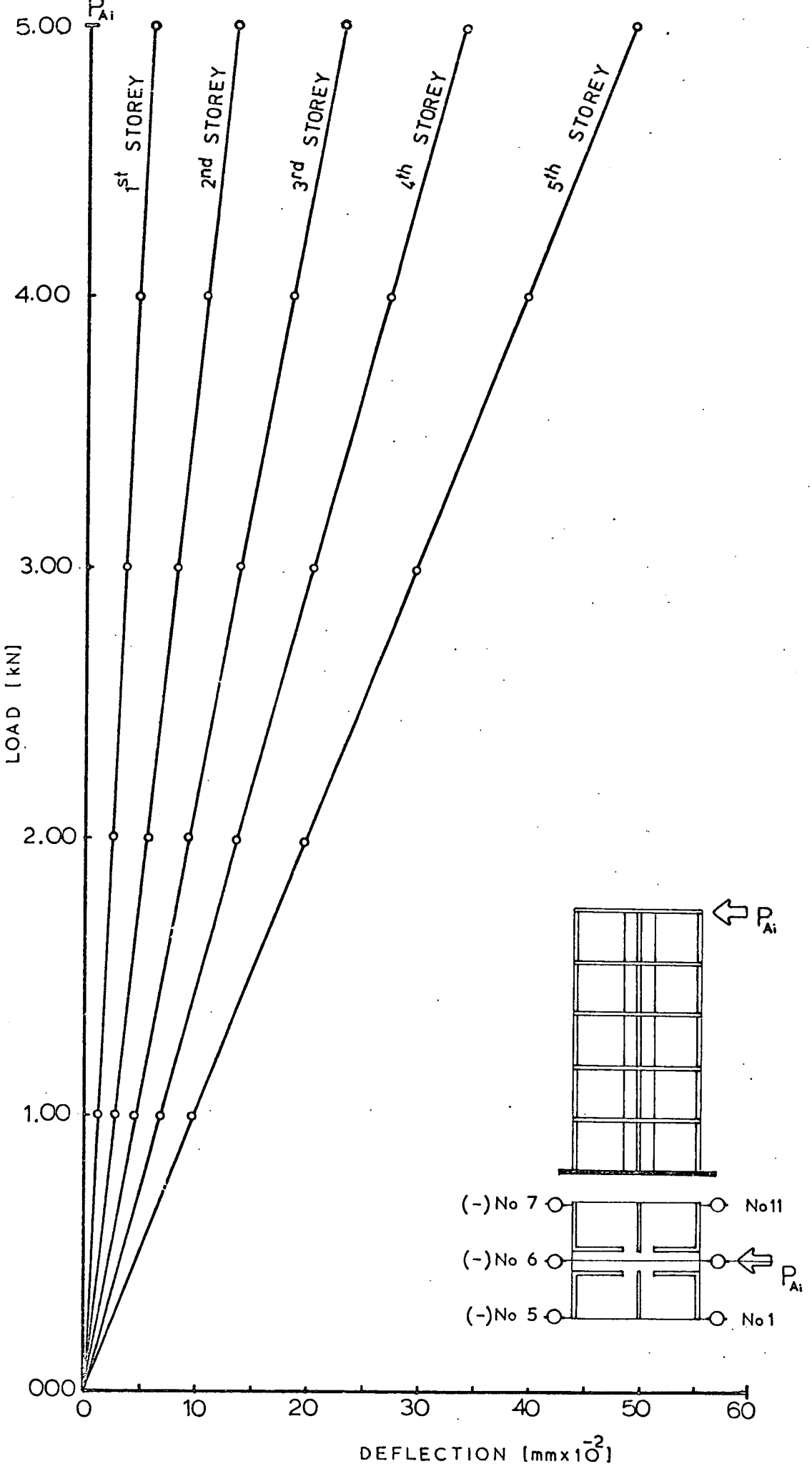

Fig. 3.5 Load/Deflection curves for structure from dial gauges position No. 1,5,6,7,11 at various floor levels (y-Direction)

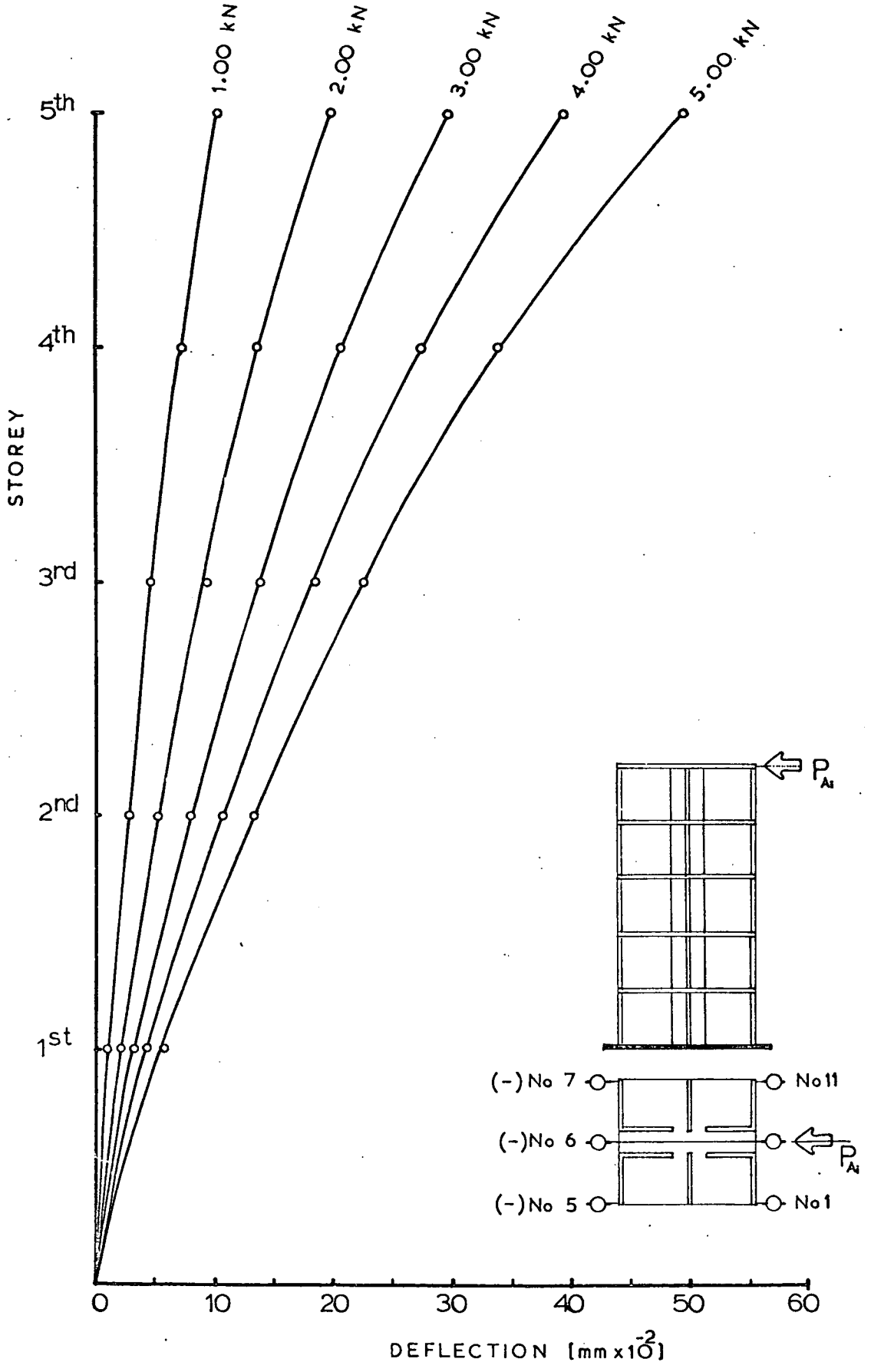

Fig. 3.6 Storey / Deflection curves for structure from dial gauges position No. 1.5.6.7.11 at various loadings (Y - Direction)

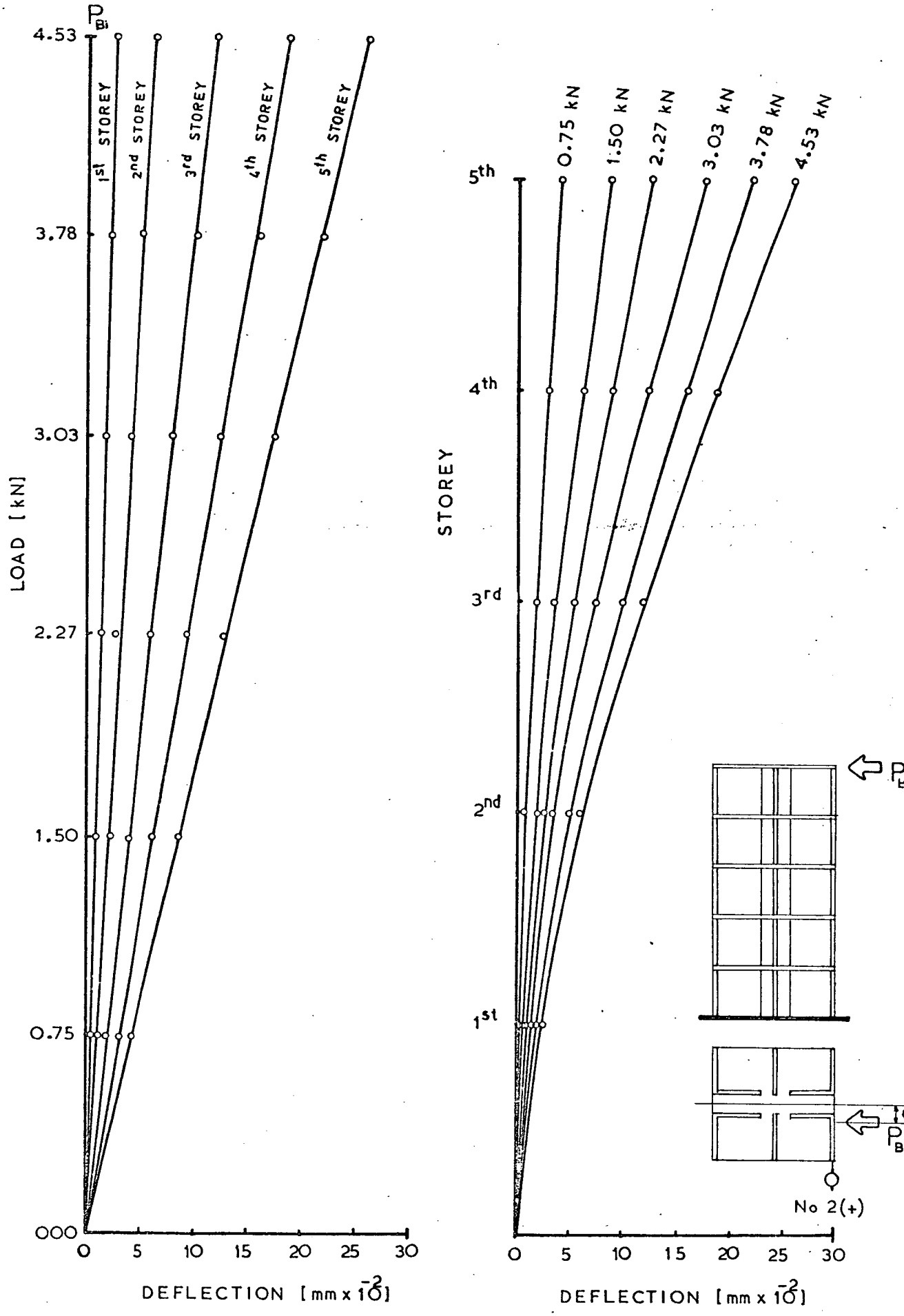

Fig. 3.7 Load/Deflection and Storey/Deflection curves for structure from dial gauge position No.2 at various floor levels and loadings respectively. (X-Direction)

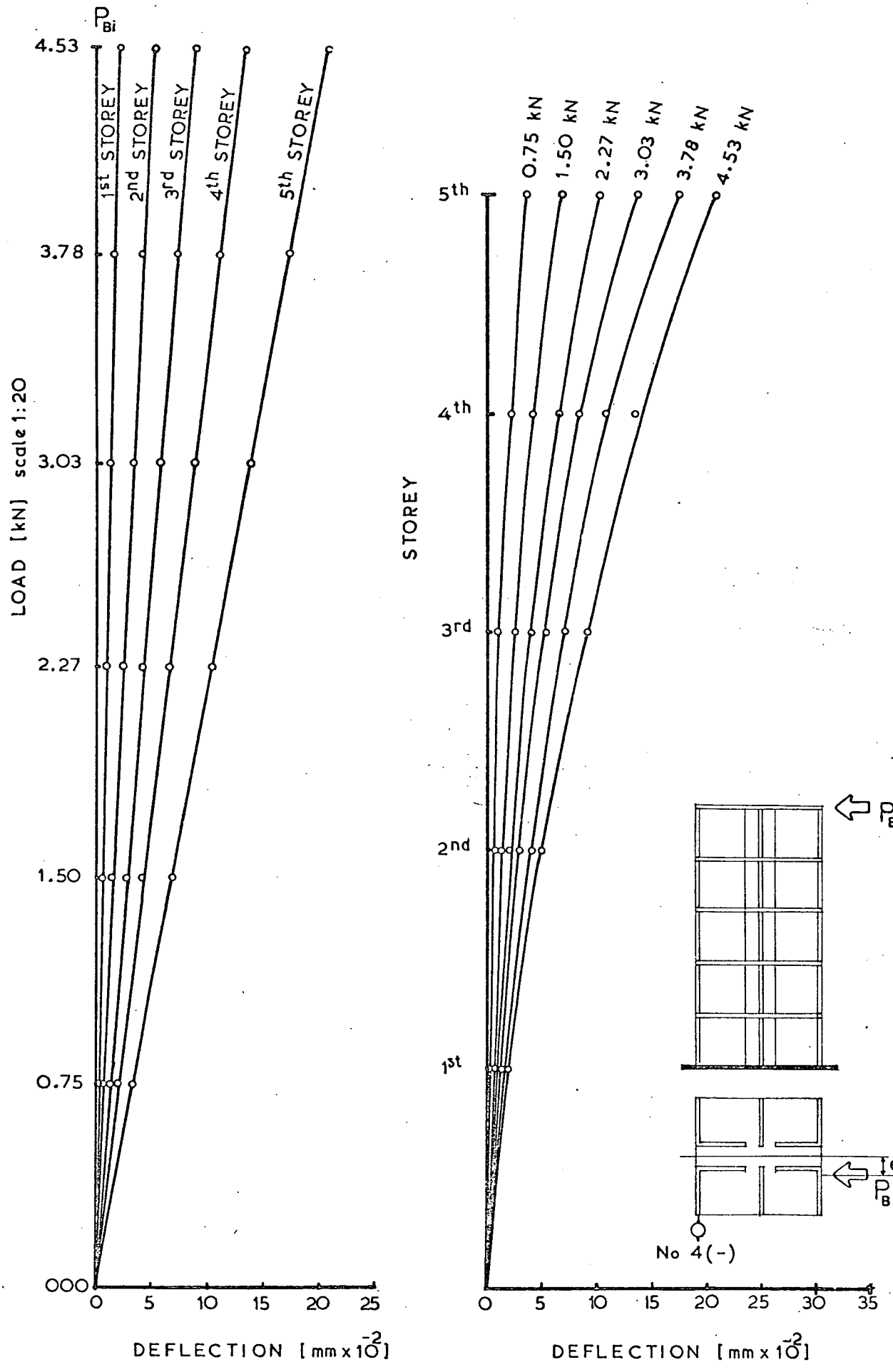

Fig.3.8 Load/Deflection and Storey/Deflection curves for structure from dial gauge position No.4 at various floor levels and loadings respectively (X-Direction)

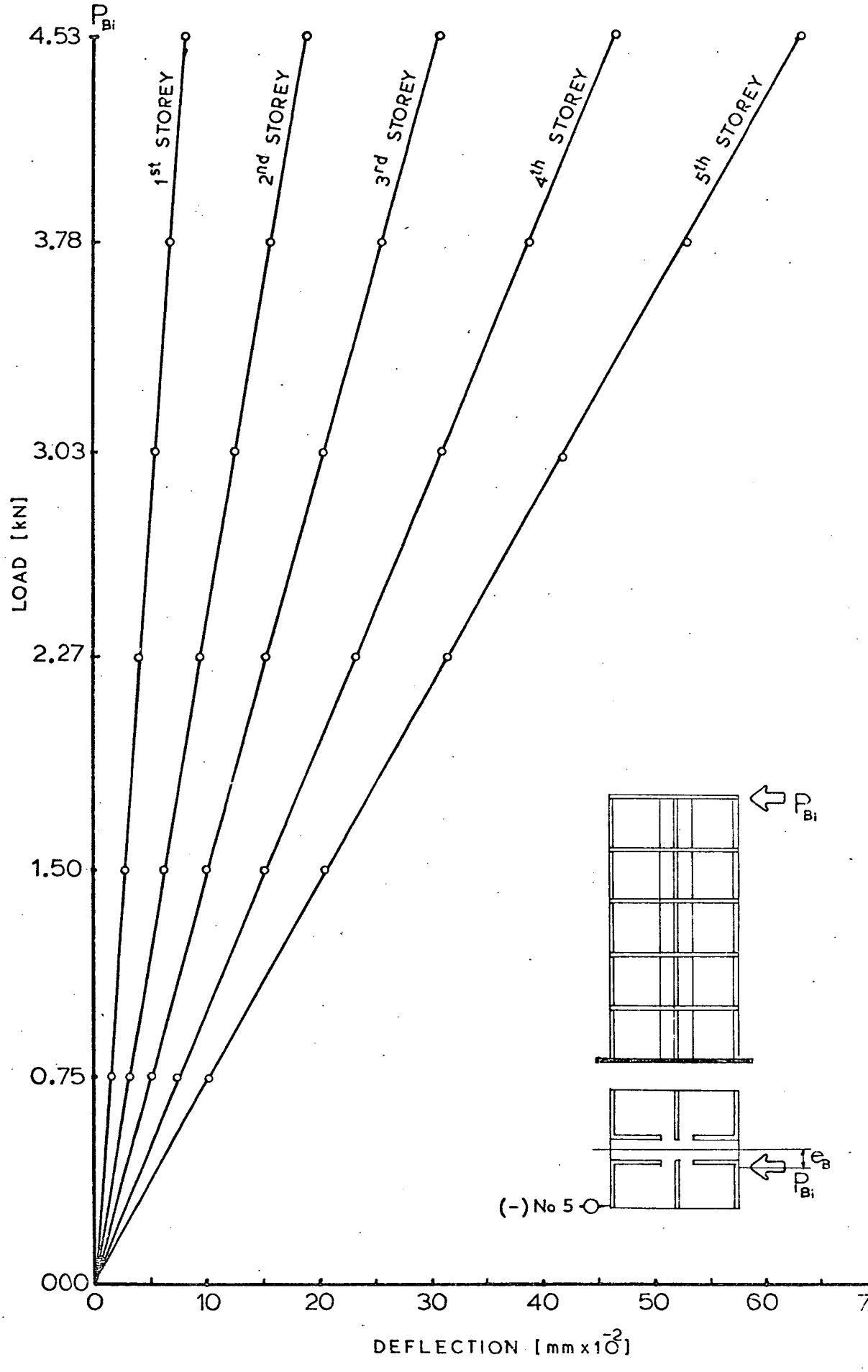

Fig. 3.9 Load/Deflection curves for structure from dial gauge position No. 5 at various floor levels (Y- Direction)

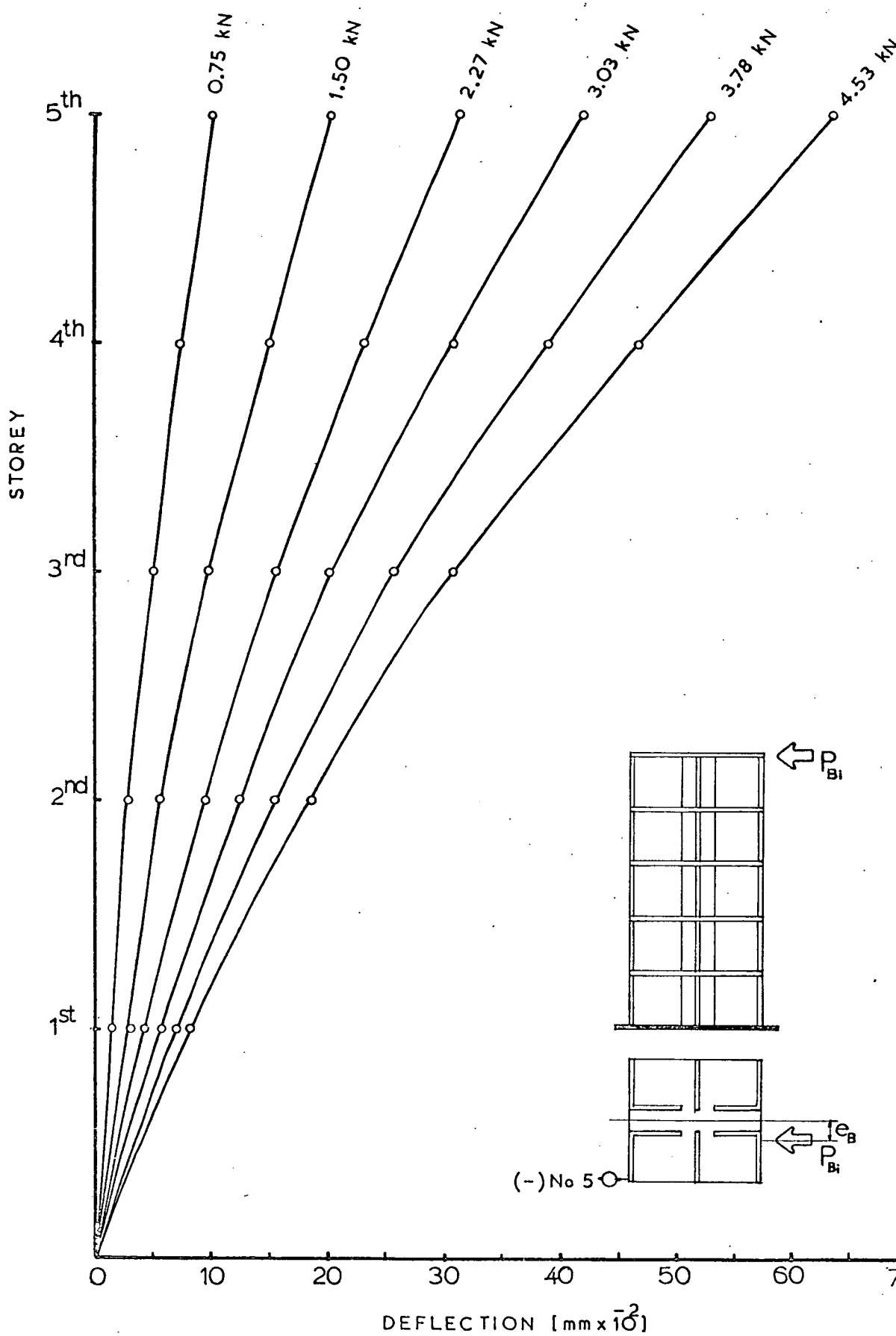

Fig.3.10 Storey/Deflection curves for structure from dial gauge position No.5 at various loadings (Y-Direction)

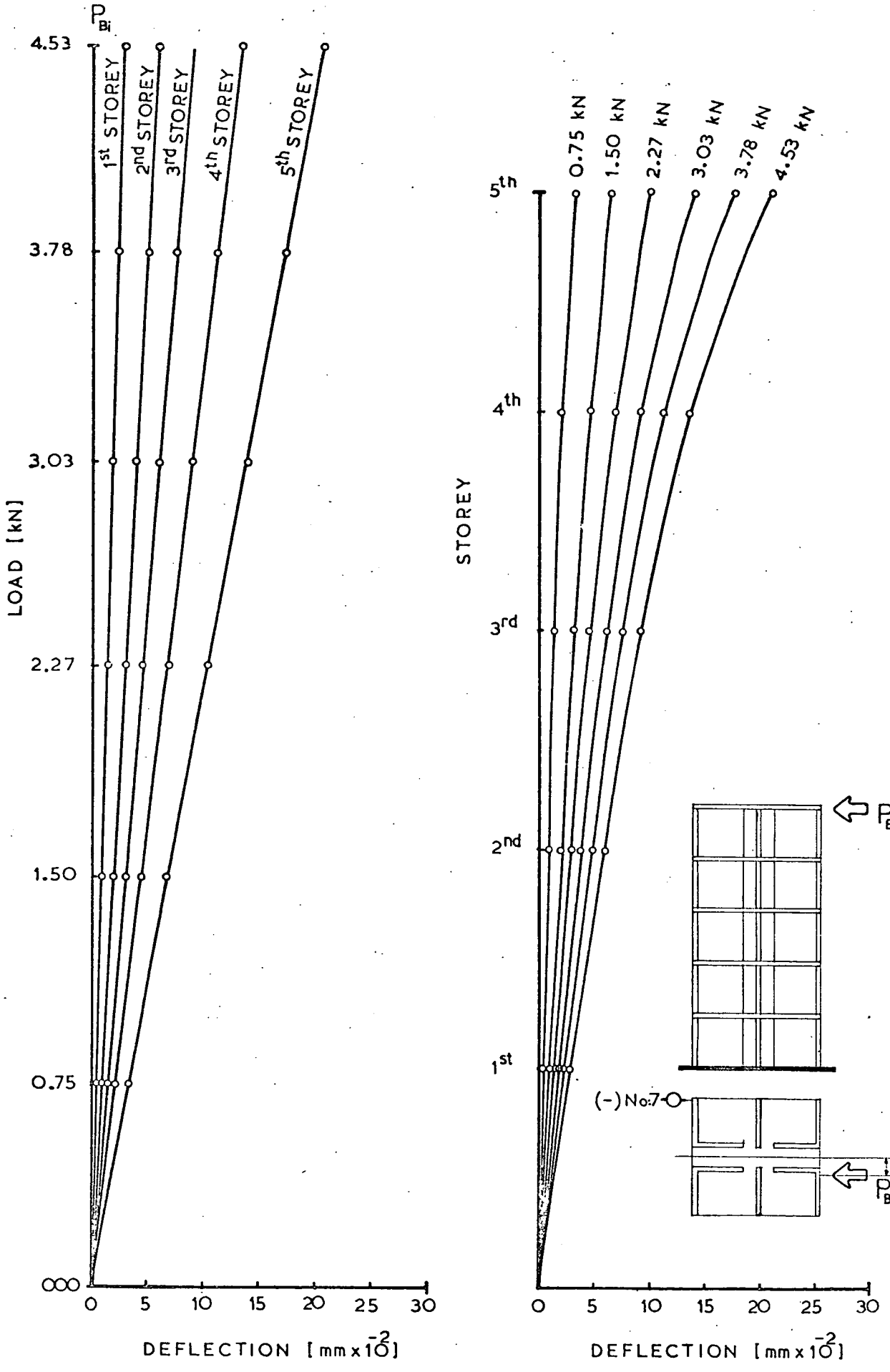

Fig.3.11 Load / Deflection and Storey / Deflection curves for structure from dial gauge position No. 7 at various floor levels and loadings respectively. (Y-Direction)

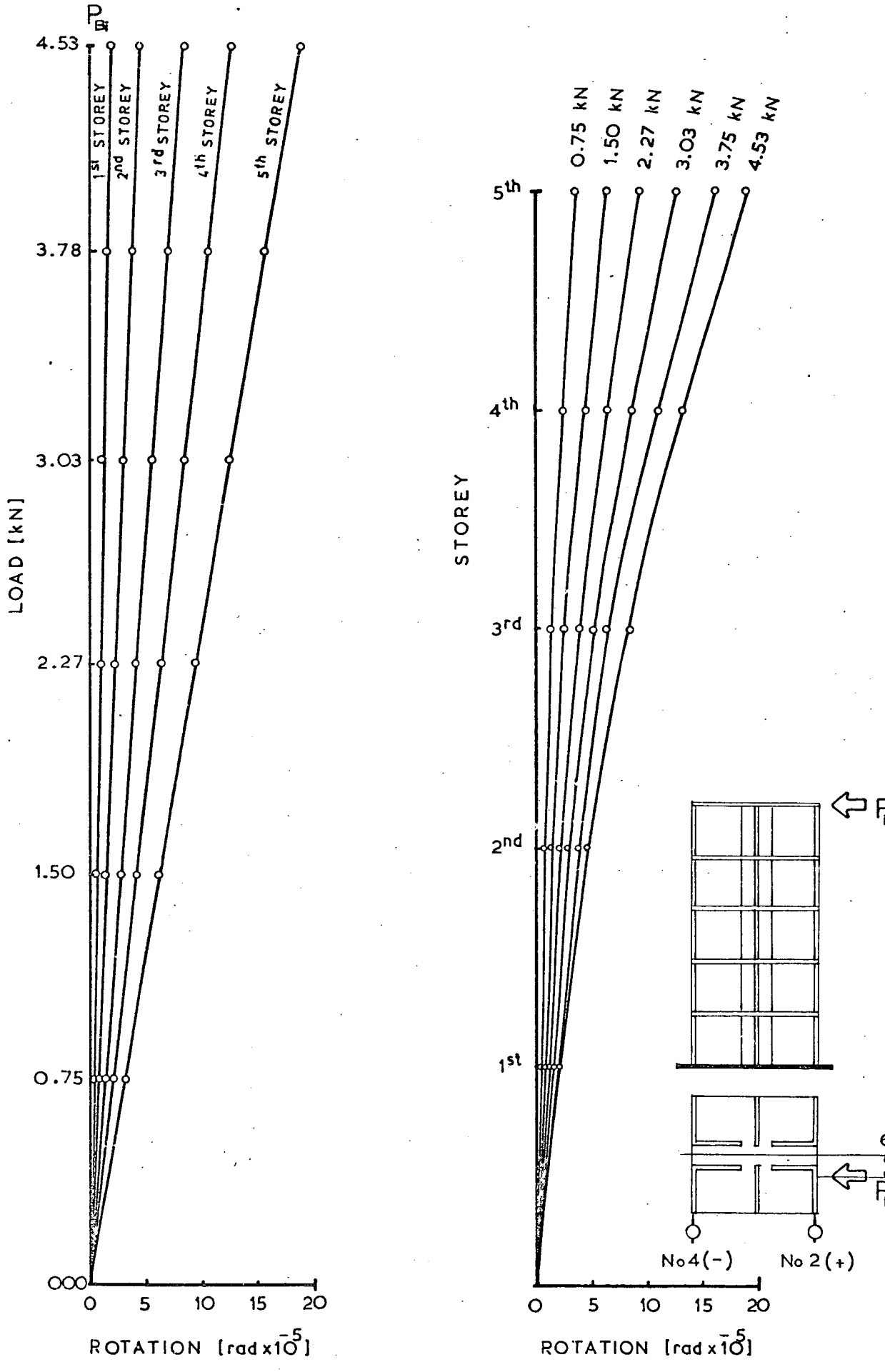

Fig. 3.12 Load/Rotation and Storey/Rotation curves for structure from dial gauges position No. 4-2 at various floor and loadings respectively. (X-Direction)

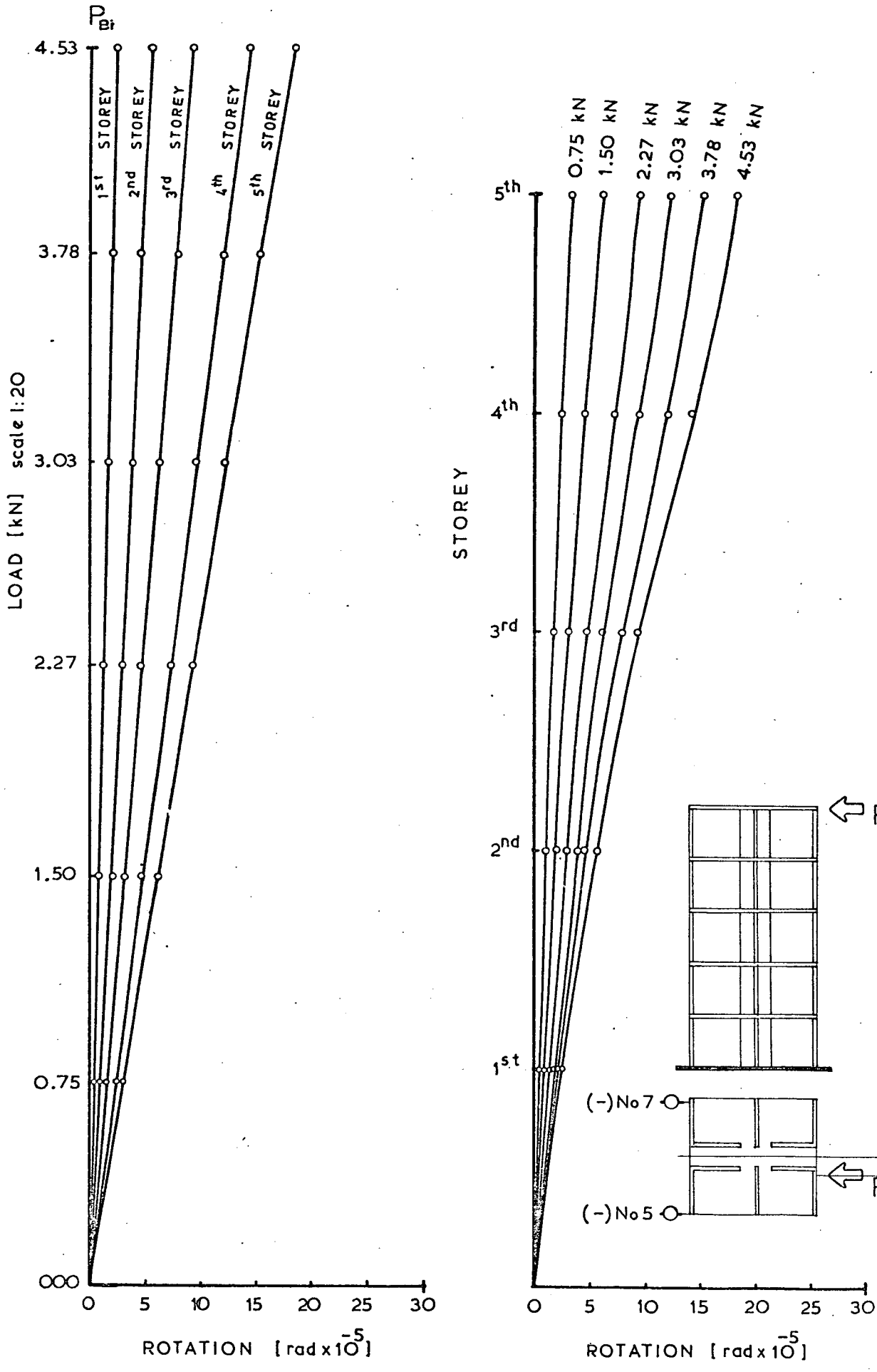

Fig 3.13 Load/Rotation and Storey/Rotation curves for structure from dial gauges position No. 5.7 at various floor and loadings respectively.

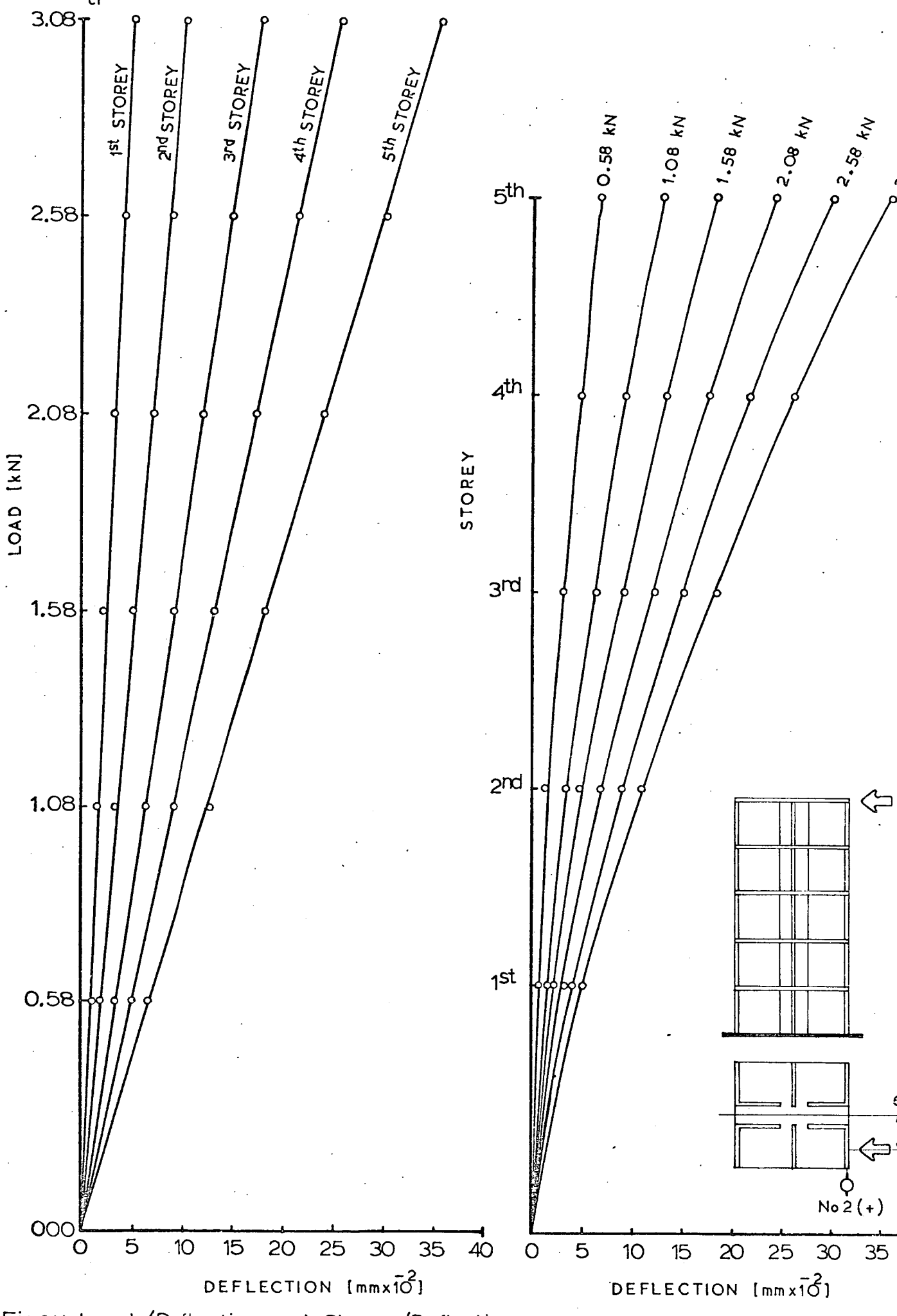

Fig.3.14 Load /Deflection and Storey/Deflection curves for structure from dial gauge position No. 2 at various floor and loadings respectively.

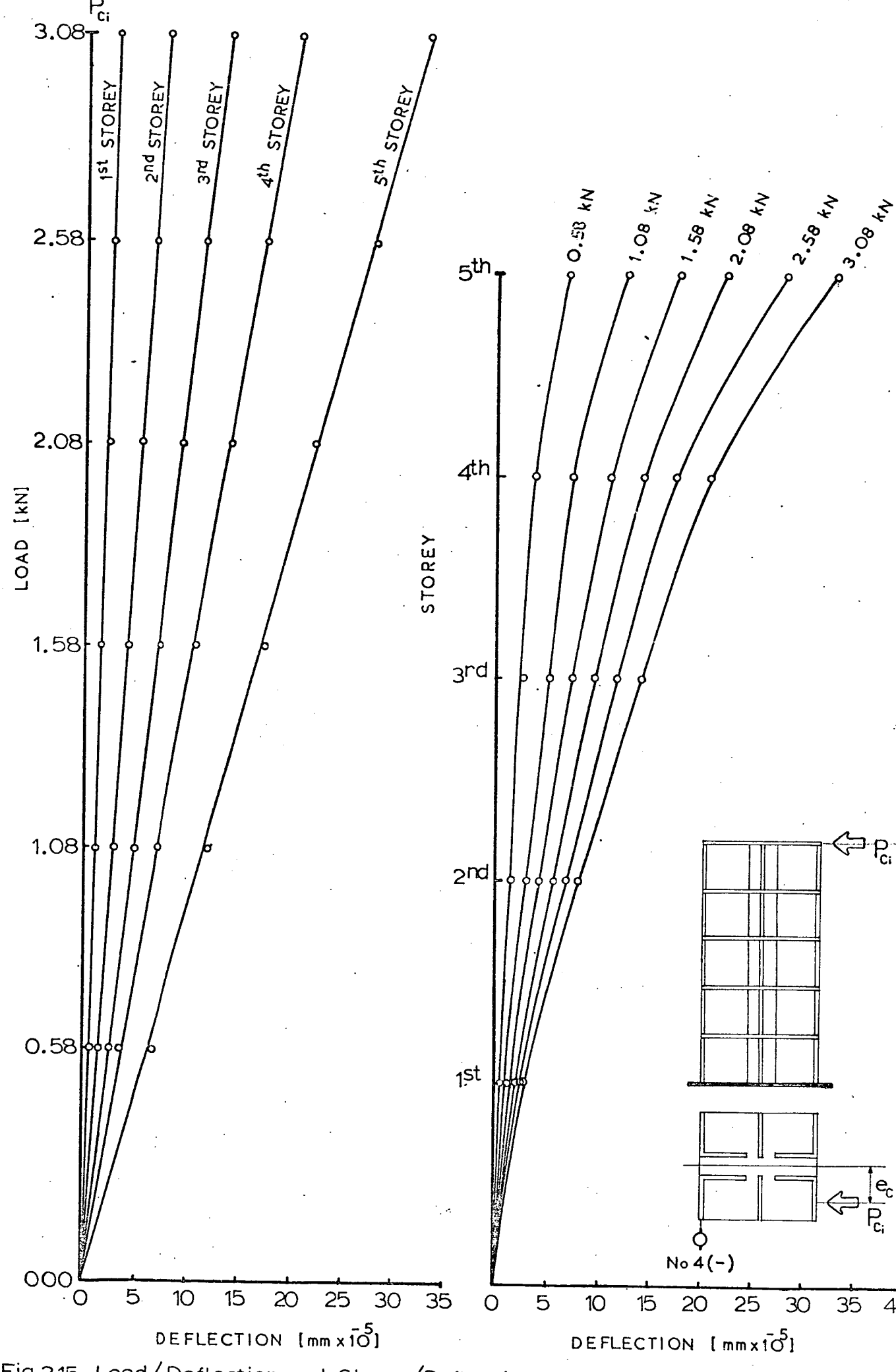

Fig. 3.15 Load/Deflection and Storey/Deflection curves for structure from dial gauge position No. 4 at various floor levels and loadings respectively.

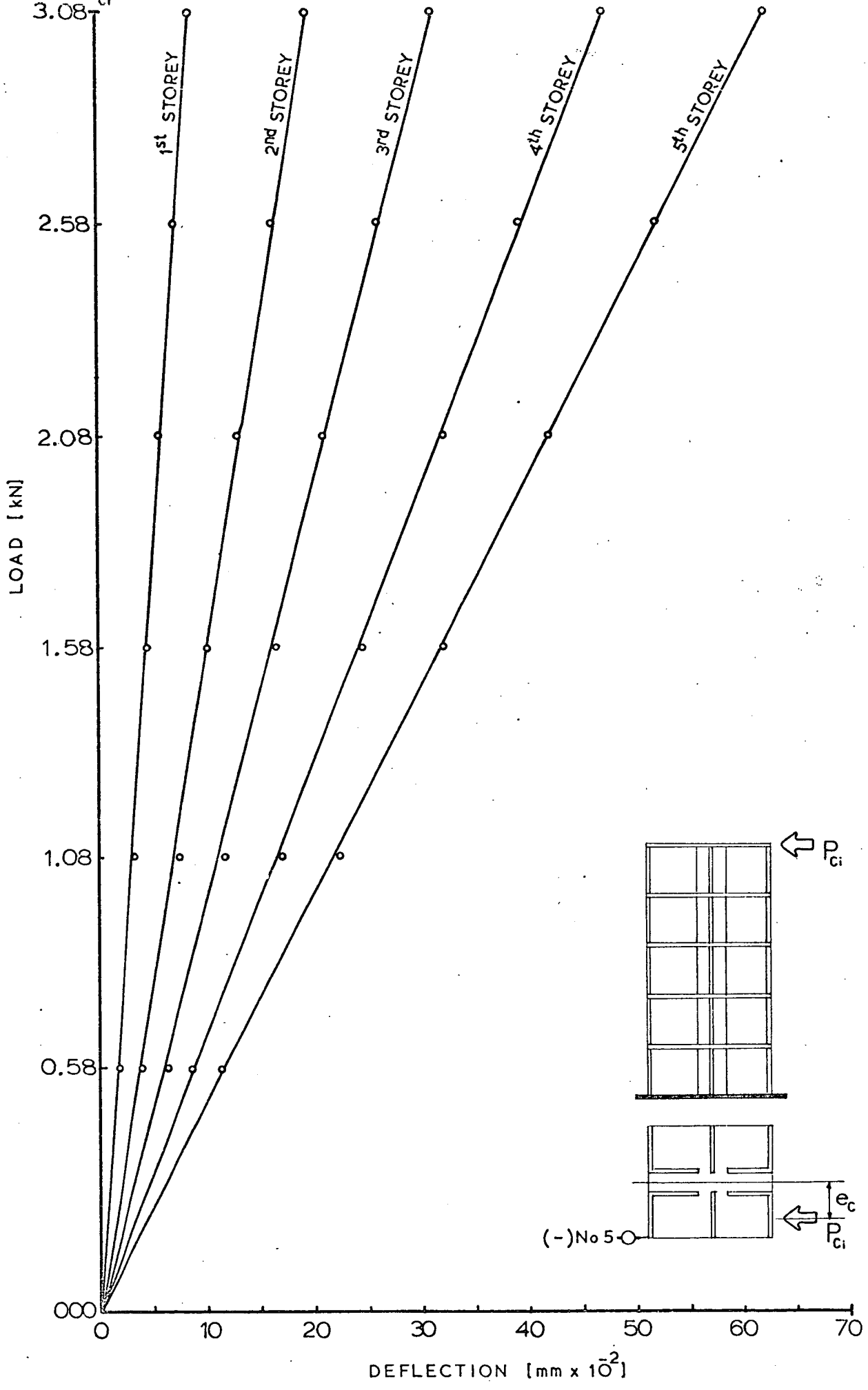

Fig.3.16 Load/Deflection curves for structure from dial gauge position No. 5 at various floor levels. (X-Direction)

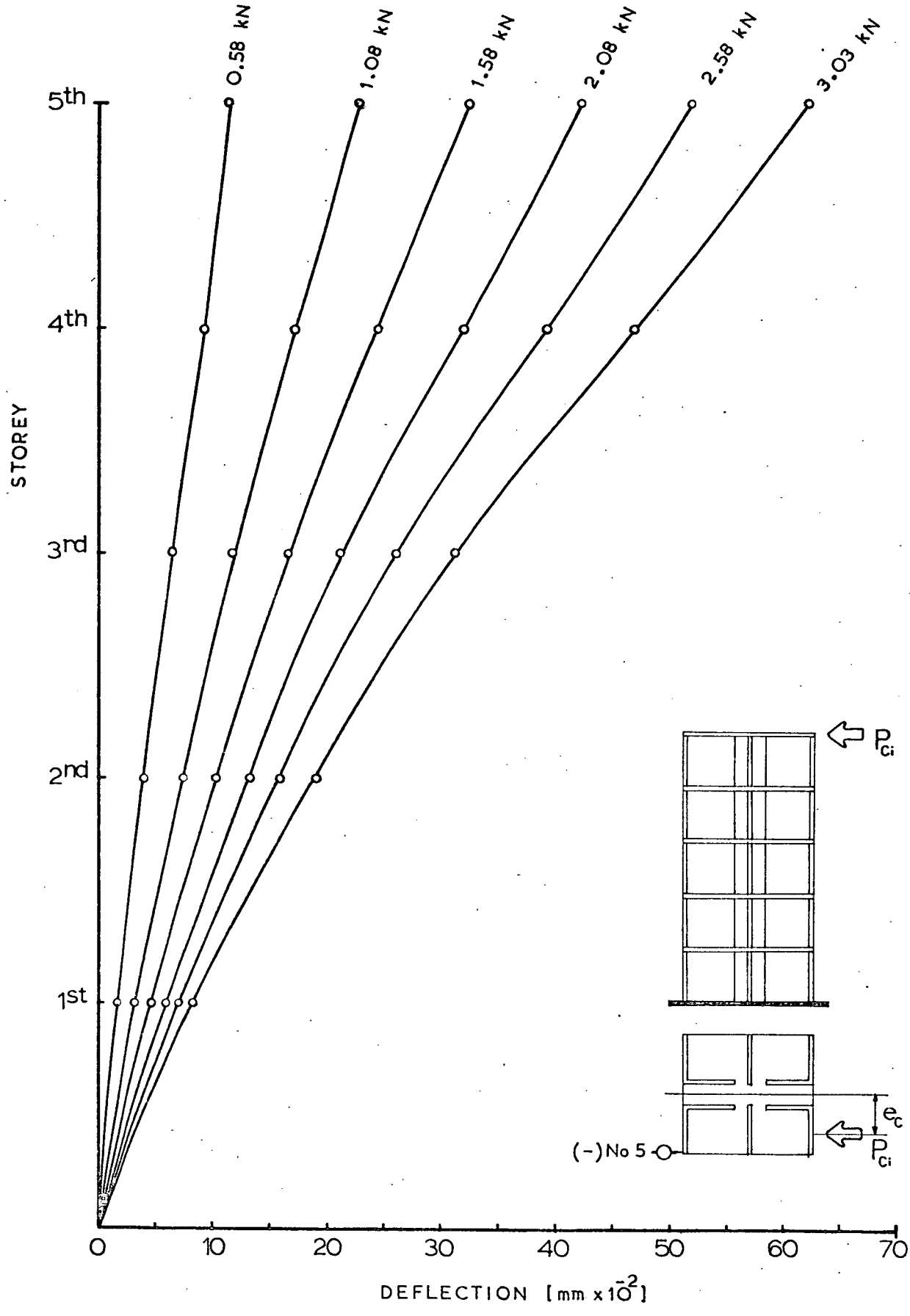

Fig. 3.17 storey/ Deflection curves for structure from dial gauge position No. 5 at various loadings (Y - Direction)

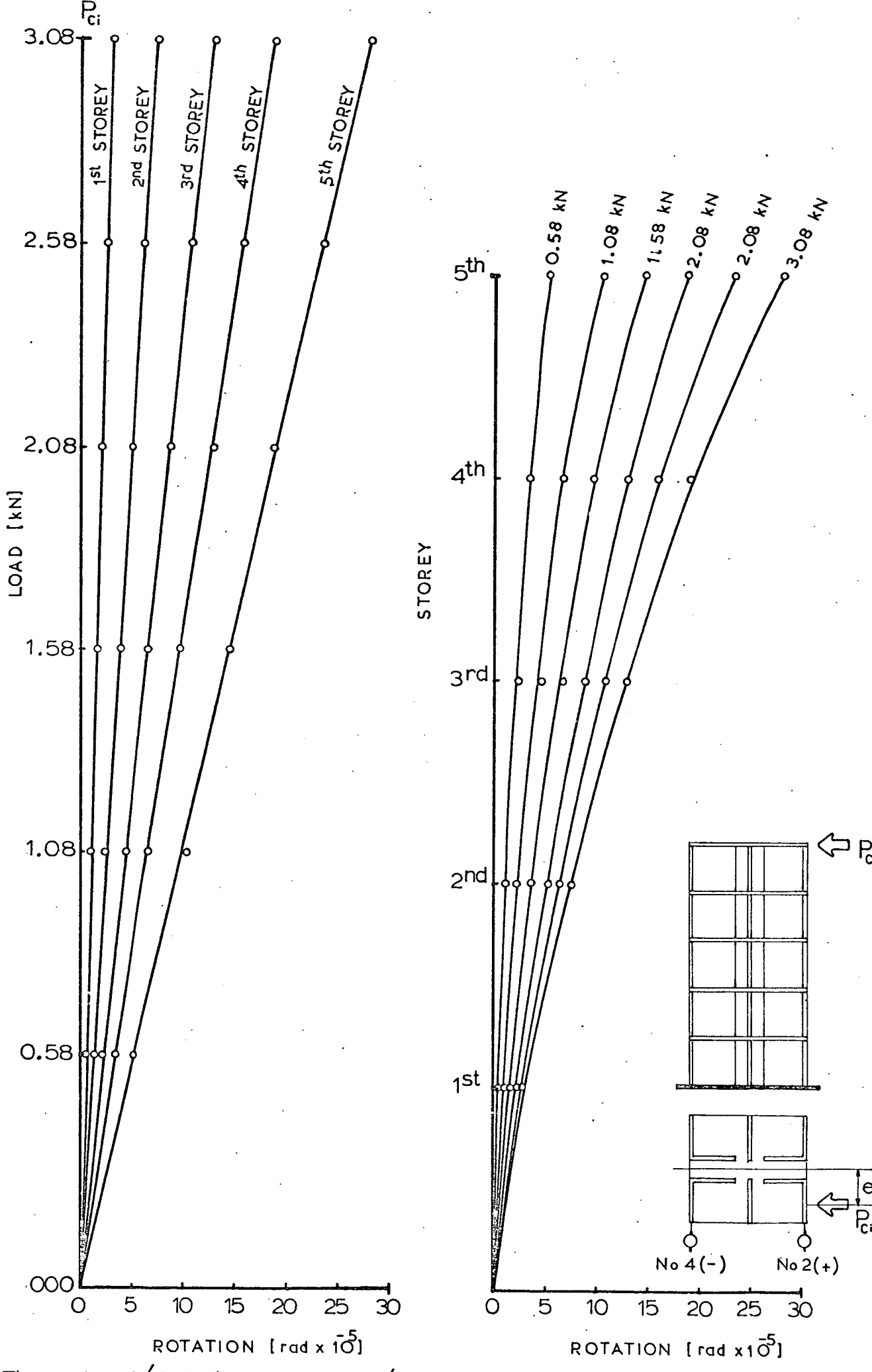

Fig.3.18 Load/Rotation and Storey/Rotation curves for structure from dial gauges position No. 4-2 at various floor and loadings respectively.

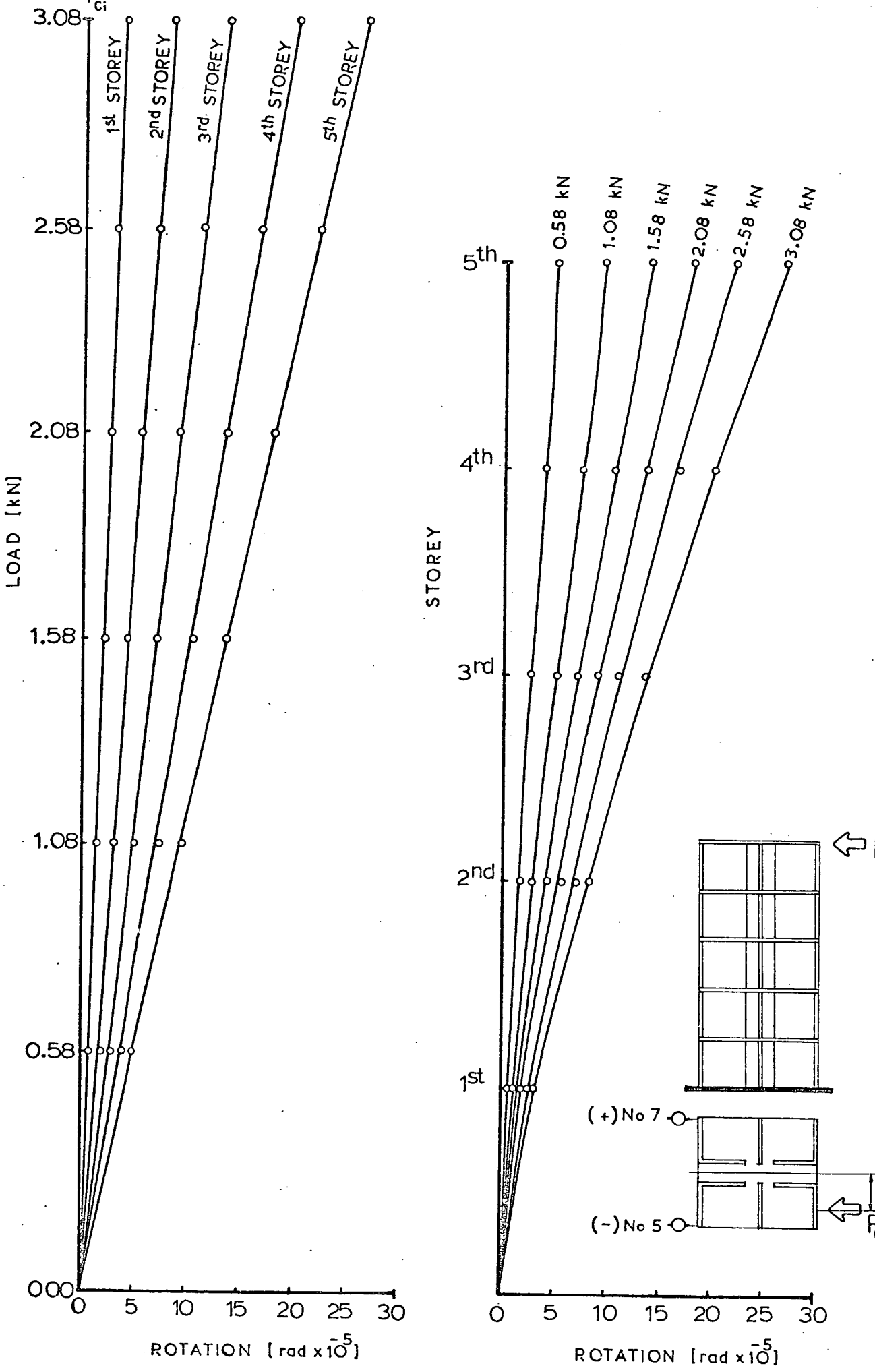

Fig. 3.19 Load/Rotation and Storey/Rotation curves for structure from dial gauges position No. 5-7 at various floor and loadings respectively.

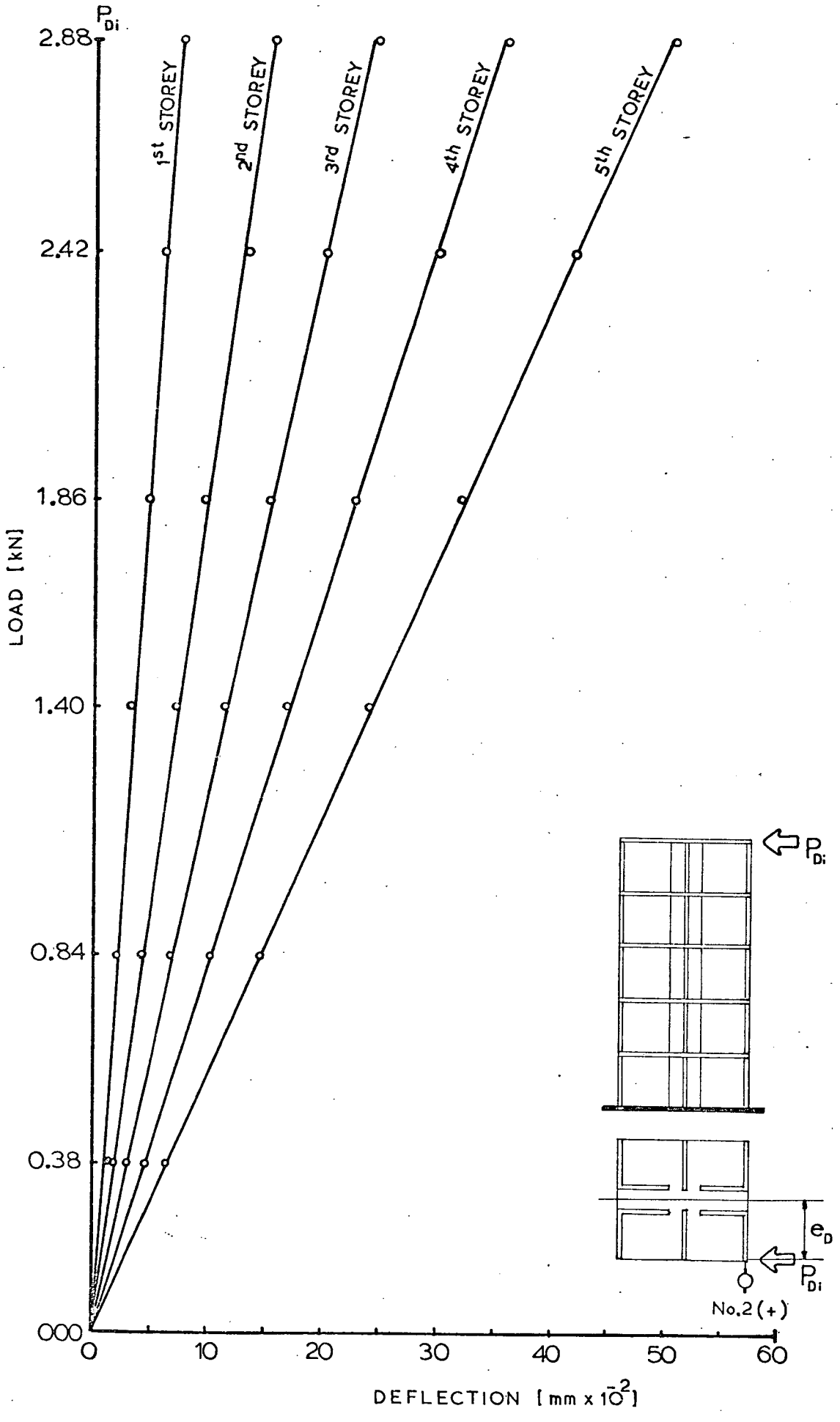

Fig. 3.20 Load / Deflection curves for structure from dial gauge position No. 2 at various floor levels. (X - Direction)

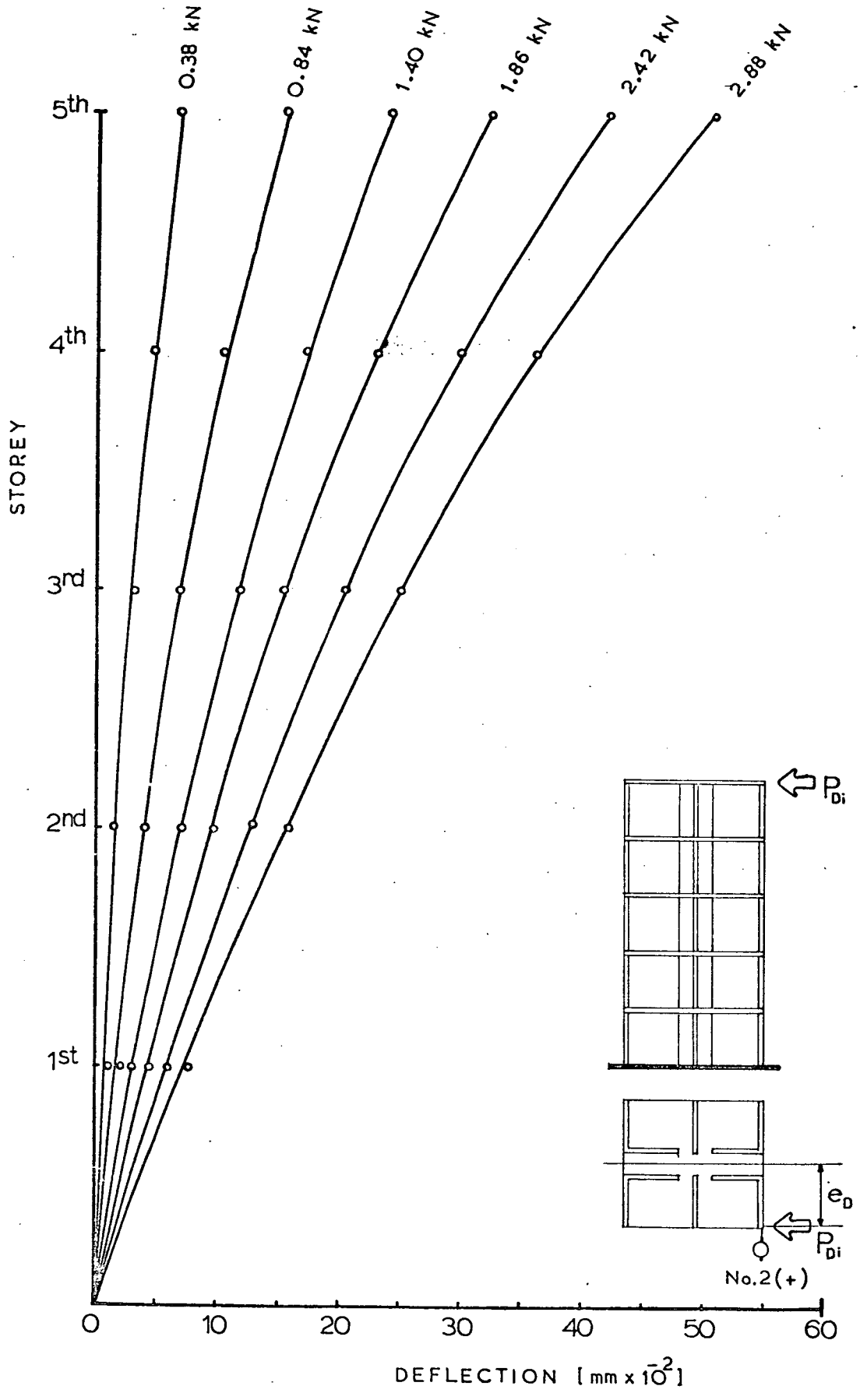

Fig.3.21 Storey / Deflection curves for structure from dial gauge position No.2 at various loadings. (X- Direction)

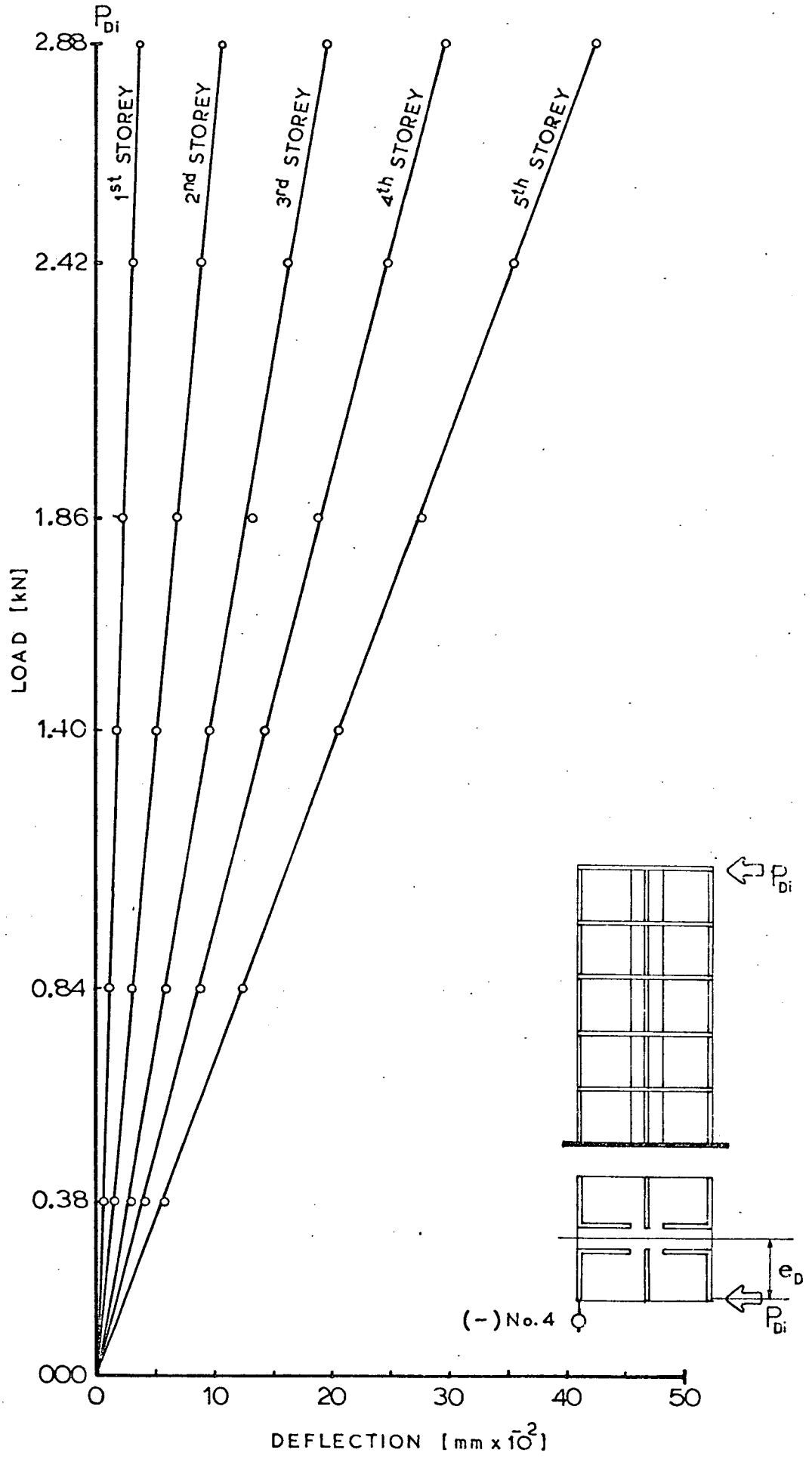

Fig.3.22 Load / Deflection curves for structure from dial gauge position No. 4 at various floor levels. (X- Direction)

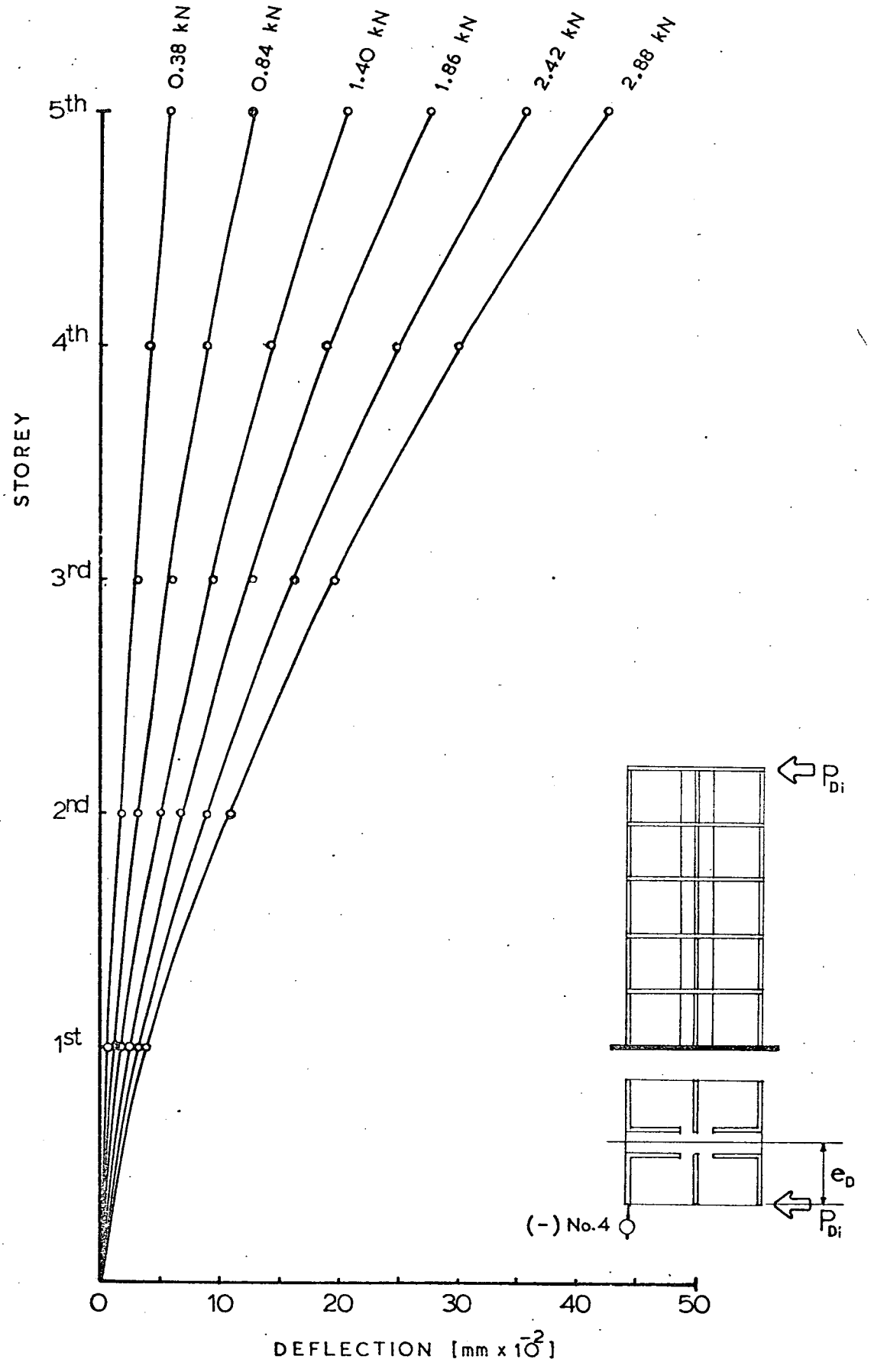

Fig.3.23 Storey / Deflection curves for structure from dial gauge position No. 4 at various loadings. (Y- Direction)

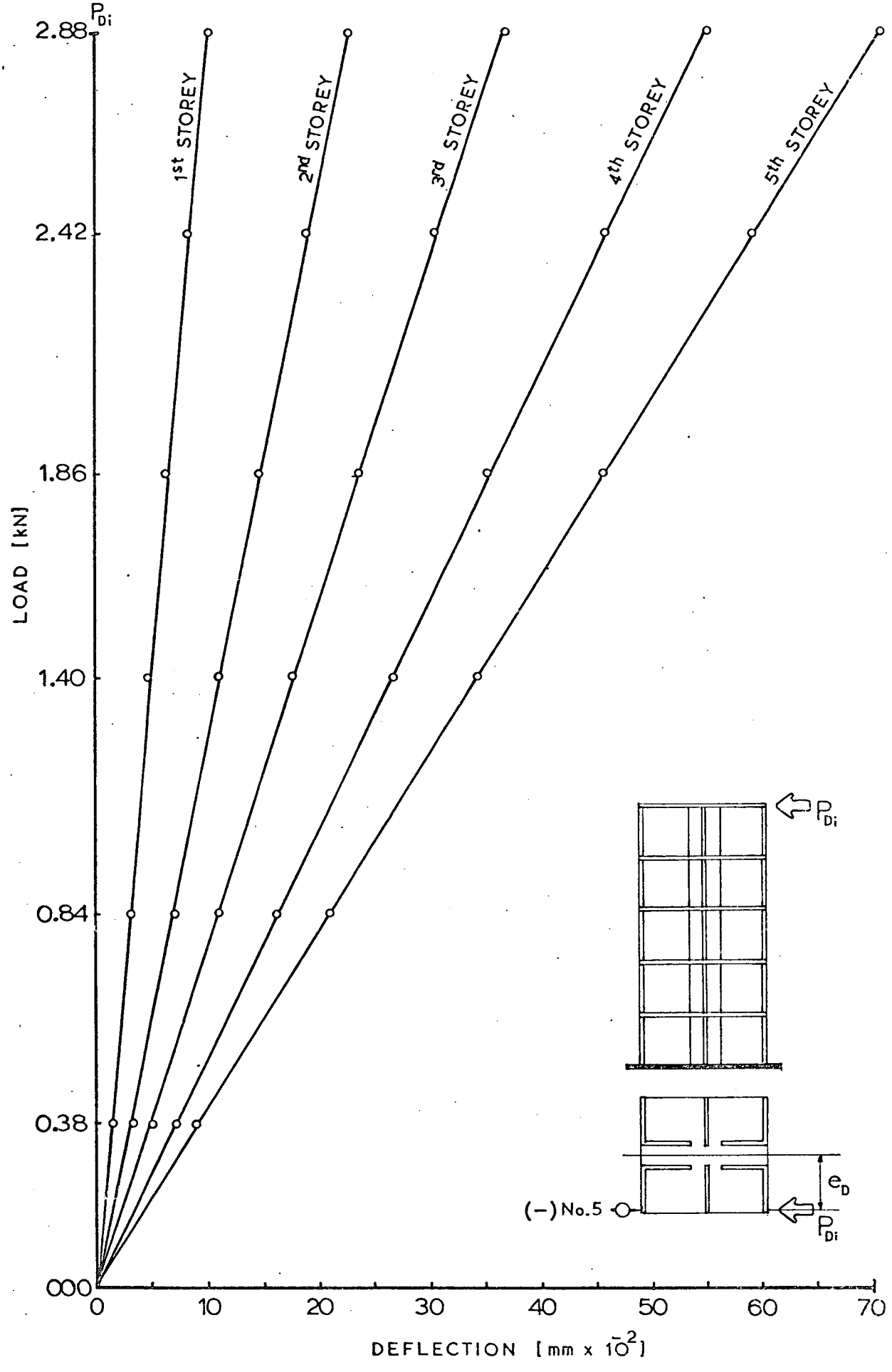

Fig. 3.24 Load / Deflection curves for structure from dial gauge position No. 5 at various floor levels. (Y - Direction)

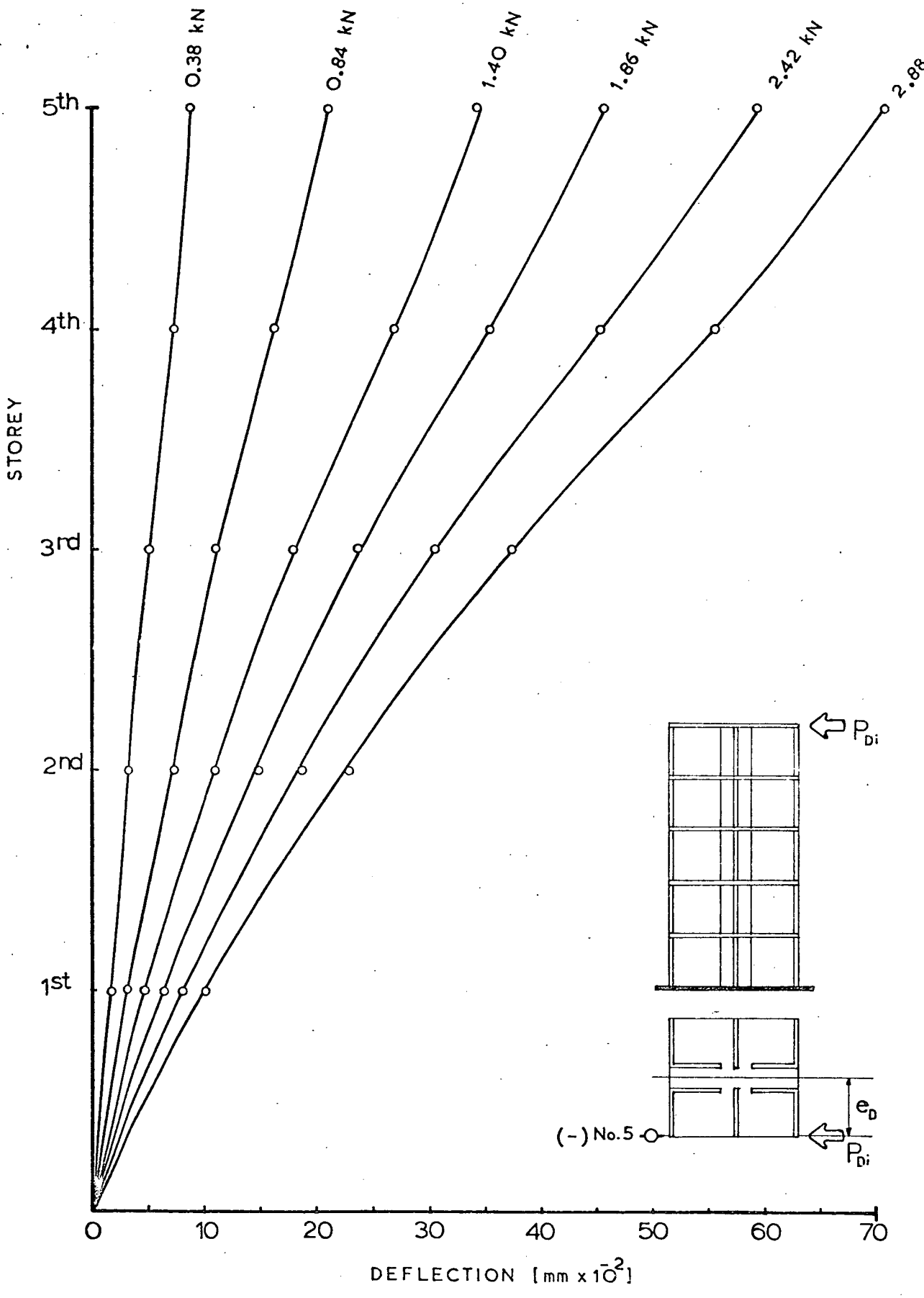

Fig. 3.25 Storey/Deflection curves for structure from dial gauge position No. 5 at various loadings. (Y- Direction)

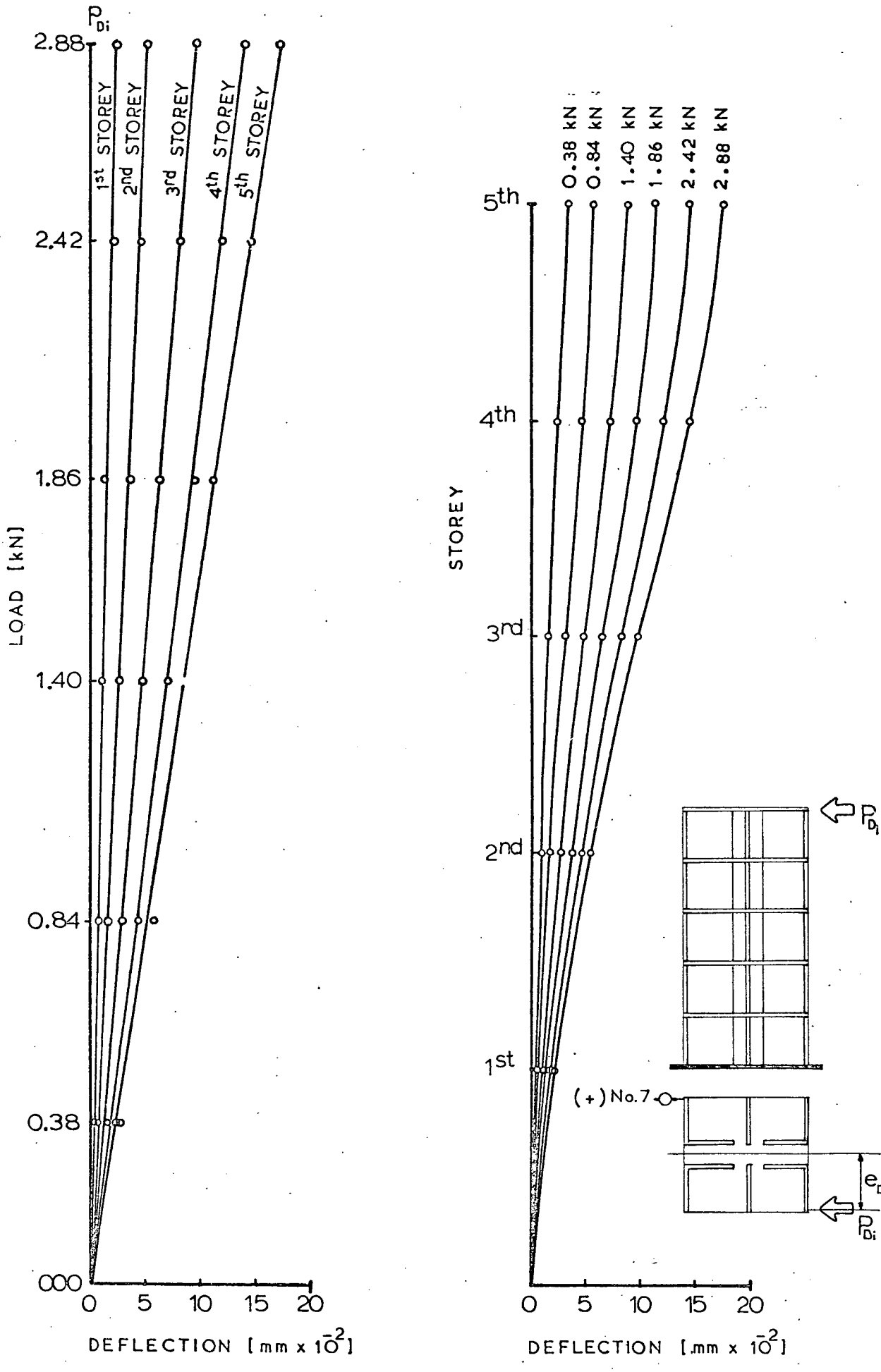

Fig.3.25 Load / Deflection and Storey / Deflection curves for structure from dial gauge position No. 7 at various floor levels and loadings respectively. (Y - Direction)

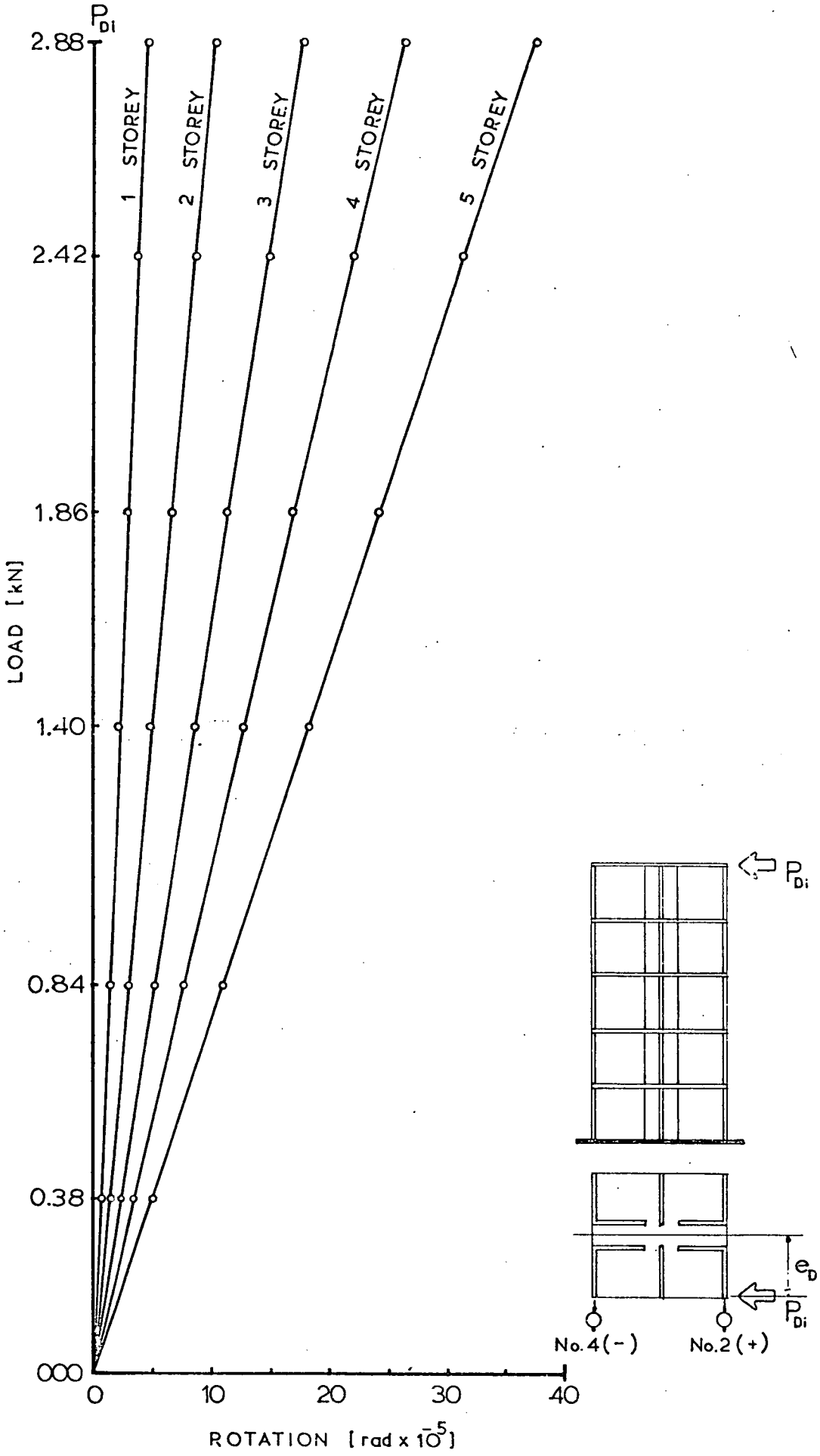

Fig. 3.27 Load / Rotation curves for structure from dial gauges position No. 2-4 at various floor levels.

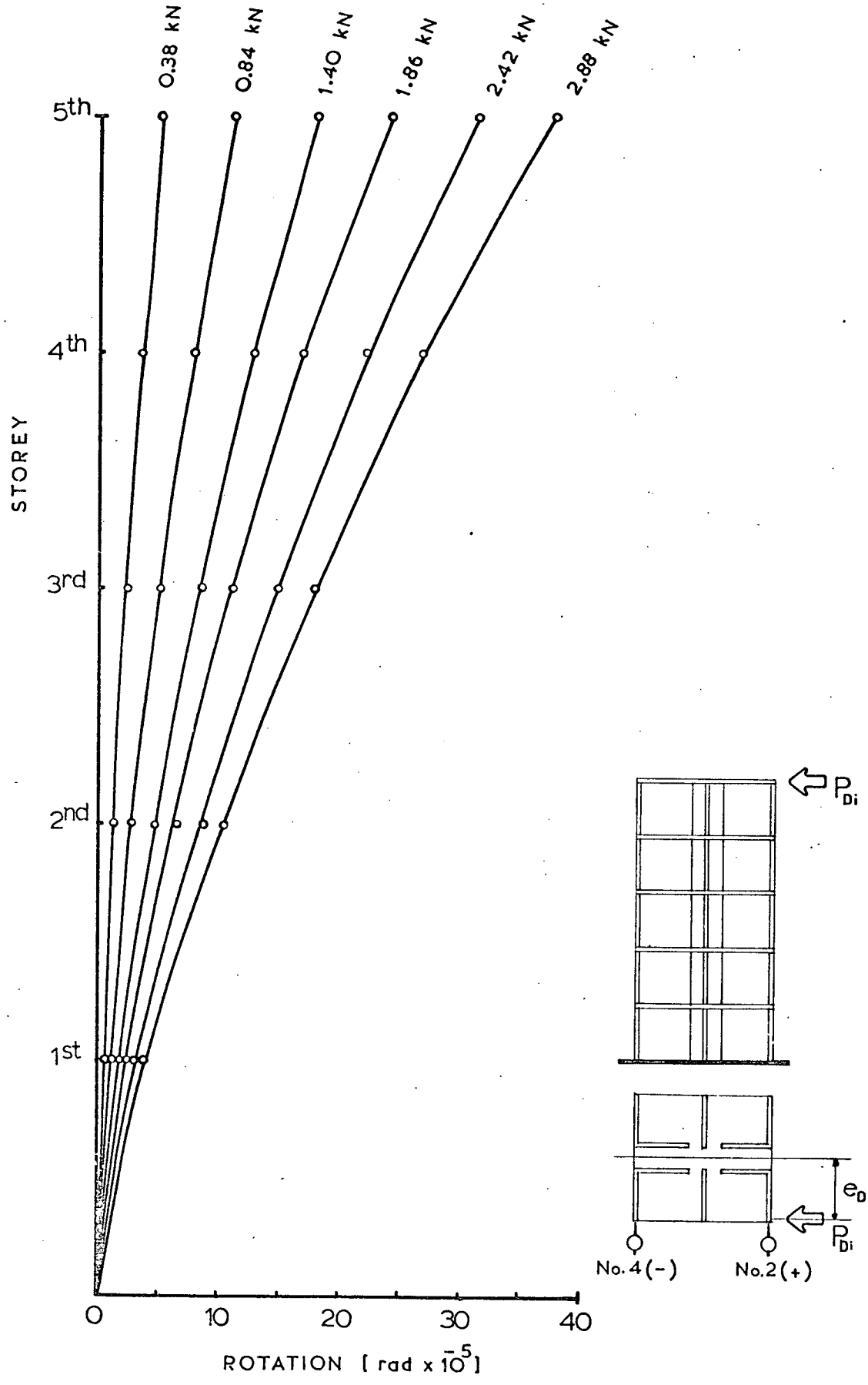

Fig.3.28 Storey Rotation curves for structure from dial gauges position No. 2-4 at various loadings.

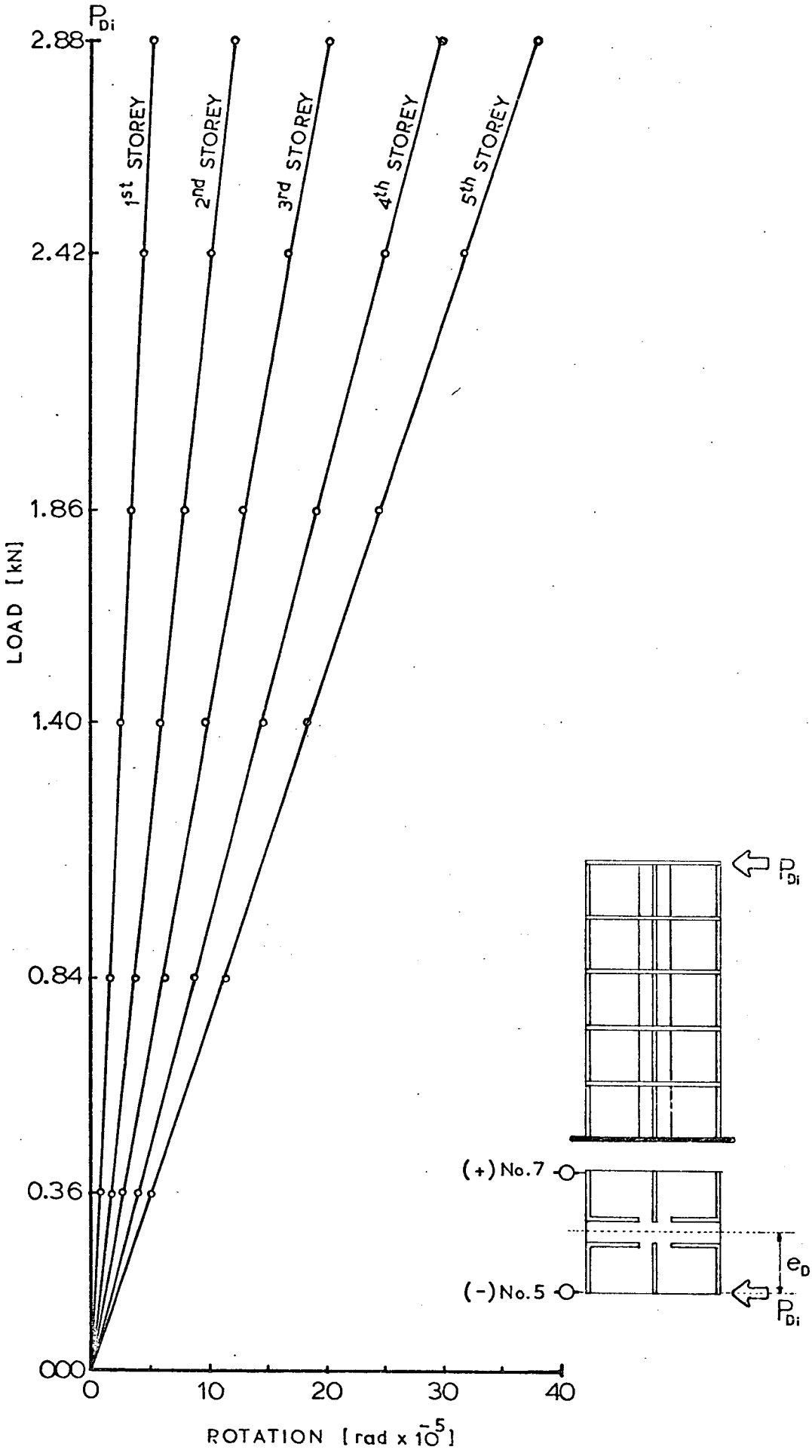

Fig. 3.29 Load / Rotaton curves for structure from dial gauges position No. 5-7 at various floor levels.

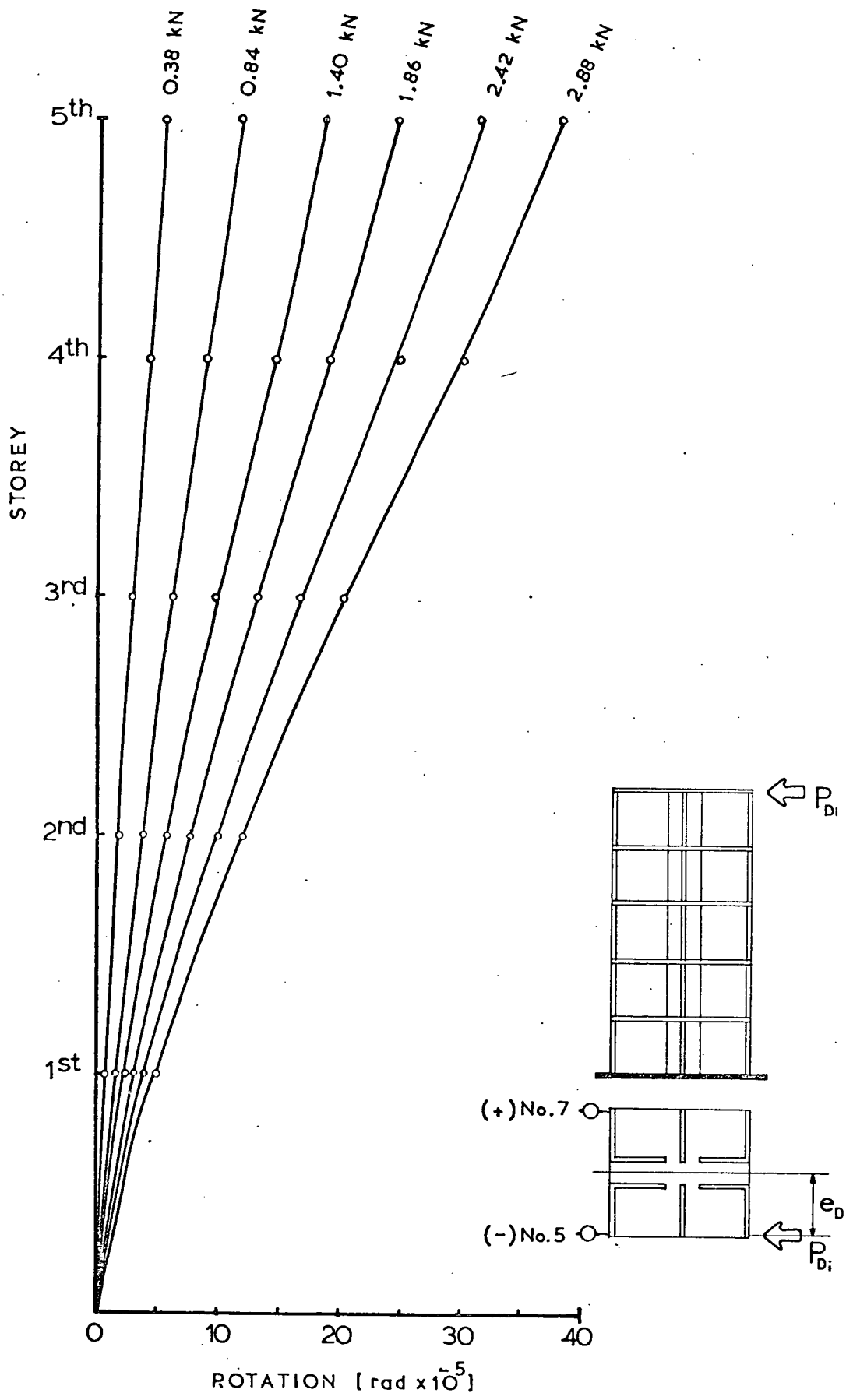

Fig 3.30 Storey Rotation curves for structure from dial gauges position No. 5 7 at various floor levels.

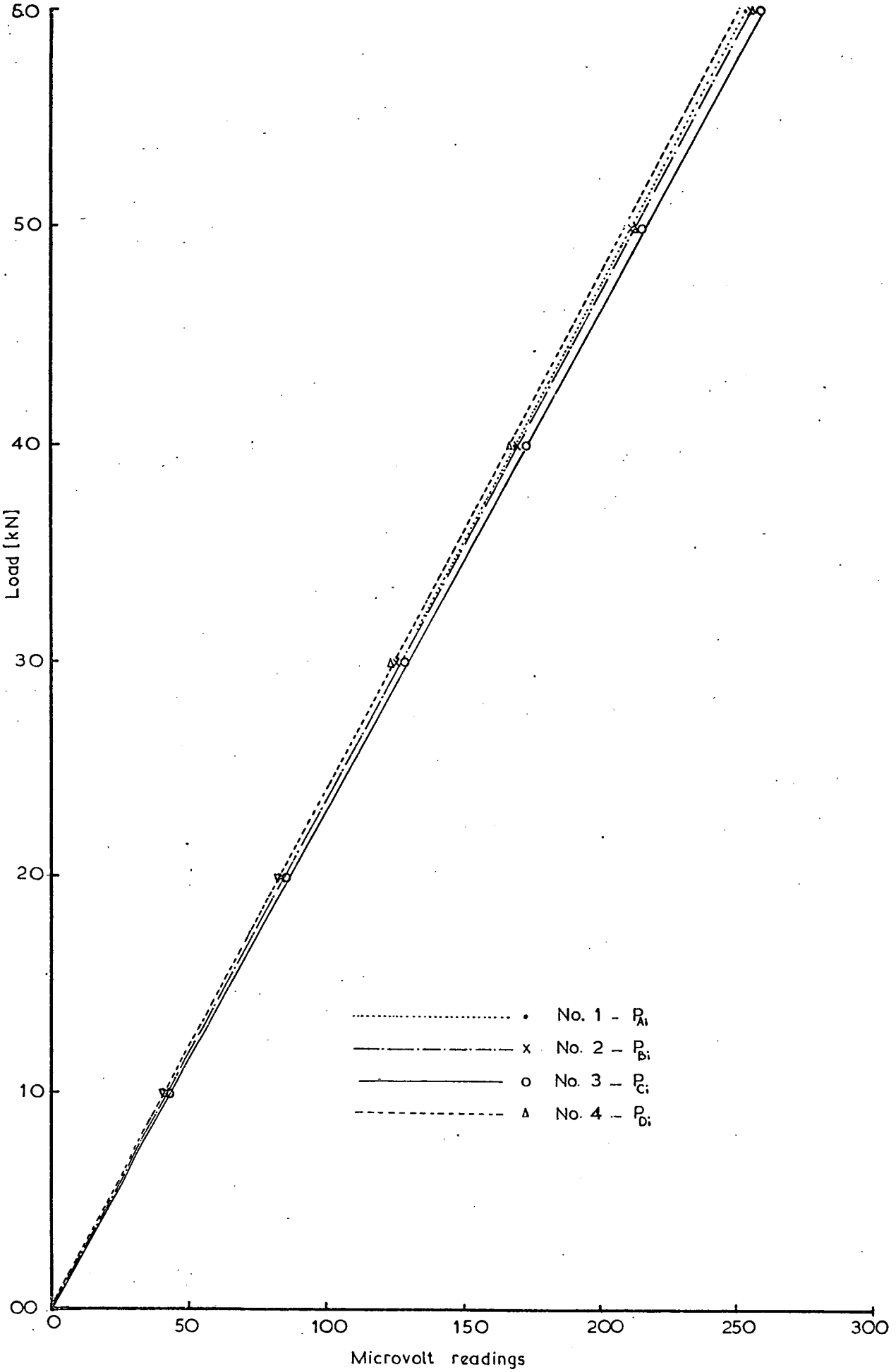

FIG. 3.31 CALIBRATION CURVES FOR 3 TON LOAD CELL

8 - DISCUSSION OF RESULTS

The primary purpose of the investigation was to obtain an understanding of the behaviour of the structure under lateral point loadings. The behaviour is best visualised from curves which relate the load to the deflection, and load to the strain, of any characteristic point on the structure. The structure is loaded by a complex system of forces, producing bending and torsional deformations. From the test results, load against deflection and load against strain graphs were plotted and the best line drawn by eye through each set of points. Linear curves were obtained for the deflection andstrain of the structure under axial loading and eccentric loadings. These results are typical of a structure behaving elastically. Therefore, the theoretical assumption of the elastic behaviour of the structure is justified. The straight line relationship can be used in calculating values of deflection and strain for any magnitude of applied load.

The various eccentric point loadingswere transferred to the axial position and the deformation curves compared with the curve from load against deflection obtained for axial loading of the same magnitude. It can be seen in Figure (4.5) that the curves are very similar, they could be considered the same within the range of experimental error. Similarly, the rotation was calculated when various eccentric loads, but with the same moment as calculated from the load times eccentricity relationship, were applied to the structure. From graph (4.10), it is seen that the curves are the same, within the range of experimental error.

In conclusion, the assumption of simplifying the analysis by considering the deflection due to pure bending separately from the deflection due to pure torsion has been demonstrated experimentally to be valid. It is apparent that the experimental results from the various load positions are in good agreement and so the results may be confidently used for comparison with the theoretically calculated data.

9 - YOUNG'S MODULUS OF ELASTICITY

A part of the work was concerned with finding the modulus of elasticity by different test methods. It was desirable to discover if the "E" value changed appreciably in the range of compressions known to be applied within the test structure. The compression on the structure varied from 10 lbf/in^2 to 50 lbf/in^2 in the fifth to the first floors, respectively. Therefore, in the wall and beam tests a maximum compression of 250 lbf/in^2 was applied. Previous workers (37) (43) used a range of Modulus of Elasticity from racking tests on one storey-height structures subjected to precompression, using the formula suggested by Benjamin (1959) (3). From the results, they used in their calculations of the structures, a different "E" value for each storey. It was apparent that they had underestimated the "E" values. With consideration to the earlier workers, numerous tests were carried out as described below.

The material for construction of the model walls and beams was obtained from full scale blocks (18" x 9" x 4") which were cut to the required dimensions in the laboratory from full scale blocks, using a clipper machine by a wetted abrasive blade. Care was taken to retain uniformity in the $\frac{1}{3}$ scale "Aglite blocks". Sand, Cement, lime and Mortar were as described previously.

Before each compression test a 2" x 2" steel plate was cemented on the ends of the wall and beams with Ferrocrete rapid hardening cement and sand. The plate was accurately levelled to ensure that the applied load was uniformly distributed over the whole section.

In the second beam test a special ball and socket joint plate was designed to give a firm connection between beam ends and top and bottom plates of the "Avery Machine" but which permitted free beam rotation, i.e. giving a hinge connection.

Test -1- The strain on the wall and deflection was measured by the flexure test on blockwork, Figure (3.32), (3.37) plate (3.8b).

Test -2- The strain on the wall was measured when under pre-compression, Figure (3.33) and plate (3.8a).

Test -3- The beam was used for the measurement of the strain with:

a) - Beam under compression, Figure (3.34).

b) - Beam in flexure, Figure (3.35)

c) - Beam under shear plus bending, Figure (3.36), plate (3.6b).

Test -4- A different beam was subjected to compression and lateral loading to measure the strain and deflection. The beam was tested

a) - Under constant compression and varying lateral loads.

b) - Under constant lateral load and varying compressions.

The calculated test results are shown in Figure (3.38), (3.39) and plate (3.6a, 3.7).

a) E value conclusion

The results from the tests to find the "E" value of the test blocks, under various conditions, showed that within the range of pre-

compression experienced in the test structure, the value did not change significantly. Therefore, it is reasonable to use a constant value for the modulus of elasticity in all calculations involved in the theoretical analysis of the test structure.

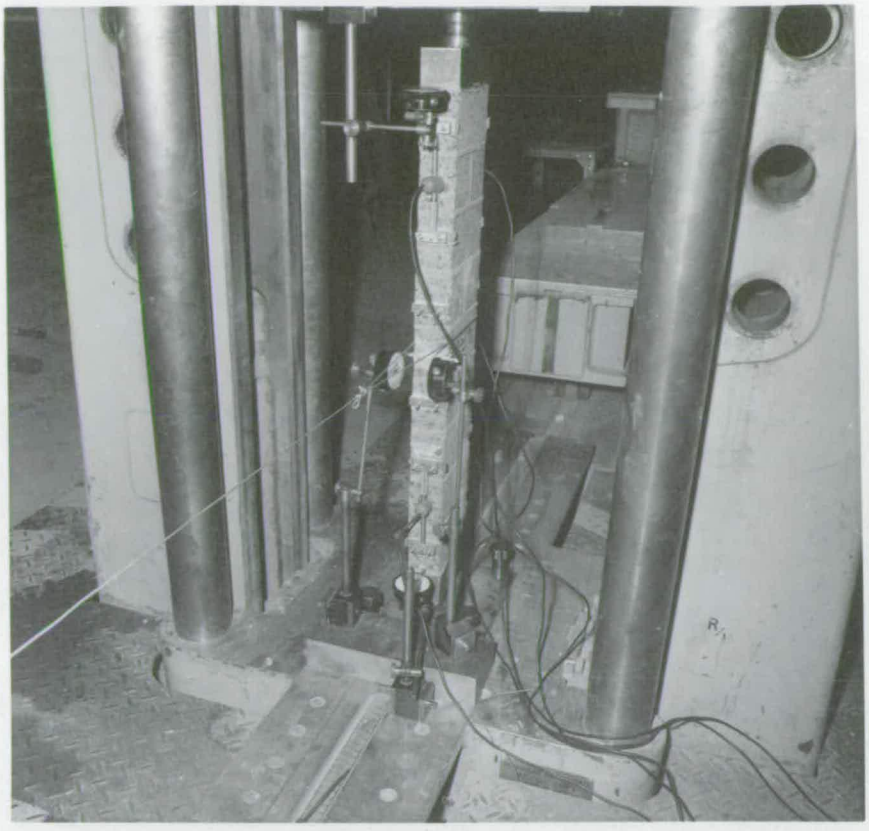

(3.6a)

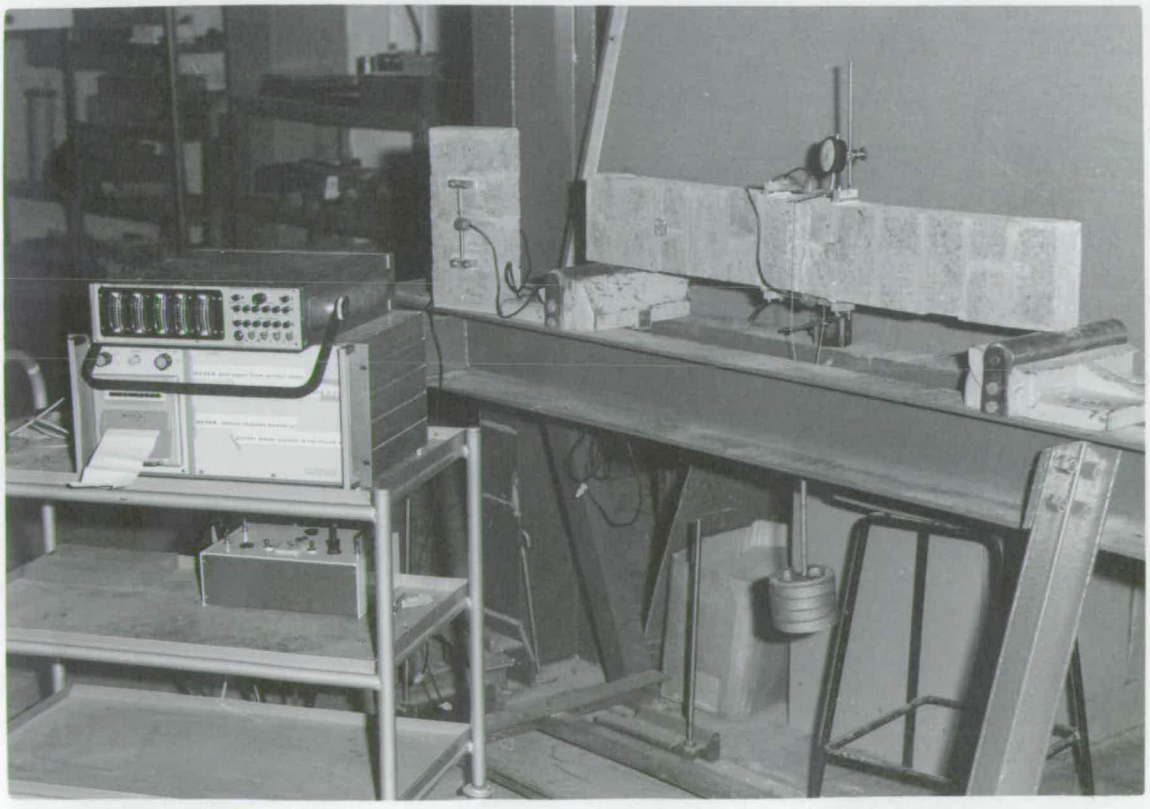

(3.6b)

PLATES (3.6a) AND (3.6b) TESTS ON BLOCKWORK BEAMS FOR MEASUREMENT OF YOUNG S MODULUS OF ELASTICITY (a) BENDING + COMPRESSION (b) UNDER BENDING

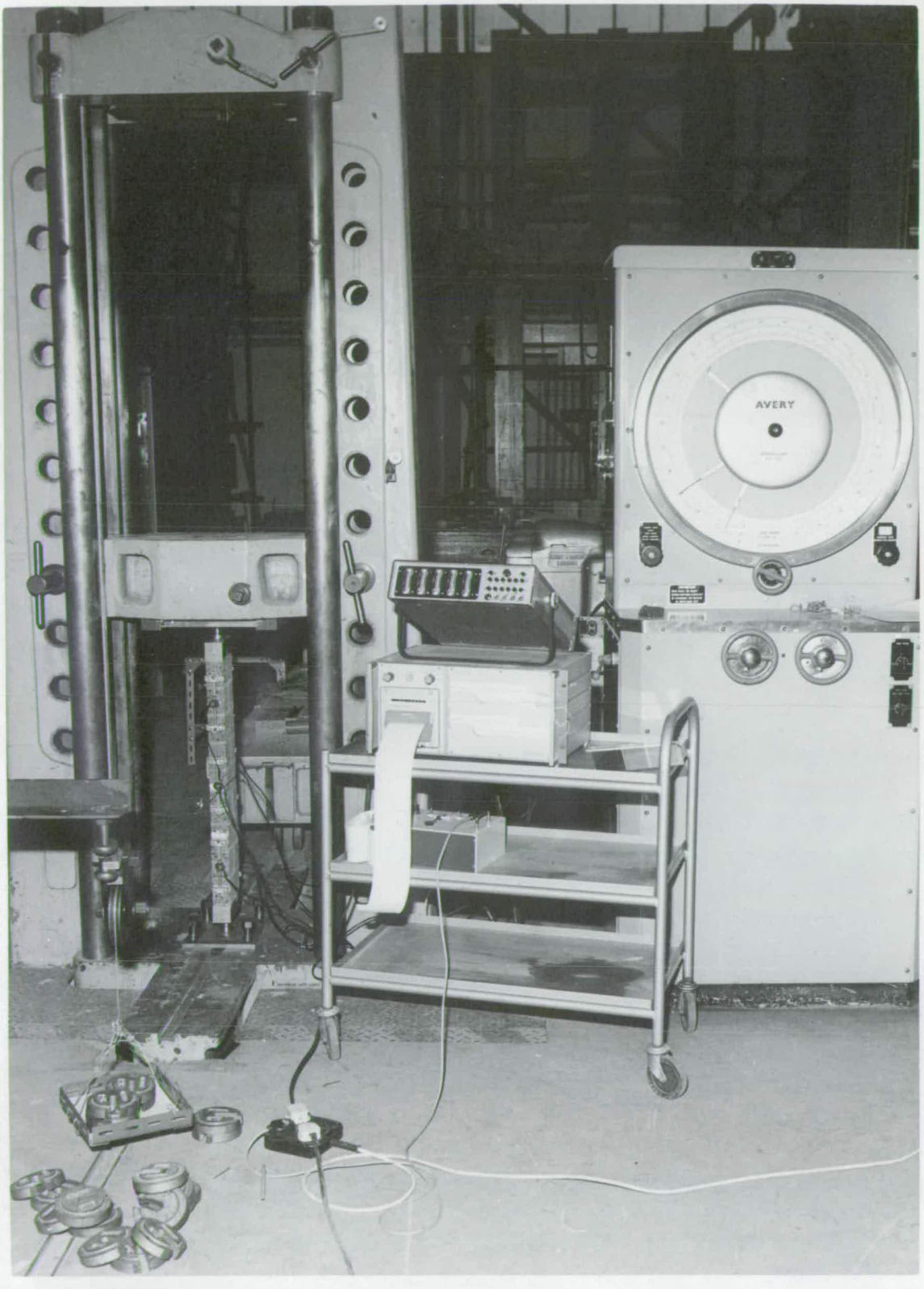

PLATE (3.7) BLOCKWORK BEAM UNDER TEST, SHOWING COMPRESSION APPARATUS AND GT UNIT TYPE DATA LOGGER

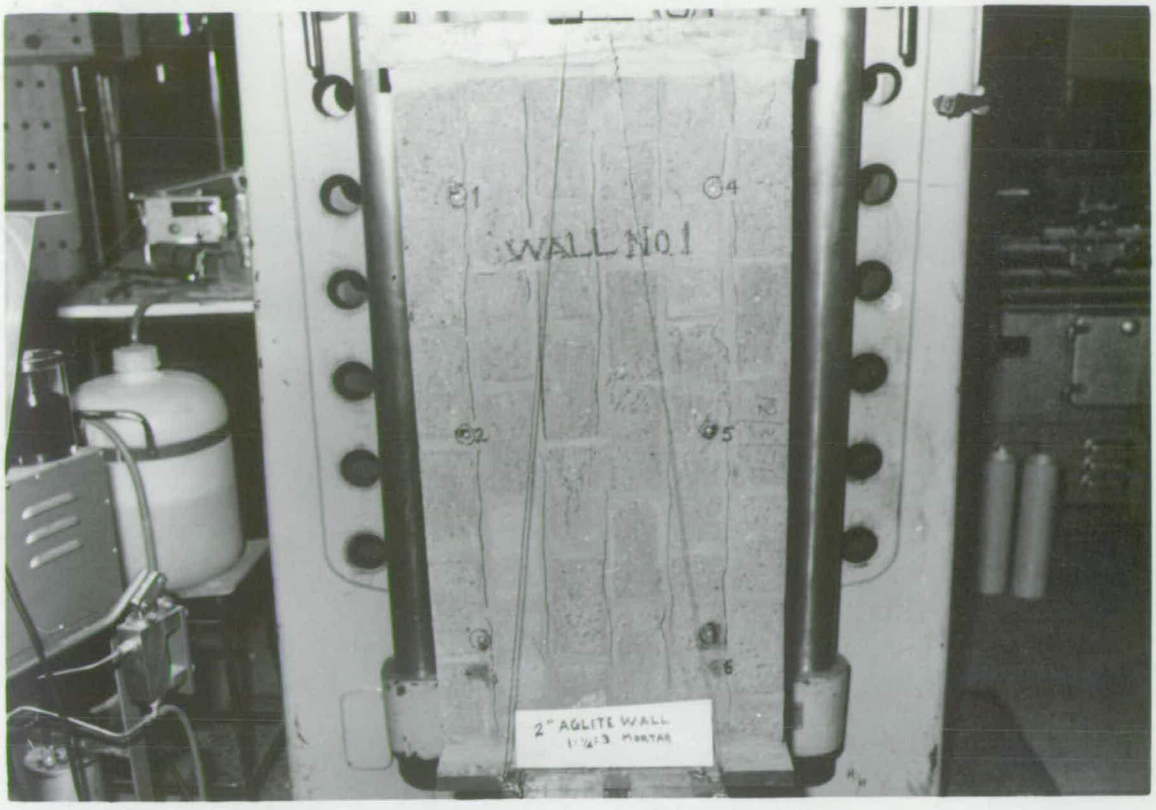

(3.8a)

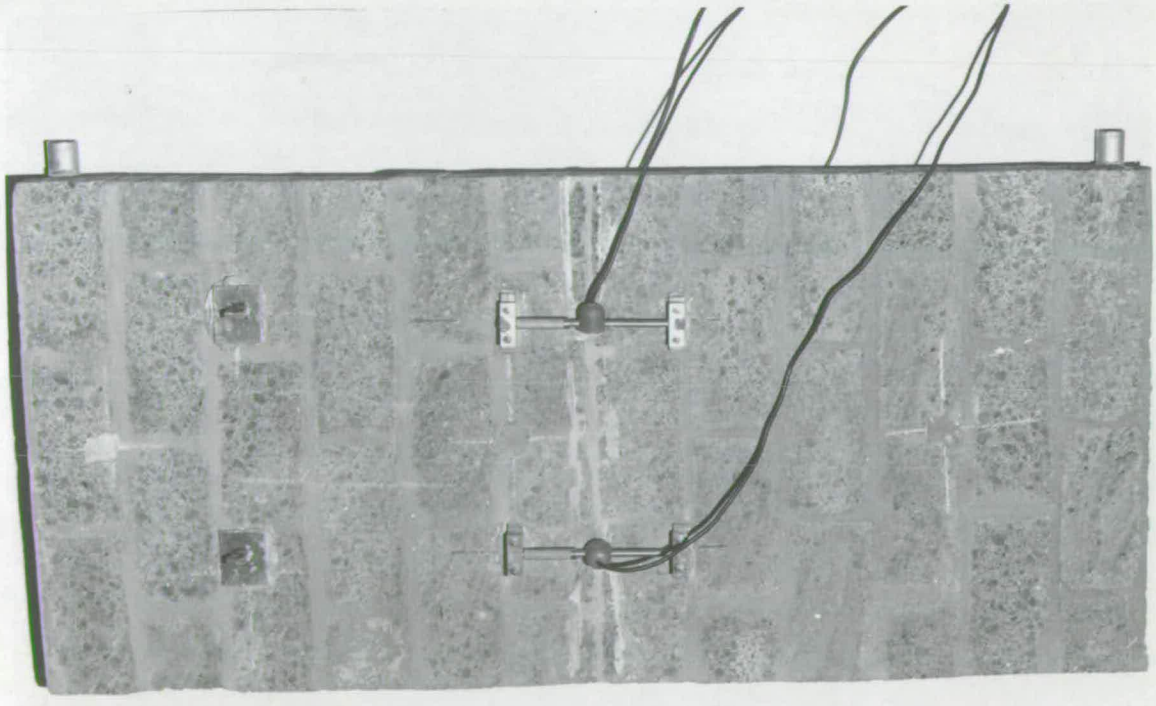

(3.8b)

PLATES (3.8a) AND (3.8b) TESTS ON BLOCKWORK WALLS FOR MEASUREMENT OF YOUNG S MODULUS OF ELASTICITY (a) UNDER COMPRESSION (b) UNDER BENDING

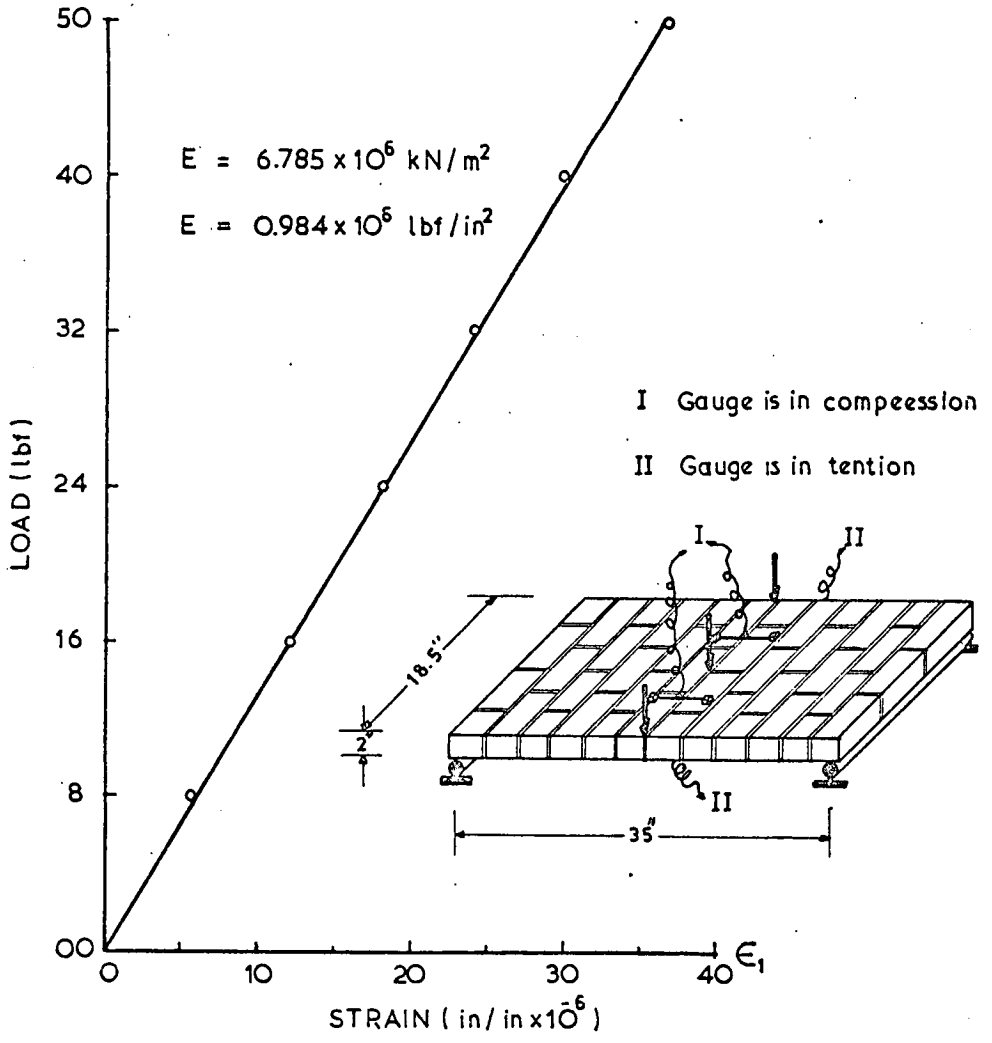

Fig 3.32 Wall in flexure

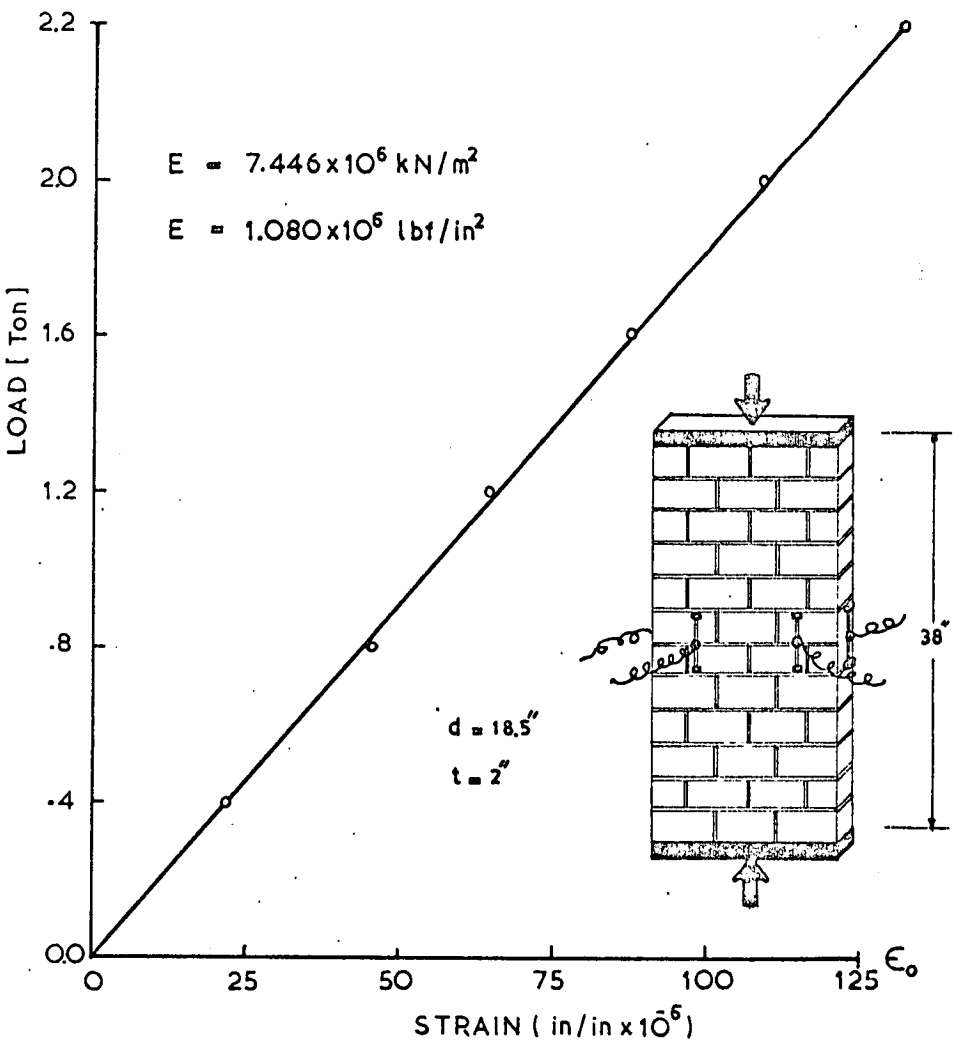

Fig 3.33 Masonry wall under compession

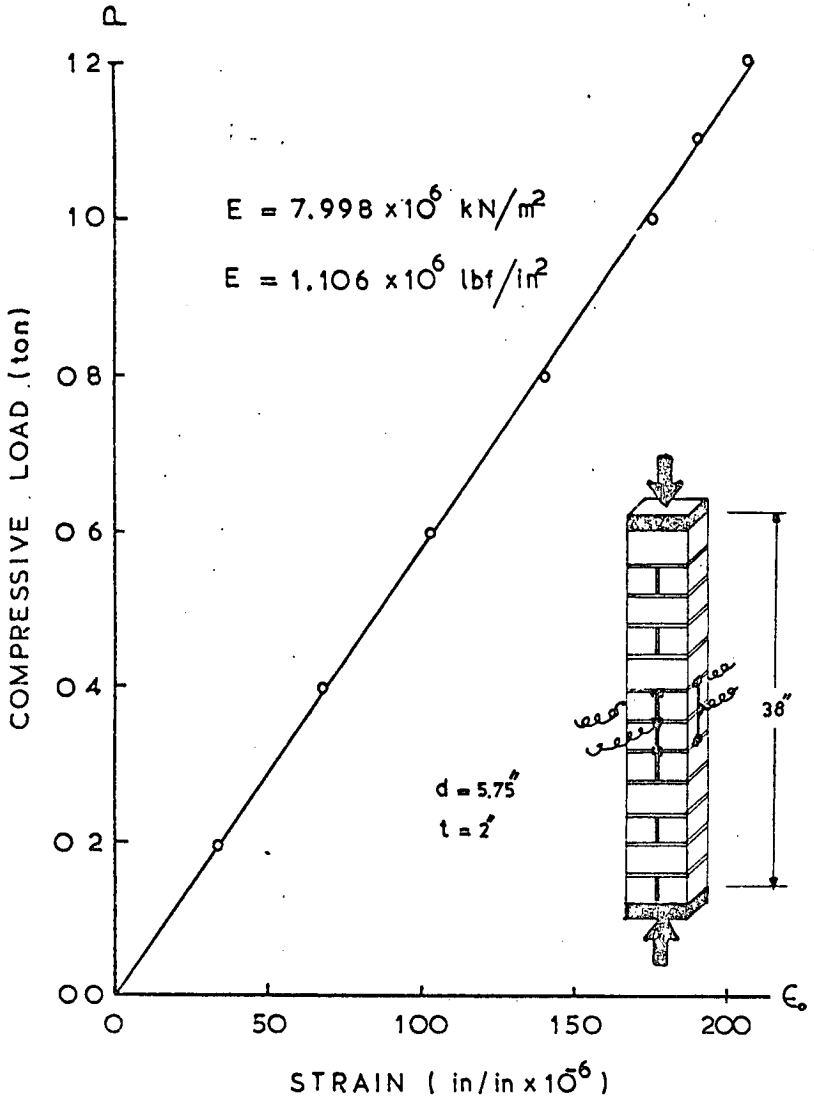

Fig. 3.34 Beam under compression

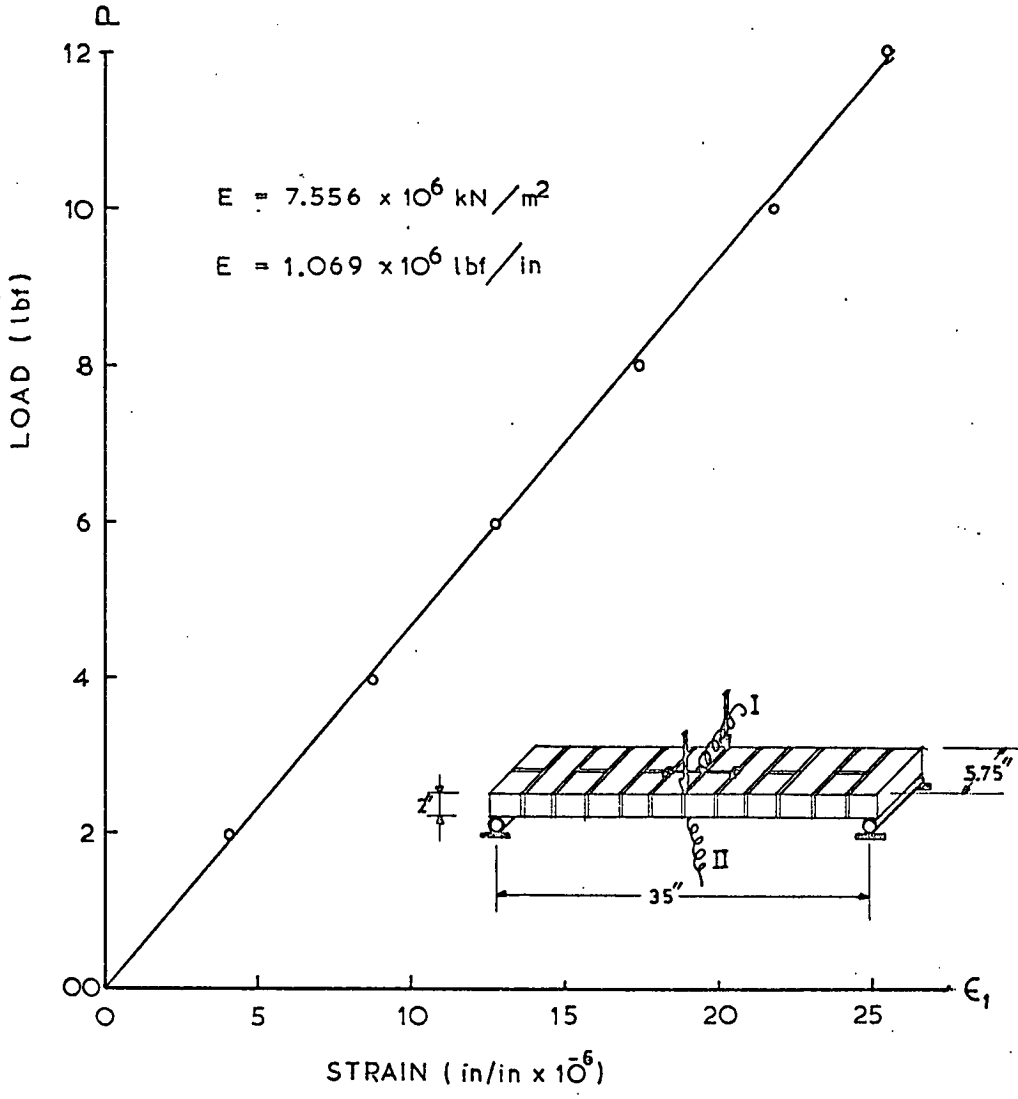

Fig.3.35 Beam in flexure positon -I-

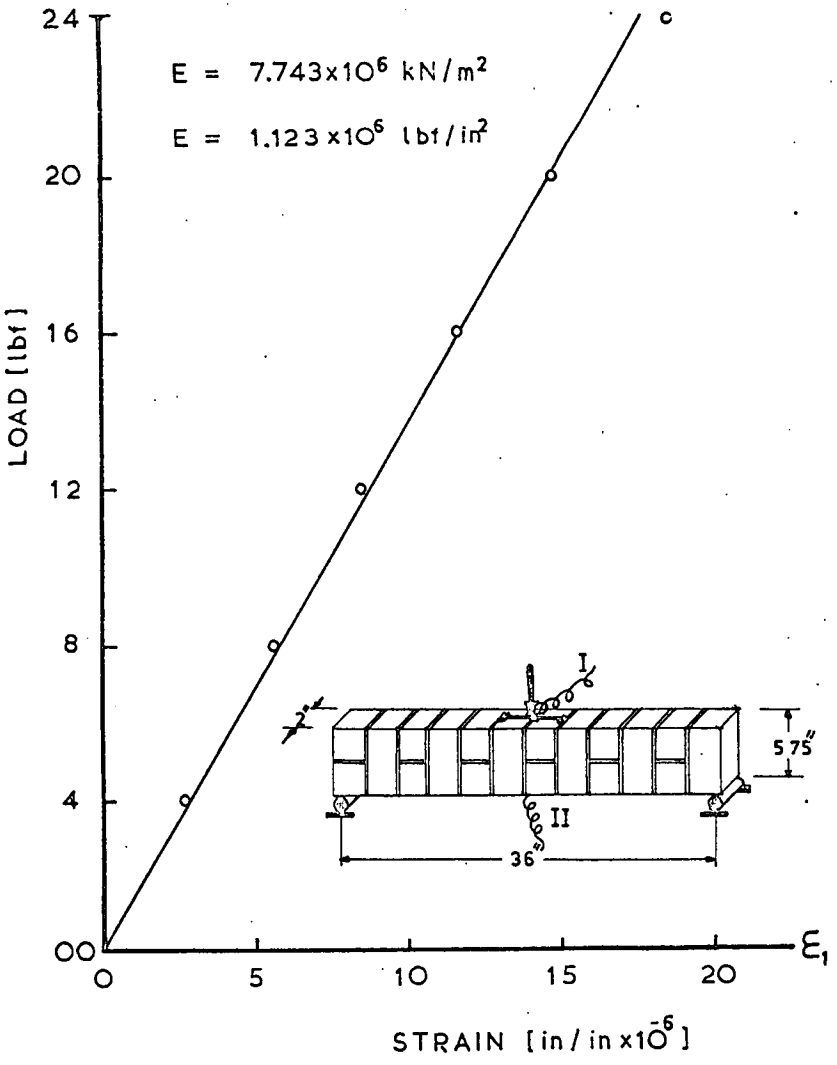

Fig 3.36 Beam in flexure position II

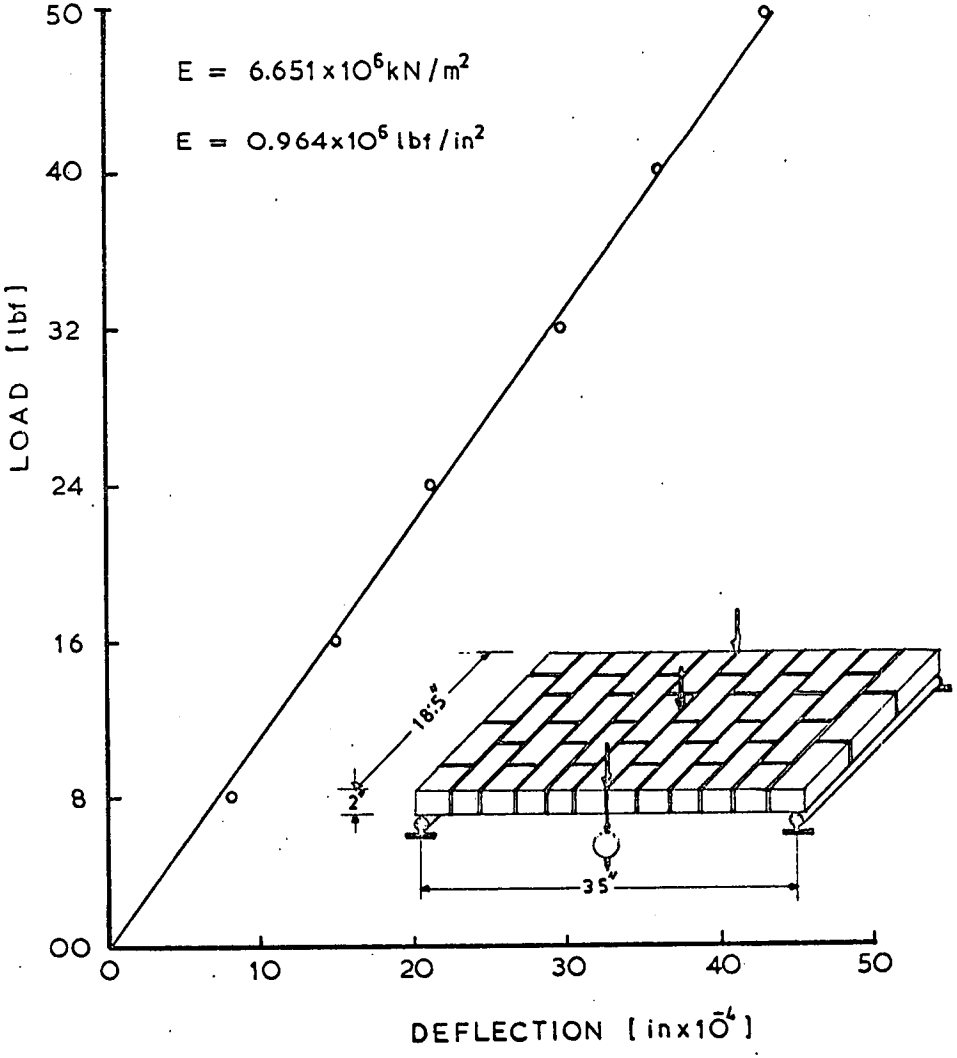

Fig 3.37 Wall in flexure

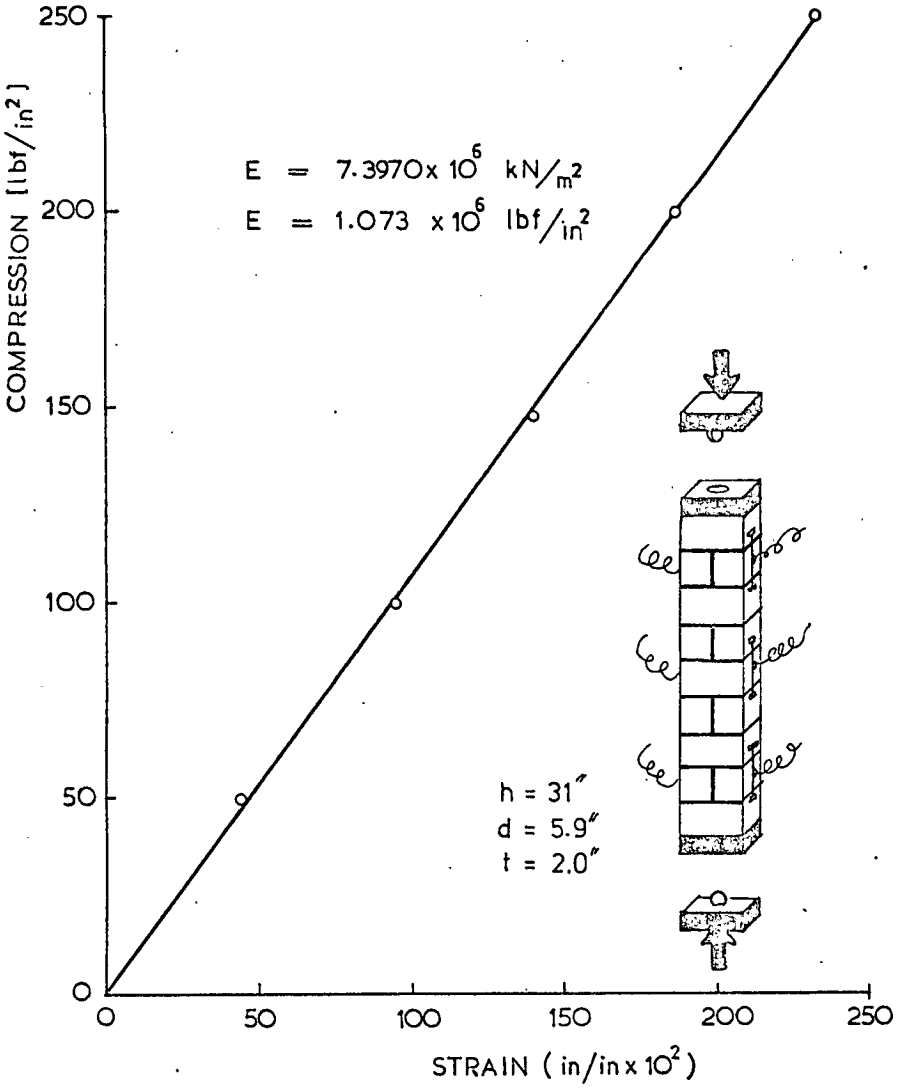

Fig 3.38 Beam under compression

Compression lbf/in²

W=Lateral load [lbf]	10	20	30	40	50	60	70
10	8	18.5	28.5	37.5	47.5	58.0	67.0
20	9	19.0	28.5	38.5	48.5	57.5	67.5
30	10	20.0	28.5	38.5	48.5	57.5	66.0
40	8	17.5	28.0	37.5	46.5	57.0	66.5
50	8	17.5	28.0	37.0	47.0	57.5	66.0

Average strain

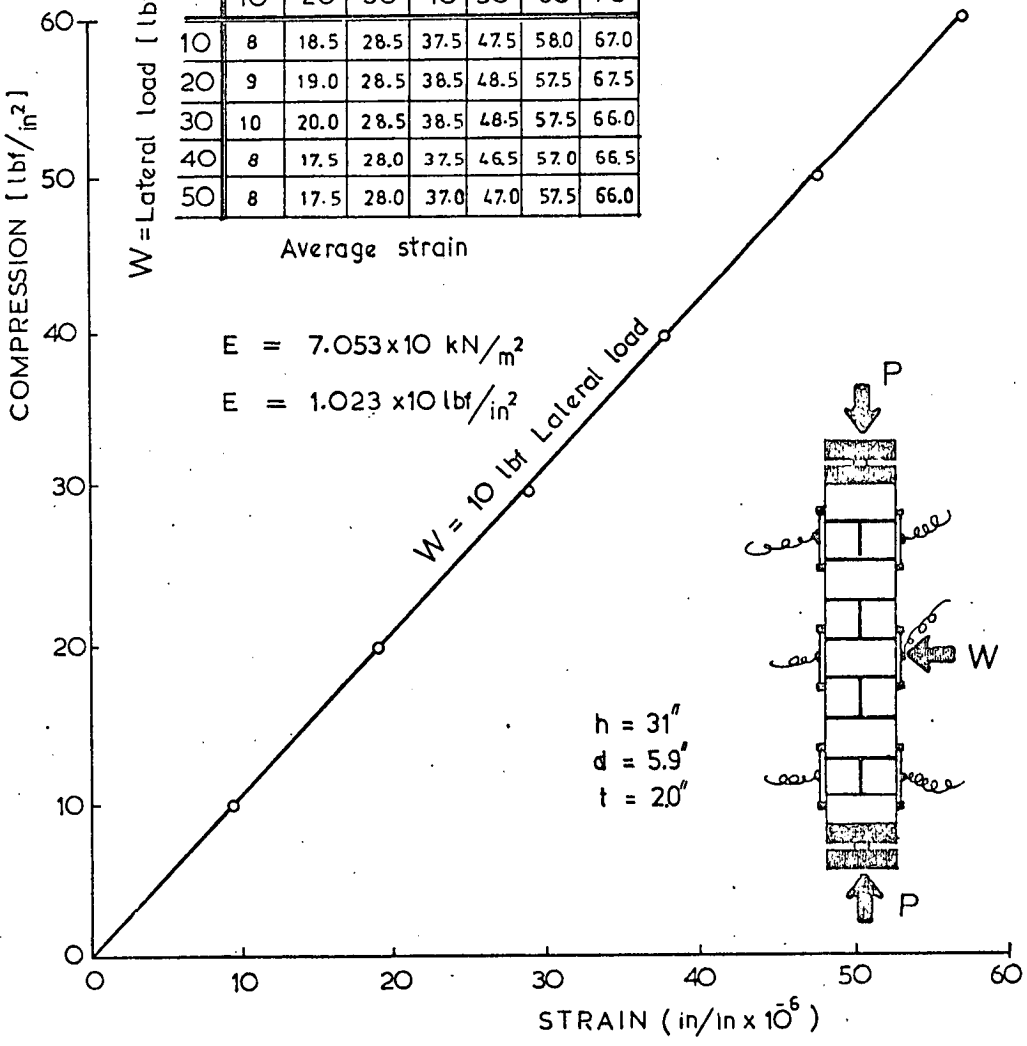

Fig 3.39 Beam under various compression and beanding loadings. The table shows average values of measured strain.

CHAPTER IV

GENERAL DISCUSSION AND CONCLUSION

1 - INTRODUCTION

In recent years shear wall structures have been increasingly used in tall buildings, for both commercial and residential purposes, to resist lateral loads. Therefore an efficient and simple method of analysis is of the utmost importance. At the present time, numerous theories exist for the analysis of multi-storey shear wall structures under bending and torsional forces, but each theory has its disadvantages, mainly due to the simplifying assumptions which have to be made to permit the analysis of the structure. The more widely used theories for bending analysis are discussed in following section.

The present studies describe a method applicable to the torsion analysis of multistorey buildings with shear walls. The method does not require the use of a computer and would be of particular use to the design engineer in the early stages of design. The experimental results obtained in this investigation, from a model structure, are compared with the experimental data taken from the work of Kalita [37] on a 1/6 scale model brickwork structure, as

well as with the results calculated using the theories of other workers.

2 - ANALYSIS OF THE STRUCTURE UNDER LATERAL LOADING

The analytical methods for the solution of multistorey shear wall buildings and the assumptions on which they are based, are briefly discussed in the following section. The methods were previously outlined in Chapter I. In the following methods, due to the symmetry, half of the structure was considered in the analysis. Young's modulus of elasticity was found experimentally, in Chapter III to be 7.171 kN/m^2 (1.04×10^6 lbf/in^2) for blockwork and 29.647 kN/m^2 (4.30×10^6 lbf/in^2) for slabs. Poisson's ratio was taken to be 0.18 and 0.15 for blockwork and concrete, respectively.

In the finite element method, the structure is subdivided into 324 two-dimensional elements, rectangular in shape, connected at 364 nodal points or joints, as demonstrated in Figure [4.1]. The program provides for the solution of plane strain, plane stress and deflection problems. In a typical building, the walls are frequently combined to form units consisting of two or more walls orientated at right angles. A wall can act either as a shear wall, a flange or a cross-wall depending on the direction of lateral loading. In resisting lateral loading, only an effective width rather than the total width of the flange is included in the calculations of area and moment of inertia in the analysis, as given in Figure [4.2]. Work has been published suggesting effective flange widths e.g. (37, 54, 55, 62). The effective flange width is calculated using

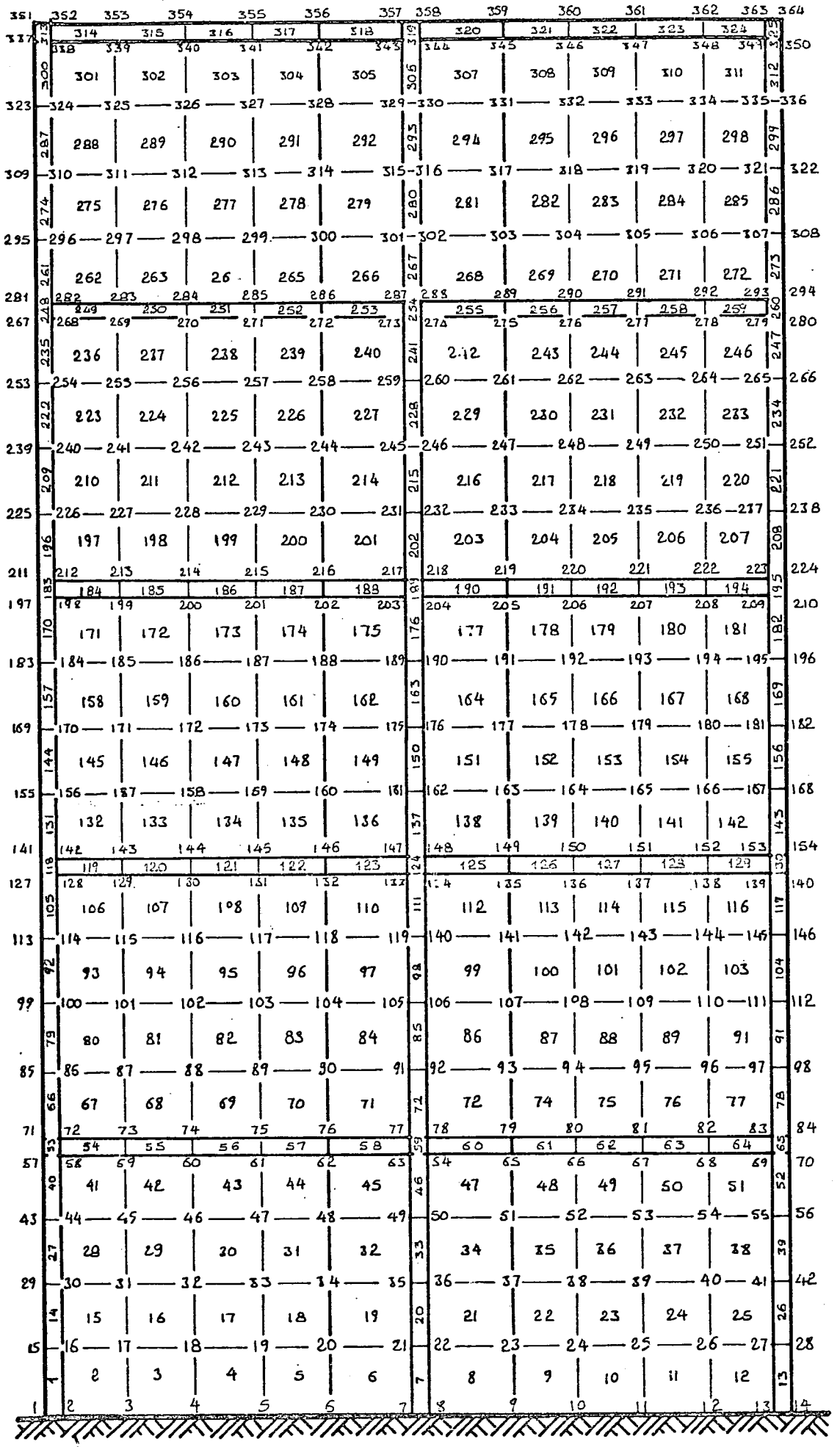

Fig. 4.1 Finite Element representation of the five storey structure

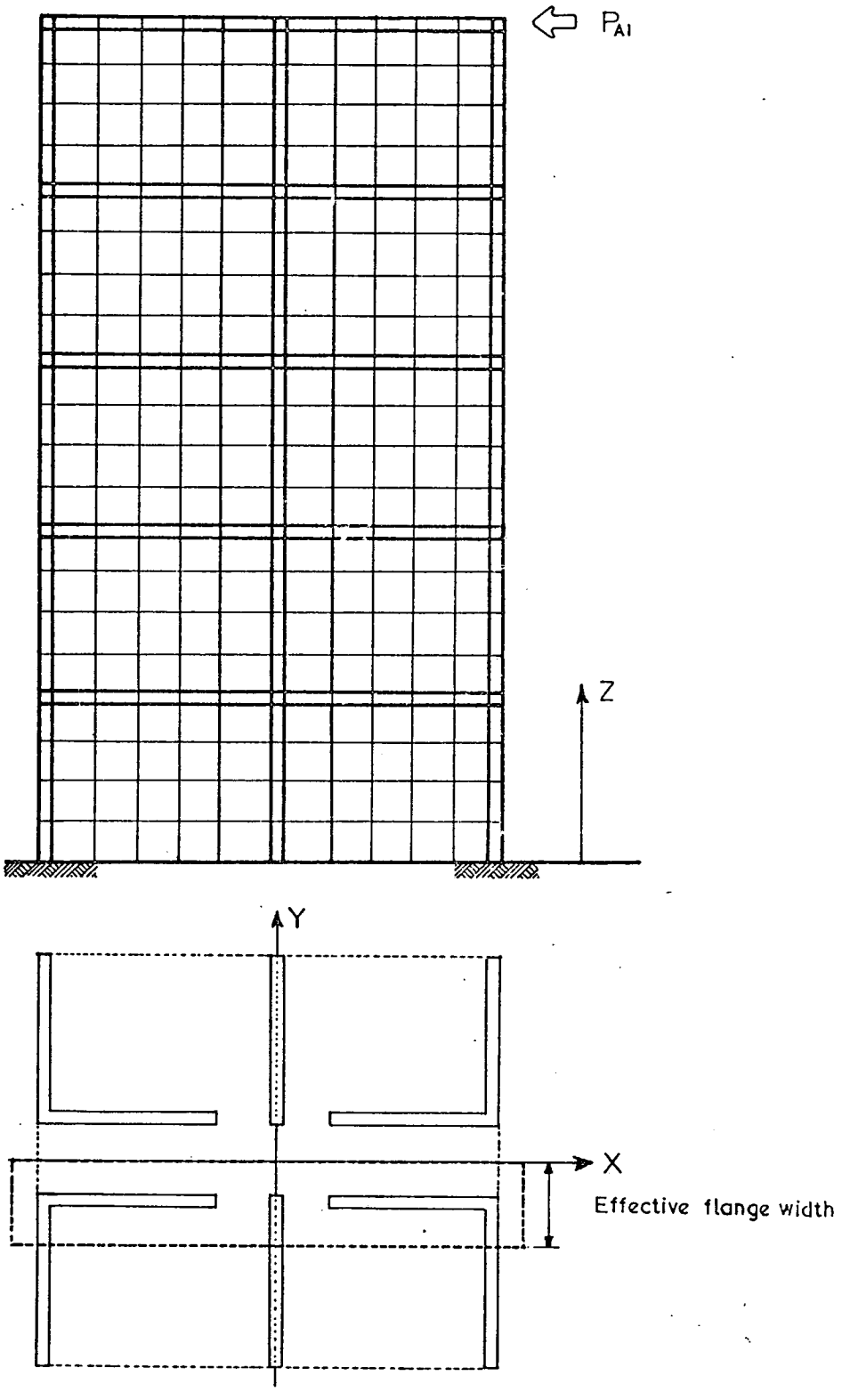

FIG. 4.2 PLAN AND ELEVATION

FIVE-STOREY STRUCTURE DIVIDED INTO FINITE ELEMENT

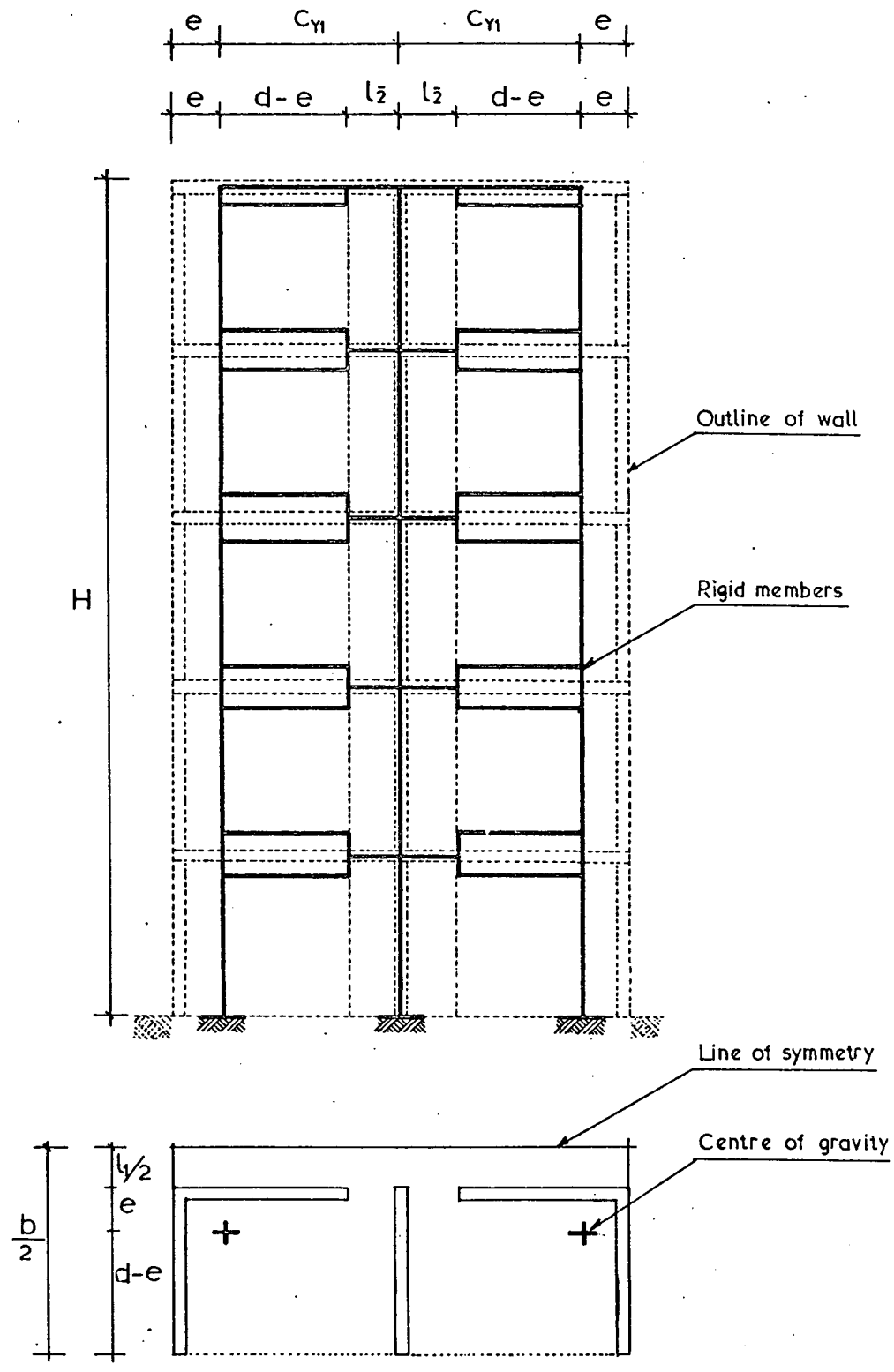

FIG. 4.3 PLAN AND ELEVATION OF BUILDING

WIDE COLUMN FRAME ANALOGY

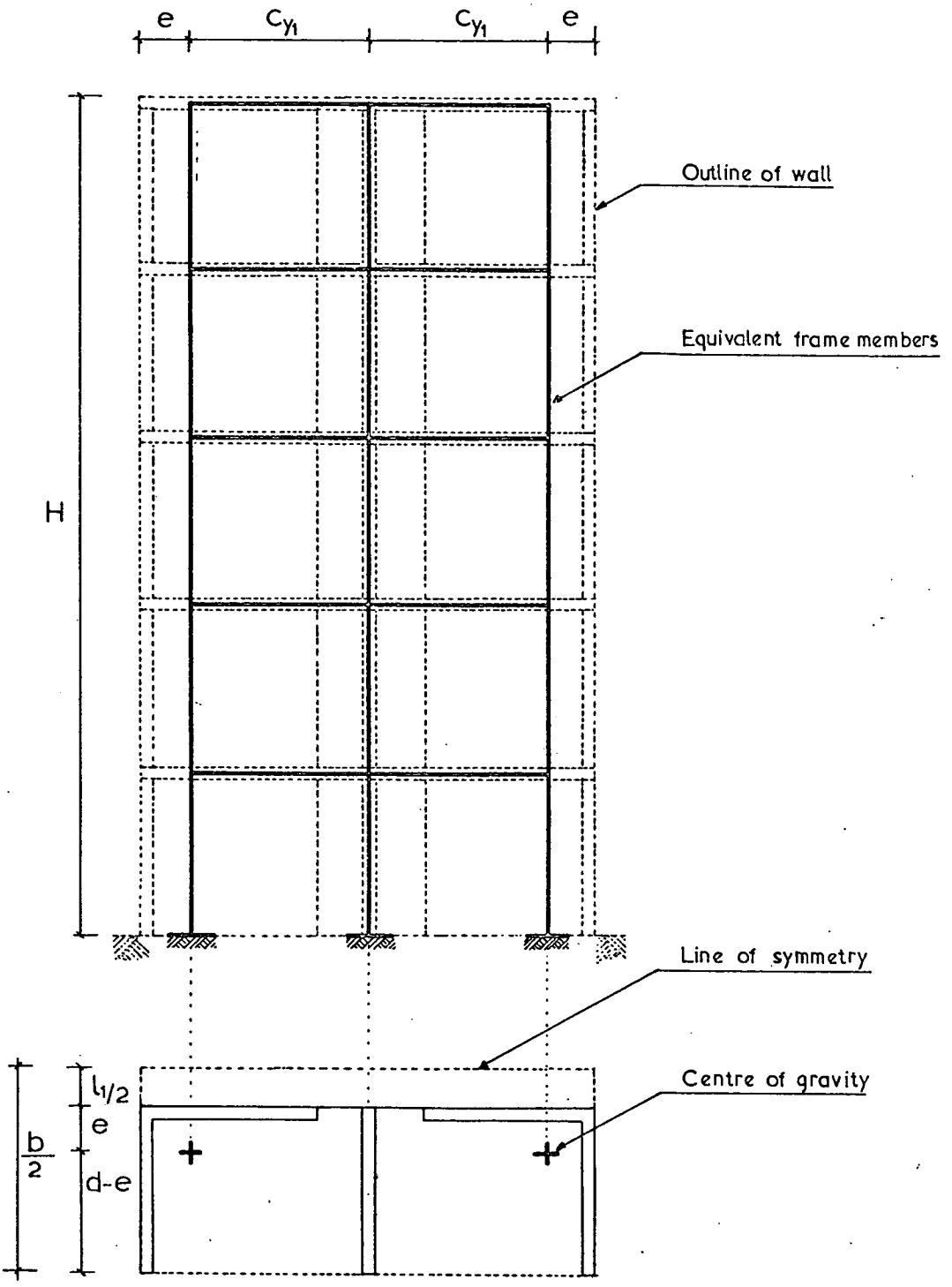

FIG. 4.4 ELEVATION AND PLAN OF BUILDING EQUIVALENT FRAME IDEALIZATION

the BS. CP 114 [61], from the equation 0.17h + t_w where h is the storey height and tw is the wall thickness.

The vertical strain distribution in the shear walls of the ground floor, under axial loading, was calculated by the finite element method. A reasonable agreement with the experimental values can be seen from Figure [4.9a]. The principal strain distribution in the ground floor, as shown in Figure [4.6] was also calculated. A similar pattern of strain distribution on the shear wall was obtained from experimental data shown in Figure [4.7]. The closest agreement is found near the foundations. The deflection, when calculated by the finite element method, is underestimated by 37% at the top storey, compared to the experimental, as shown in Figure [4.5]. The structure seems to be more flexible than expected analytically.

The wide column frame analogy considers the structure as a frame with beams which are assumed to be infinitely stiff from the centre of gravity of the angle section, to the edge of the actual opening, as shown in Figure [4.3]. By this method, the deflection was underestimated by 34%, about the same as by the finite element method. When the shear deformation on the columns and beams are included in the analysis, the discrepancy is reduced slightly.

In the equivalent frame analogy, the shear wall structure is replaced by columns having the same flexural rigidities as the walls. The slabs are replaced by beams with the same stiffness and with lengths equal to the distance between the centroidal axes of the neighbouring columns, as shown in Figure [4.4]. The deflection is overestimated by 10% at the top storey when compared with experimental

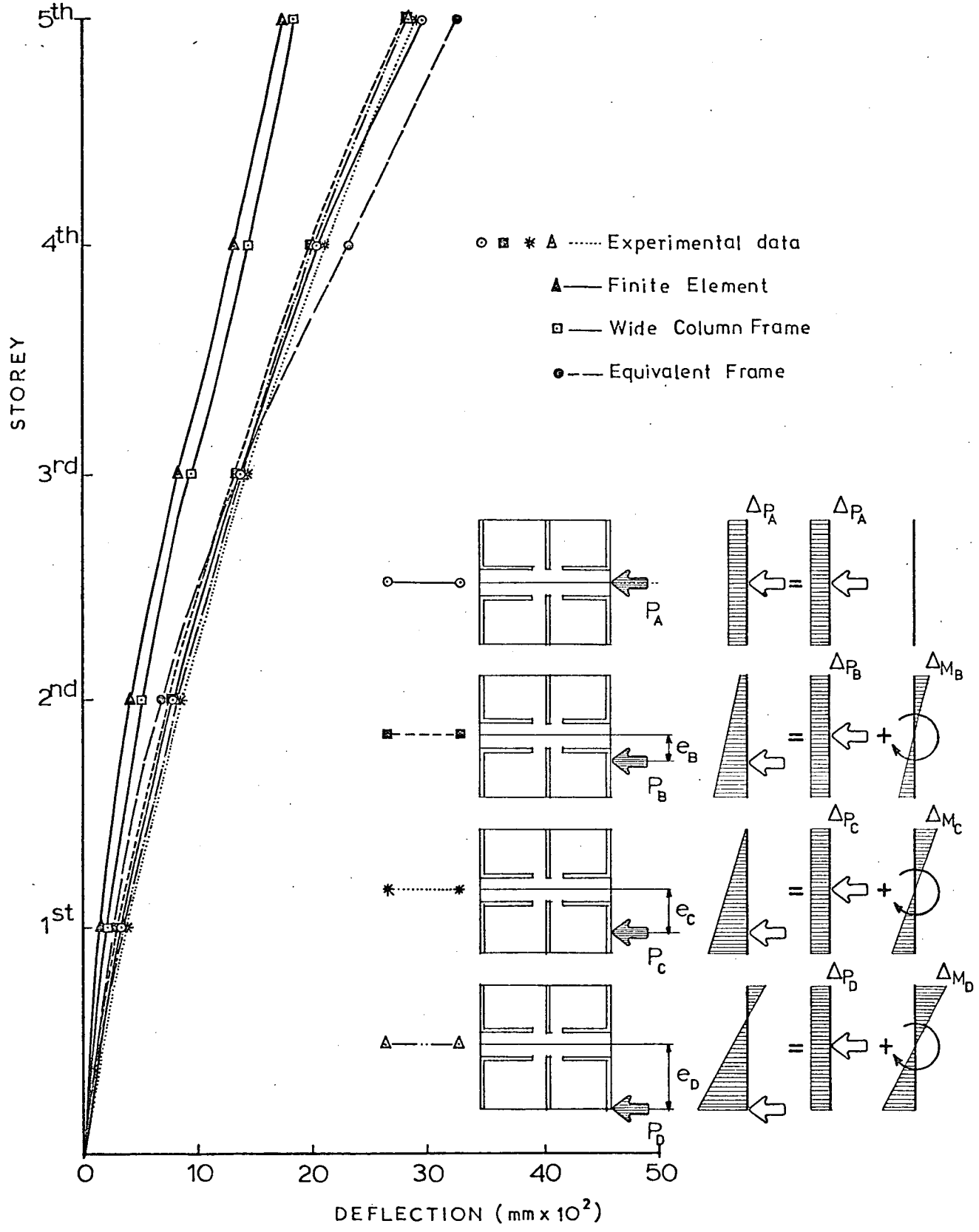

Fig. 4·5 Comparison of the analytical and experimental deflection results. $P_A = P_B = P_C = P_D = 2.88$ kN

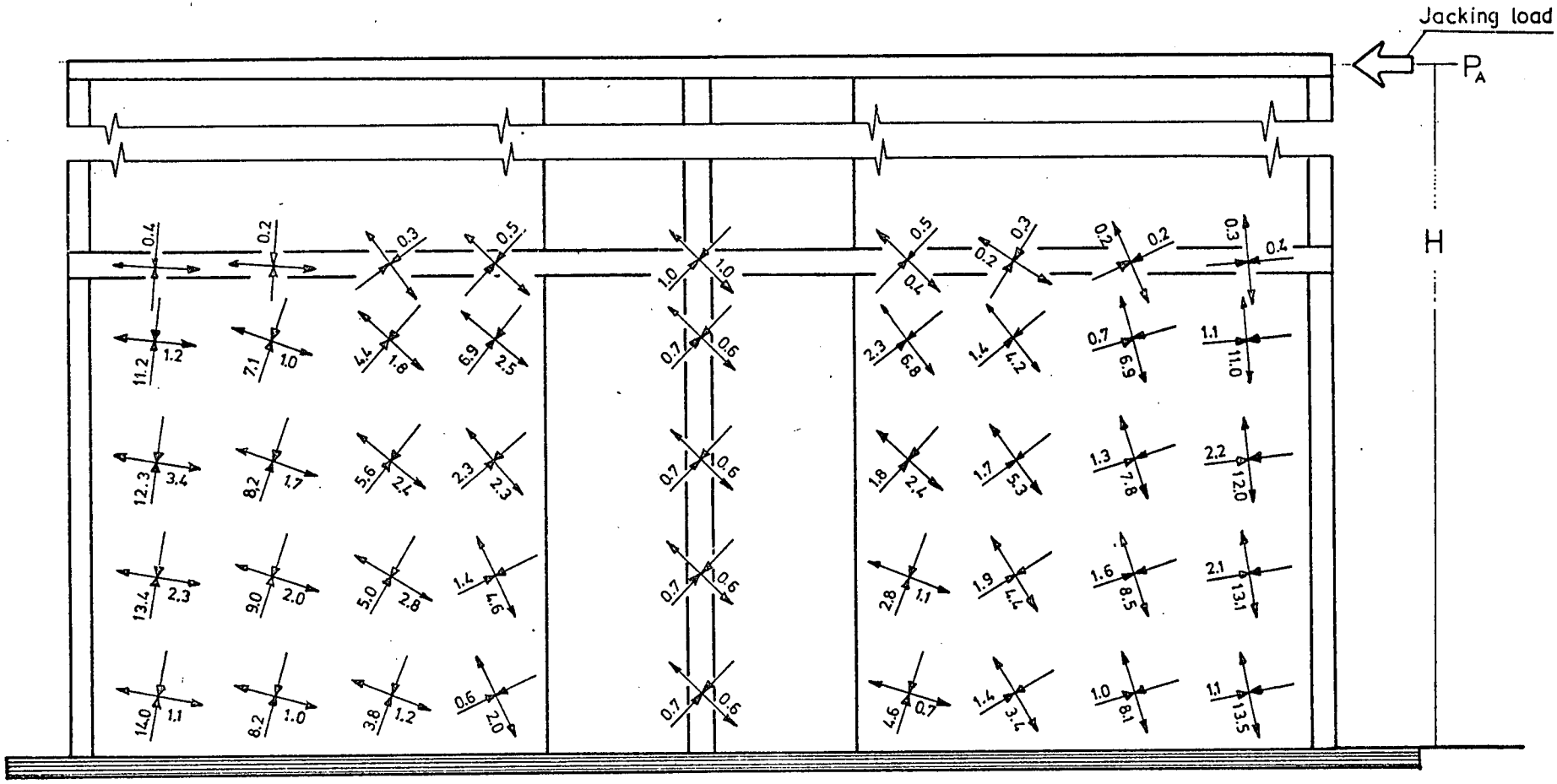

Fig. 4.6 Principal strain distribution in the ground floor shear walls, calculated from Finite Element. Load P_A = 3.00 kN

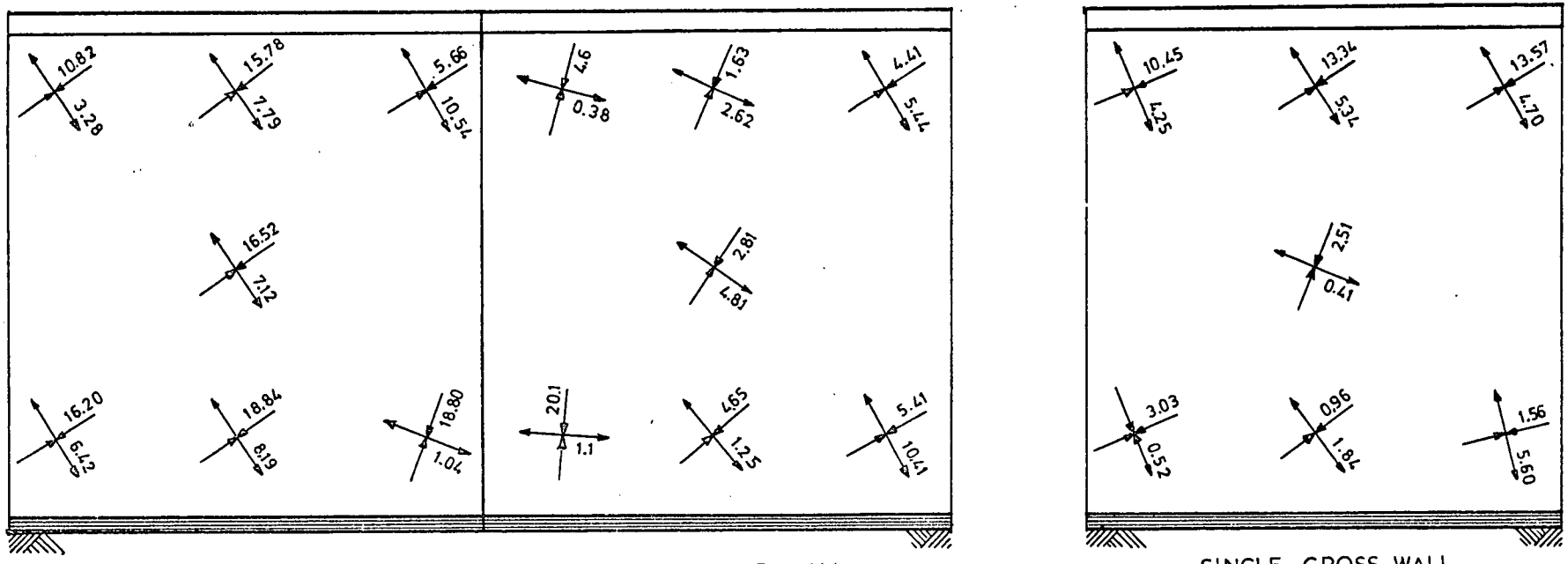

CROSS WALL AND CONNECTING SHEAR WALL

SINGLE CROSS WALL

Fig. 4.7 Principal strain distribution in the ground floor shear and cross walls, calculated from experimental results of axial loading (P_A). P_A = 3.00 kN

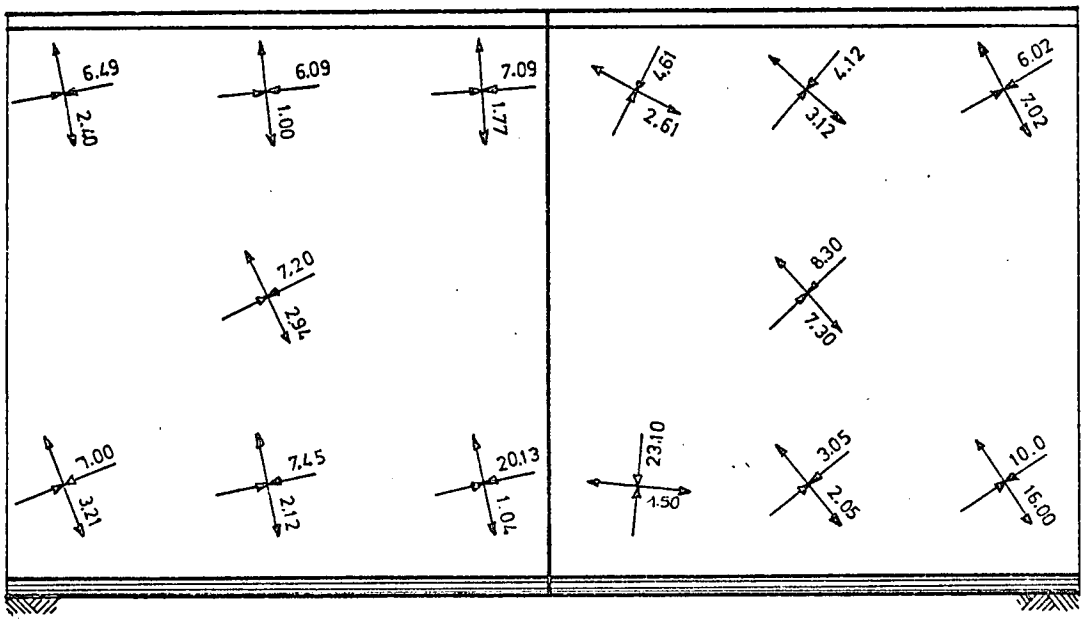

CROSS WALL AND CONNECTING SHEAR WALL

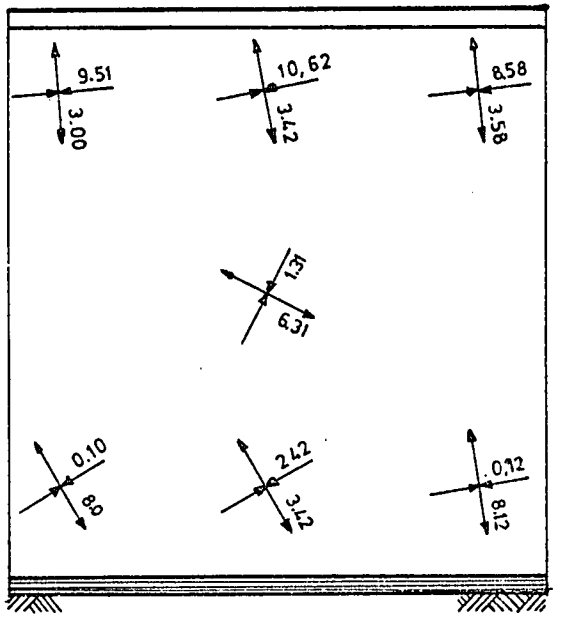

SINGLE CROSS WALL

Fig. 4.8 Principal strain distribution in the ground floor shear and cross wall, calculated from experimental results of eccentric loading (P_B) P_B = 3.00 kN

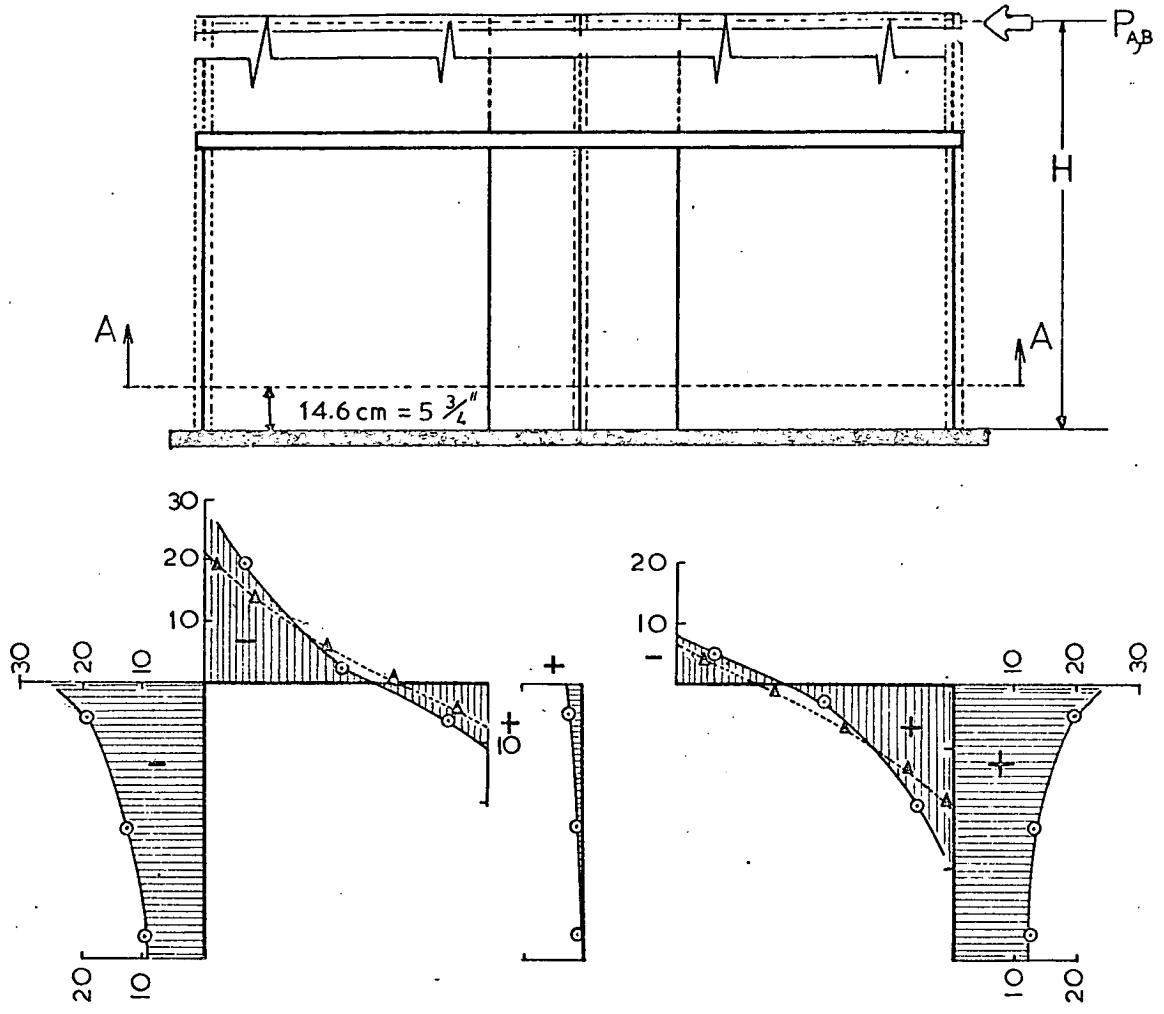

Fig. 4.9a

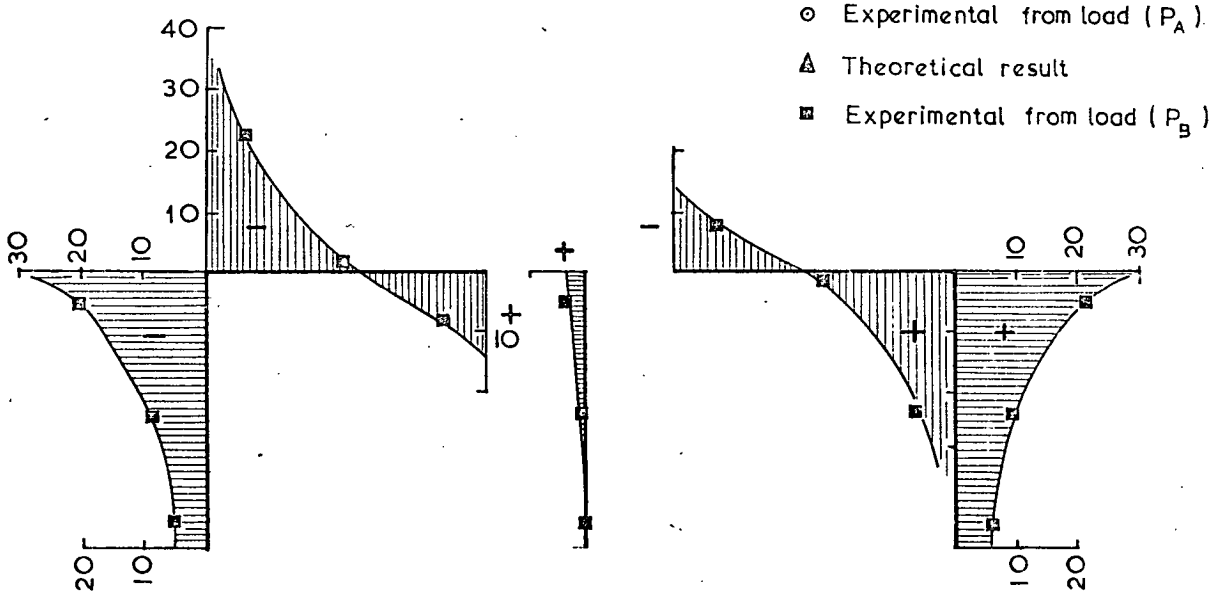

Fig. 4.9b

Vertical strain (ϵ_y) distribution in the shear walls, flanges and centre walls across section A - A Loads, $P_{A,B}$ = 3.00 kN

Fig. 4.9a Direct loading (P_A) experimental results compared with Finite Element

Fig. 4.9b Eccentric loading (P_B) experimental result.

results, but the discrepancy is reduced towards the base of the structure (Figure 4.5).

The same pattern of results, for the three methods presented, has been reported by numerous workers e.g. [40, 47, 50], but the degrees of discrepancy vary in the different reports.

3 - TORSIONAL ANALYSIS FOR STRUCTURE

A - INTRODUCTION

The solution for the experimental test structure by the proposed theory is presented below. The experimental structure is constructed of four angle and two single wall sections. In the theoretical assumptions, all the elements were considered independently and the stiffnesses calculated individually for each element. Consequently the warping stiffness is calculated as zero. In this type of section with only one joint, as exemplified,

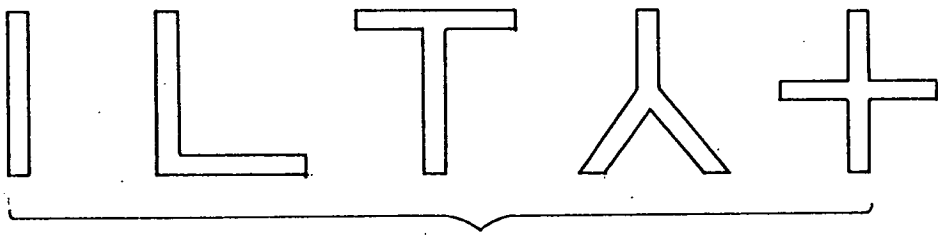

$\omega(s)_j = 0$ and $I_\omega = 0$

the cross-section has the shear centre CS_j at the intersection of the flanges and therefore the sectorial properties vanish everywhere; the sectorial co-ordinate $\omega(s) \equiv 0$ and the sectorial moment of inertia $I_\omega = 0$ (Appendix I). Thus there is no warping developed in such sections and these elements resist eccentric load by free torsion only. The value of Young's

modulus of elasticity (E) used in the calculation for the analyses of the test structure, was found by simple beam and wall tests, under pure bending and under compression, as described in Chapter III. The average of numerous test was taken and a value of 7.171 kN/m^2 (1.04 lbf/in^2) is used in the numerical solution. Poisson's ratio for blockwork was taken to be 0.18 and the shear modulus of elasticity (G) was calculated from the relationship $G = E/2(1+r) = E/2.36$.

B - DETAILS OF THEORETICAL SOLUTION AND EXPERIMENTAL RESULTS

H = 482.60 cm, (190 in)

h = 96.52 cm, (38 in)

a = 243.90 cm, (96 in)

b = 228.60 cm, (90 in)

C_{x1} = 48.26 cm, (19 in)

C_{y1} = 96.52 cm, (38 in)

e_B = 38.10 cm, (15 in)

e_C = 76.20 cm, (30 in)

e_D = 116.84 cm, (46 in)

e_{x1} = 25.40 cm, (10 in)

e_{x2} = 69.85 cm, (27.5 in)

e_{y_1} = 119.38 cm, (47 in)

t = 5.08 cm, (2 in)

l_1 = 45.70 cm, (18 in)

l_2 = 28.00 cm, (11 in)

Applied force and moment

P_B = 8800.22 N 1978.38 lbf

P_C = 4400.11 N 989.19 lbf

P_D = 2869.64 N 645.12 lbf

M_T = 3352.8825 Nm (29675.52 lbf in)

Moment of inertia

$I_{x1} = I_{y1}$ = 810870.434 cm^4 (19481.26 in^4)

I_{x2} = 1026.67 cm^4 (24.667 in^4)

I = 4832673013.3217 cm^6 (17996383.325 in^6)

Due to the symmetry of the structure about both axes, X-X and Y-Y, the calculations are simplified. The rotations were calculated by two forms of the governing equation; in one the slab effect was taken into consideration and in the other, it was neglected. Both sets of results are shown in Figure (4.10).

The experimental results plotted in Figure (4.10) show the average rotation calculated under various eccentric loadings, but with the same moment, as calculated from the load times eccentricity relationship. The longitudinal strain distribution of the walls in the ground floor at section A-A under eccentric loading (P_B) is given in Figure (4.8).

C - COMPARISON BETWEEN THEORY AND EXPERIMENTAL RESULTS

A comparison is made in Figure (4.10) between the theoretical and experimental results, by the angle of rotation. The difference between these two results is expressed as a percentage of the experimental

results, calculated for the top storey only. When a slab effect, which is based on the continuum approach of coupled shear wall analysis, is included in the calculations, the rotation is grossly underestimated compared with the experimental results. The predicted rotation is smaller by 38% at the top storey level but the analysis gives a close agreement with the experimental when the slab effect is neglected. In both forms of the theory, the warping stiffness is not taken into account. When the structure rotates under eccentric loading, the floor slabs, being coupled with the wall elements, attempt to warp and bend out of their plane but will be restrained by their stiffness. The experimentally measured vertical displacements given in Chapter III demonstrate that the slabs rotate in their plane and do not warp. The slab stiffness will also increase the torsional stiffness of the whole system. The discrepancies between the theoretical, including the slab effect and the experimental and theoretical neglecting the slab effect are likely due to the overestimation of the slab stiffnesses by the continuum method of analysis. Therefore, by the theory, slabs can have a large influence on the stiffness of the structure. The calculated rotation can be reduced by a maximum of about 38% of the rotation calculated without the slab effect. When, half the effective width of the floor slabs is considered in the theoretical calculations of area and moment of inertia the rotations approached nearer the experimental; they underestimated by about 30% of the experimental.

The total stresses can be obtained by the principal of superposition of the stresses due to direct loading and the stresses due to the

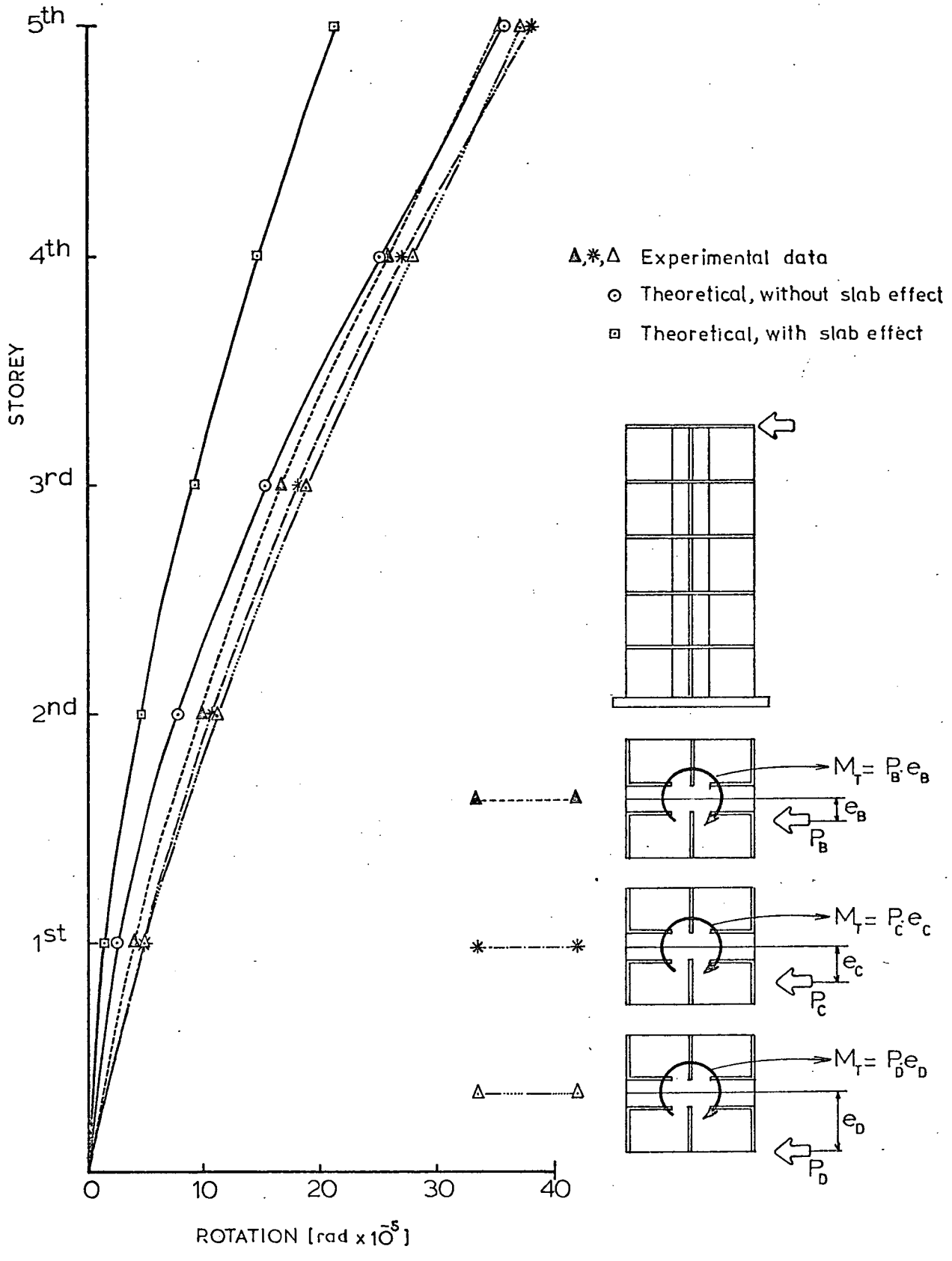

Fig. 4.10 Comparison of the experimental rotation results with theoretical results considering with and without the effect of slabs.

twisting moment. For direct loading stresses can be calculated using the finite element method. Figures (4.6),(4.7)and (4.9a) show that the experimentally measured strain distribution compares reasonably with the strains also calculated by the finite element method. The complementary warping stresses due to the twisting moment can be calculated using the sectorial area but in the test structure, the sectorial area becomes zero and so the warping stresses cannot be calculated.

Another typical structure was similarly analyzed to discover if this pattern of results was the general case and to verify the accuracy of the theory. Particularly since, in the test structure, warping is calculated as zero, due to the sectorial properties of the elements. It was desirable to analyze a structure where the magnitude of the stiffness contribution from warping could be found, as well as that from the slab effect.

4 - SYMMETRICAL CHANNEL STRUCTURE

A - INTRODUCTION

In this section a method is presented for the analysis of a symmetrical channel cross-section connected by floor slabs, using the modified theory as previously detailed in Chapter II. The experimental results referred to were obtained by Kalita [37] from tests on a four storey, one-sixth scale brickwork model. The model structure is shown in plate (4.1) and (4.2). The bricks had a mean crushing strength of 3865 lbf/in^2. The loads were applied eccentrically at each floor level to simulate wind loading and produced both bending and torsional deformations. The loads on the 1st to 3rd storeys were equal and the load on the roof slab was half of the load applied at the other slab levels.

B - EXPERIMENTAL RESULTS

The results of the deflections produced on walls A and B, under eccentric loadings are shown in Figures (4.11) and (4.12). The storey against the rotation results are given in Figure (4.13) and Table (4.1). The stresses calculated from the measured strain on the web are shown in Figure (4.14).

C - NUMERICAL SOLUTIONS

The numerical values for the theoretical calculations are given below. The test structure dimension terms are shown in Figure (2.9)

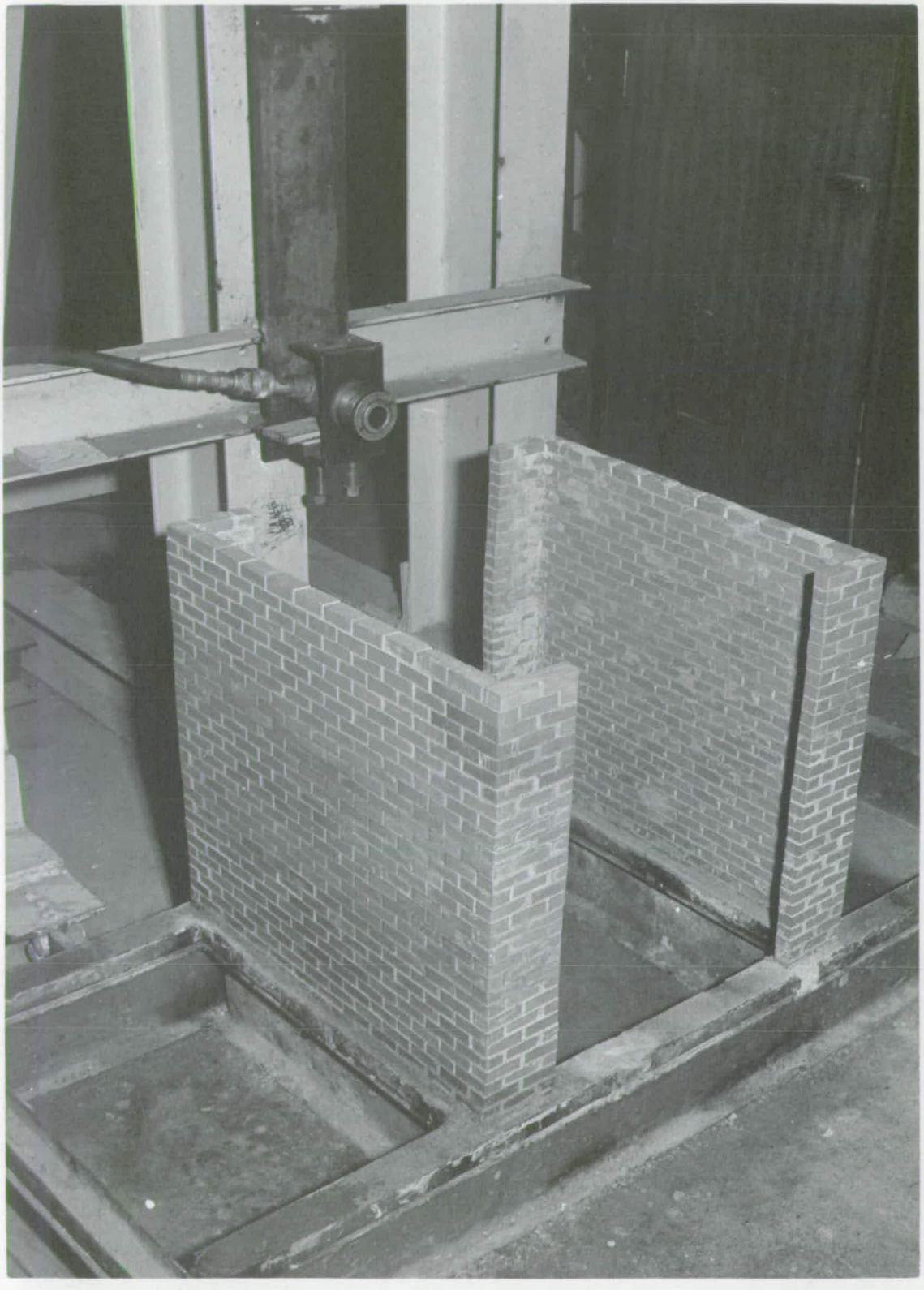

PLATE 4.1 TORTION CORE WALLS OF STRUCTURE USED BY KALITA SHOWING CONSTRUCTION IN SITU.

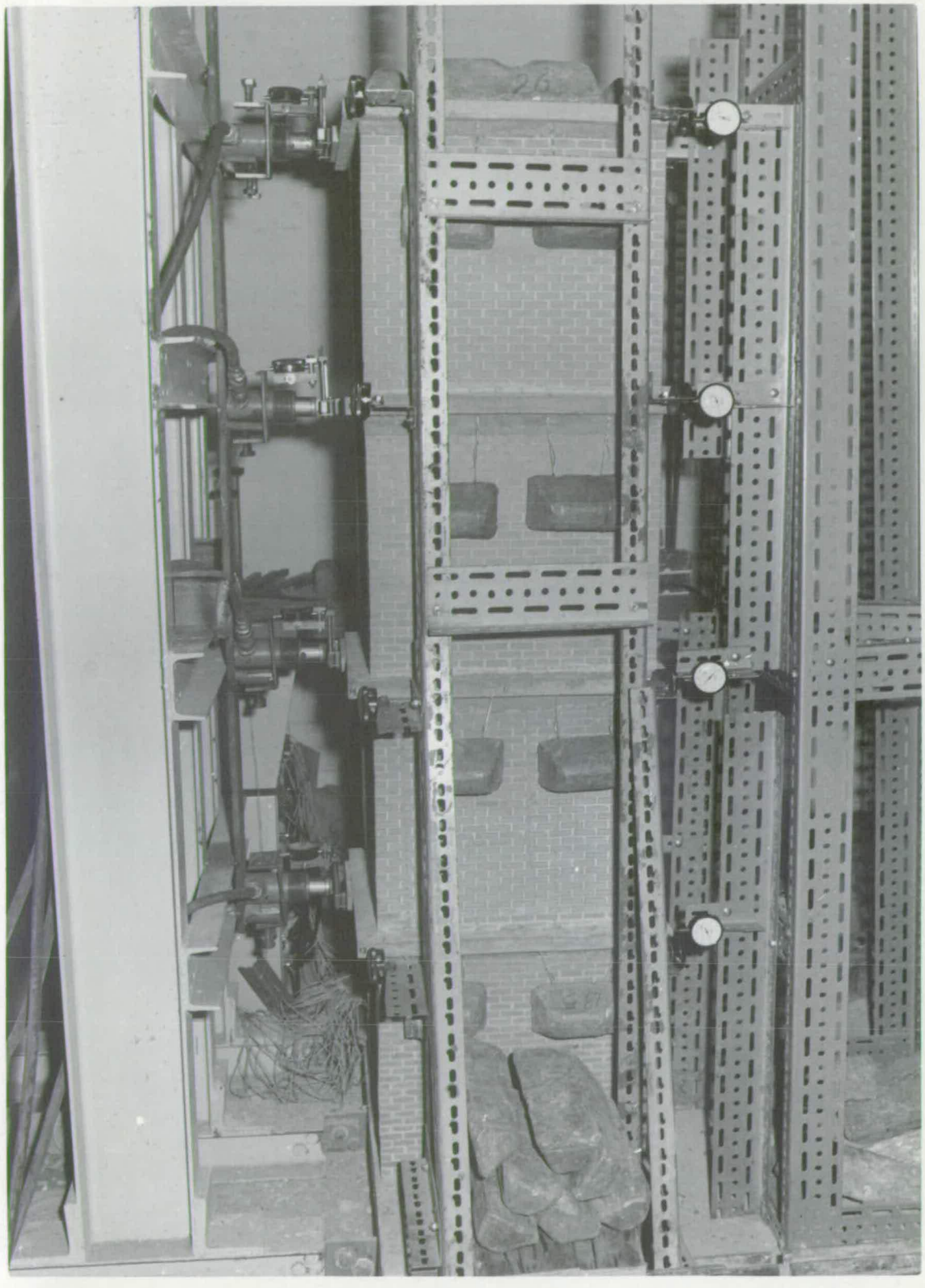

PLATE 4.2 ONE SIXTH SCALE BRICKWORK FOUR STOREY MODEL STRUCTURE UNDER TEST BY KALITA

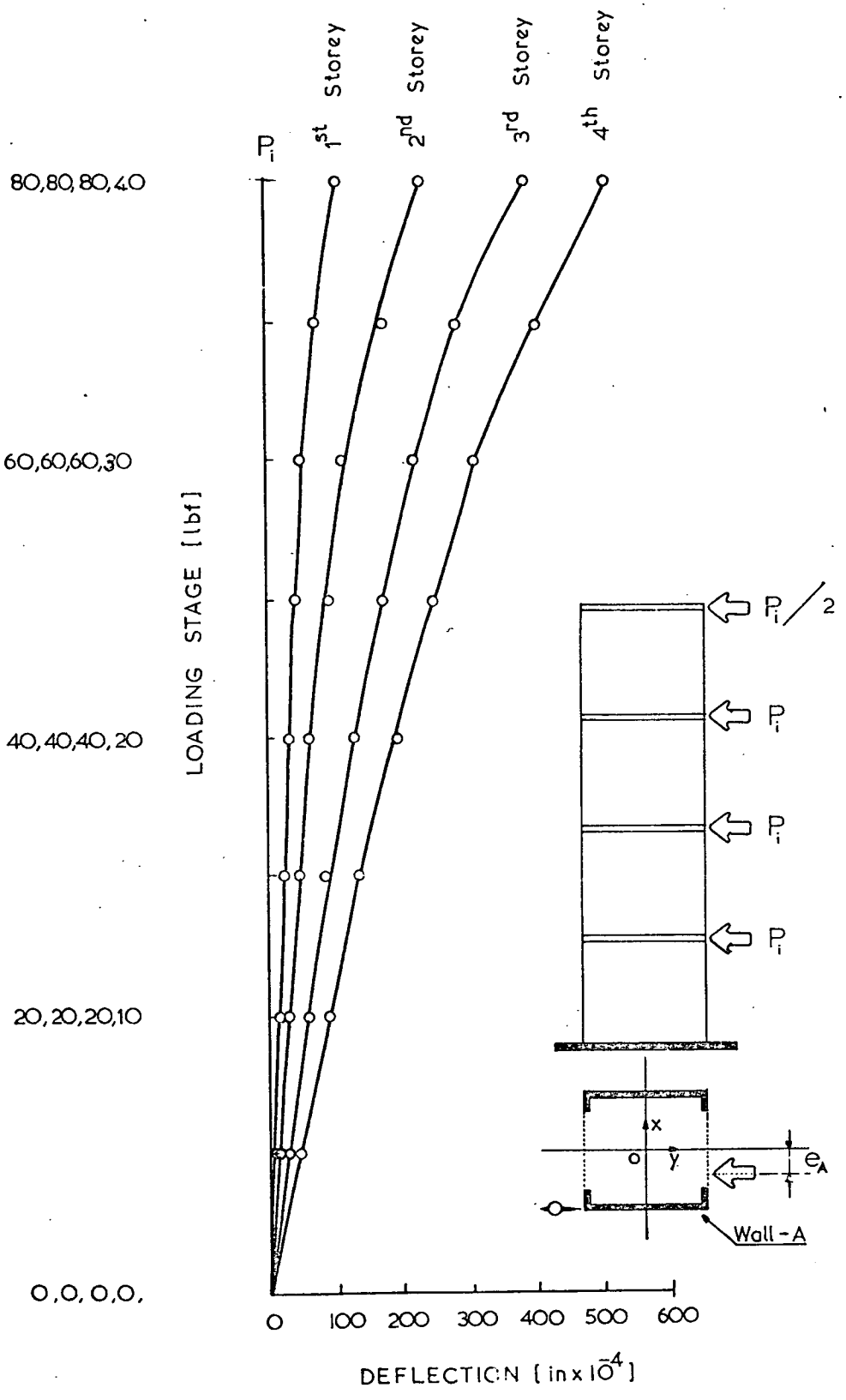

Fig. 4.11 Load / Deflection curves for wall A at various floor levels (Y- Direction) from 'Kalita'

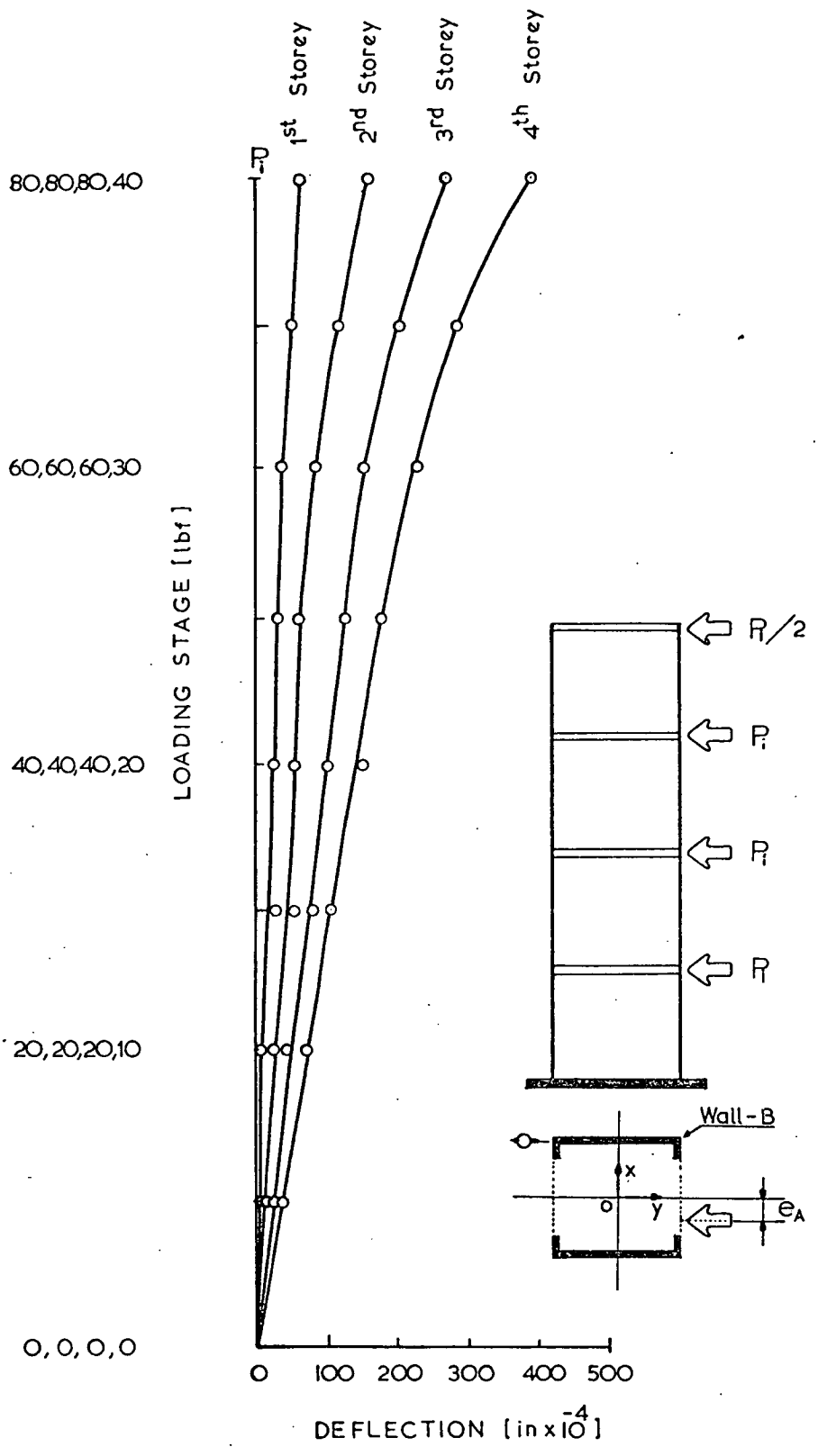

Fig. 4.12 Load / Deflection curves for wall-B- at various floor levels (Y.-Direction) from 'Kalita'

$H = 68^{1}$ in

$h = 17$ in

$a = b = 16.69$ in

$C_{x1} = C_{x2} = 8.02$ in

$d = 2.655$ in

$e_{x1} = {}_{x2} = 8.995$ in

$e_{1} = {}_{2} = 0.65$ in

$l_{1} = {}_{2} = 11.38$ in

$t = 0.69$ in

$\rho = 1.0$ in, slab depth

$G = E/2.2$ lbf/in^2

$I_{x1} = I_{x2} = 522.61$ in^4

$P_{1,2,3} = 40$ lbf for each storey

$p_{4} = 20$ lbf top floor

$e_{A} = 3.0$ in load eccentricity

Young's modulus of elasticity was taken as 0.98×10^6 lbf/in^2, from Sinha [50] and was constant throughout the structure.

D - COMPARISON AND DISCUSSION

Comparisons are made between the experimental results and various forms of the proposed theory, in Figure (4.13) and Table (4.1). The difference between the theory and experimental results is expressed as a percentage of the experimental results, calculated for the top storey only.

When all terms (St. Venant torsion, slab effect, shear forces and warping effects) of the governing equation are considered in the solution of the rotation of the structure, the results were 22%

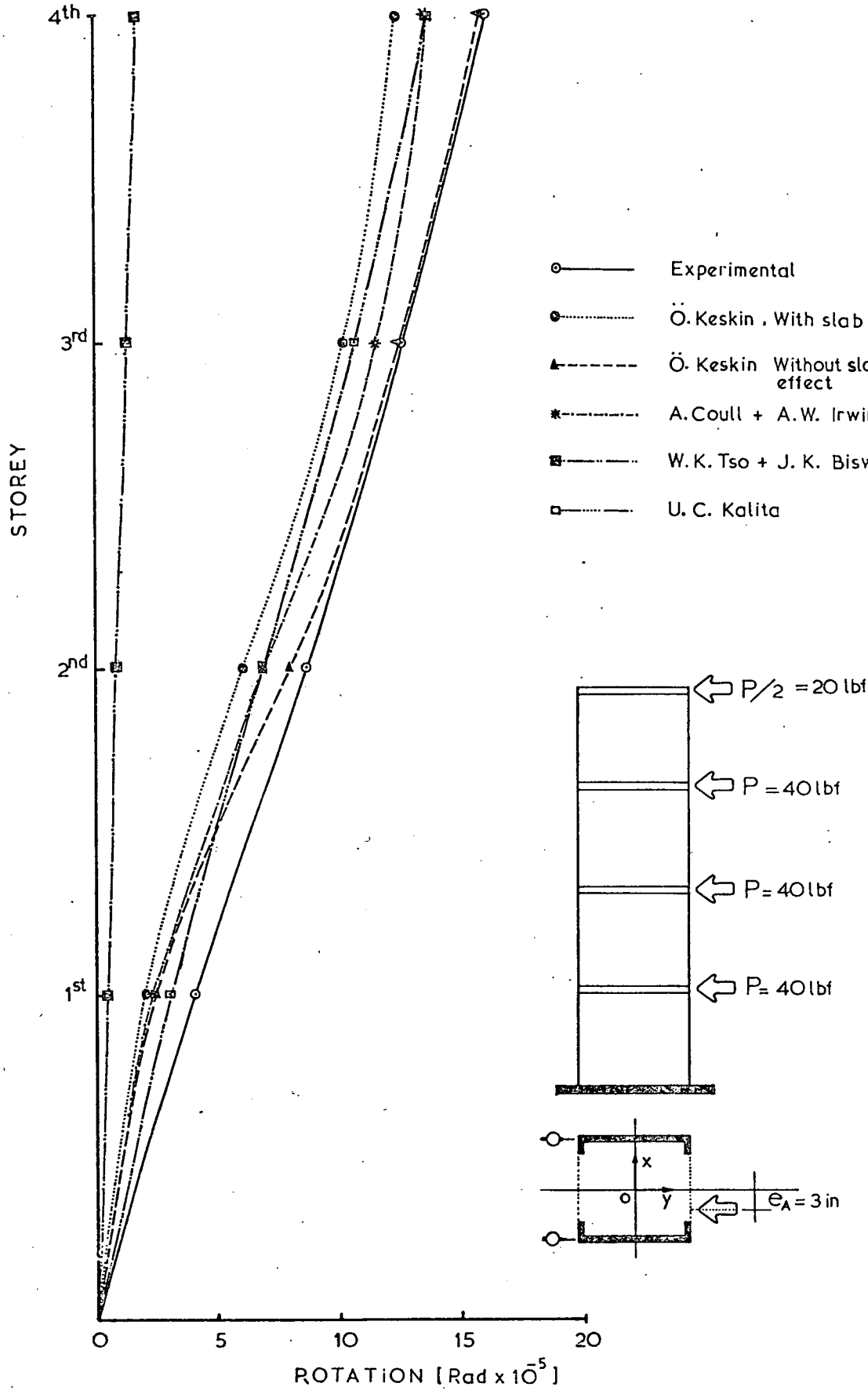

Fig.4.13 Storey / Rotation curves for structure. Comparison of theoretical and experimental results from "Kalita

$E = 0.98 \times 10^6$ lbf/in^2		St. Venant Torsion	Slab Effect	Shear Forces Effect	Warping Effect	ROTATION, [Rad $\times 10^{-5}$] For EACH STOREY				Percentage difference from experimental
						1st	2nd	3rd	4th	
A. COULL A.W. IRWIN		GK_T	EK_{SC}	EI^*	EI_{WC}	2.2	6.8	11.4	13.6	15 %
W.K. TSO		GK_T	EK_{ST}	EI^*	EI_{WT}	0.4	0.9	1.2	1.5	91%
Ö. KESKİN	1	GK_T	EK_{SK}	EI^*	EI_{WK}	2.0	6.2	10.3	12.3	22%
	2	GK_T	—	EI^*	EI_{WK}	2.4	7.6	13.0	15.5	2%
	3	GK_T	—	EI^*	—	2.4	7.7	13.2	15.7	1 %
	4	GK_T	—	—	EI_{WK}	98.0	263.	386.	431.	—
U.C. KALITA*		FROM J.R. BENJAMIN				3.2	6.8	10.1	13.6	15%
U.C. KALITA'S EXPERIMENTAL DATA						4.1	8.6	12.5	15.9	

Table 4.1 Comparison of theoretical and experimental results, showing the terms of rotation included in the formulae and the percentage difference. The terms are listed below

$$EI_{WC} = \frac{Eb^2t}{196}\left[b - l - t\right]\left[1 + \frac{b^3 t}{4\, I_{xx}}\right]$$

$$EI_{WT} = \frac{Eb^2t}{12}\left[\frac{b^2}{4}\left(b + 6d\right) + d^2\left(3b + 2d\right)\right]$$

$$EI_{WK} = \frac{Eb^2t}{12}\left[be + 2d^3 - 6de\left(d - e\right)\right]$$

AND

$$EK_{SC} = \frac{24 E I_d b^3 e_x}{hl^3}$$

$$EK_{ST} = 2E\left[be + b^2\right]^2 \lambda_1$$

$$EK_{SK} = m_{c1}\bar{m}_{c1}\lambda_1 E = \frac{Eb^2}{2}\left[b + e_x\right]\left[b + c_x\right]\lambda_1$$

AND

$$GK_T = \frac{2G}{3}\left[b + 2d\right]t^3 \qquad \text{AND} \qquad I^* = \sum_{i=1}^{i=2}\left(I_{x_i} e_{x_i}^2 + I_{y_i} e_{y_i}^2\right)$$

* $E_1, E_2, E_3, E_4 = \left[0.26 \times 10^6 \text{ to } 0.12 \times 10^6\right]$ lbf/in^2

smaller than the experimentally calculated rotations. The discrepancy is most likely due to the overestimation of the floor slab stiffnesses in the theoretical solution. Secondly, if the slab effect is neglected in the calculations the theoretical rotation compares very closely with the experimental, there being only a 2% difference, see table (4.1). It may be suggested from these two sets of results that the slab effect is contributing to 20% of the underestimation of the calculated rotation. A very close agreement, only 1% difference is observed between theory and experimental when both the slab effect and warping effect are neglected. Therefore, the warping effect, in the theory, may be considered to contribute to 1% of the calculated rotation. The difference is so insignificant because the coupling action of the slabs makes the whole section deform in plane, when the structure rotates. Finally, when only the warping and St. Venant torsion effects are considered in the governing equation, the value of rotation is much higher than the experimental value. Therefore, the bending due to shear forces acting through the individual element's shear centre, in the X-X and Y-Y directions, has a significant influence on the torsional stiffnesses of the structure.

For further comparison, the core wall structure was analysed by the theories of other workers, who developed their theories for this type of structure. The theory recently presented by Tso and Biswas 1974 (57) for the cove wall structure, was applied to the present symmetrical channel cross section. The calculated rotation is shown in Figure (4.13) and Table (4.1). Very poor agreement is obtained with the experimental results because, according to the

authors the sectorial parameters such as the sectorial co-ordinate $\omega(s)_j$ and the warping moment of inertia I_ω are calculated with respect to the rotation centre of whole structure. Their calculated slab coefficient K_{ST} and sectorial moment of inertia $I_{\omega T}$ are given below table (4.1). Therefore, the calculated warping and slab stiffnesses are grossly overestimated. The error in this interpretation is emphasised when the structure is wider, i.e. the core walls are further apart in the X-X direction, thus the initial radius between the pole and the centre line of the wall becomes longer. The calculated sectorial moment of inertia I_ω becomes much greater compared with the bending stiffness. The calculated rotations in these circumstances become underestimated and the warping stresses can be larger than expected. Possibly, if the shear force effect acting on the elements shear centre is neglected in this formula, a reasonable agreement with the experimental may be found, as was shown by Taranath [53]. He also calculated the sectorial moment of inertia I_ω about the centre of rotation of the core, and neglected the shear force effect on the wall element. As a result of these assumptions he concluded the warping stiffness to be of major importance when the torsional load predominated.

Better agreement with the experimental was obtained by applying the theory as suggested by Coull and Irwin (21). The rotation is underestimated by 15%. This compares more favourably with the experimental, than the proposed theory including the effect of the slabs, which underestimates by 22%. This difference is mainly from the slab stiffness EK_{SC}, which is given below table (4.1). Their torsional stiffness $EI_{\omega c}$ for the channel cross section was derived from standard 'strength of materials' formulae also given below table (4.1).

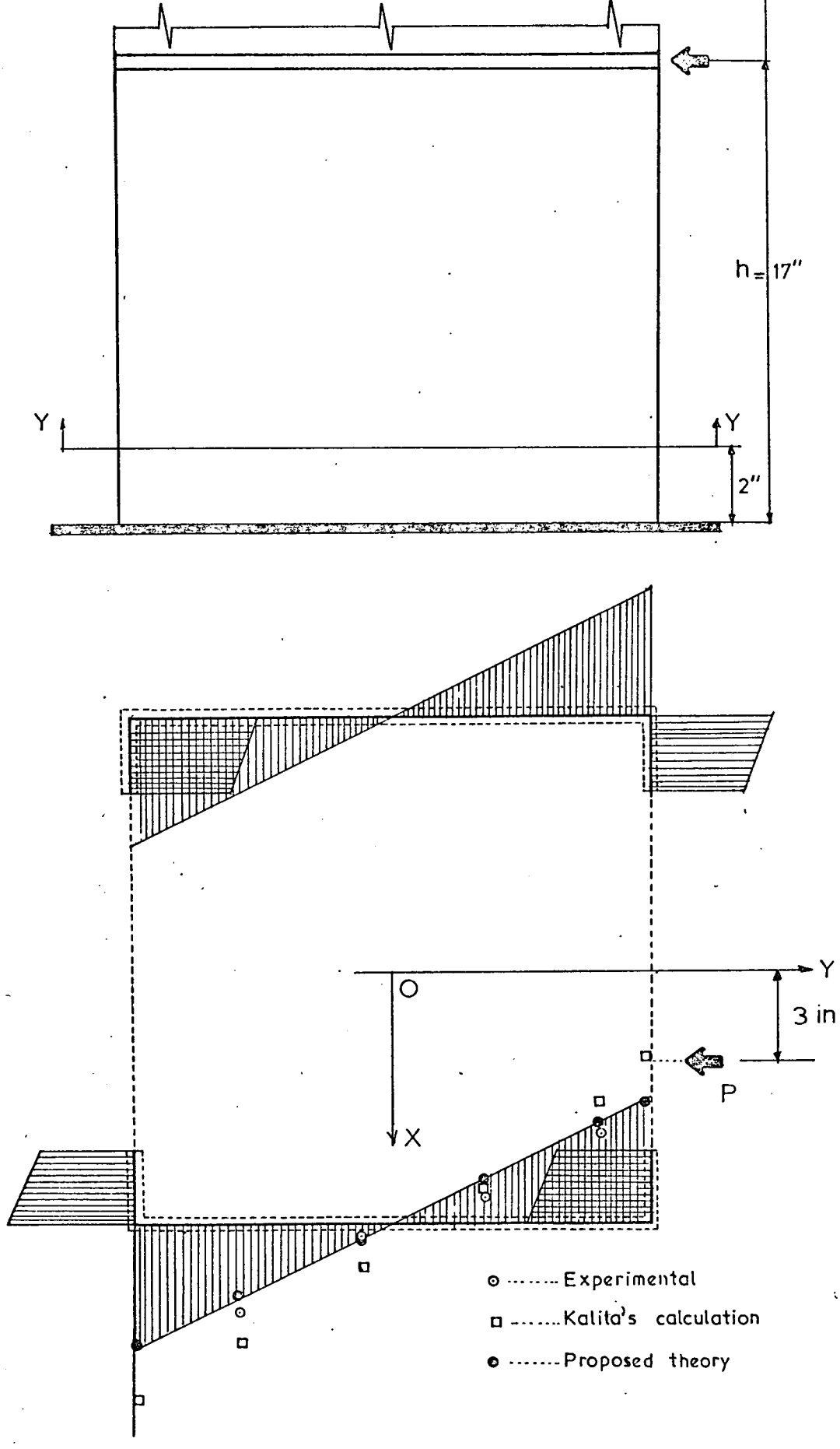

Fig. 4.14 Vertical stress distribution in the web at section Y-Y.

Finally, when this structure is analysed by the method presented by Kalita [37] the calculated rotation is underestimated by 15% compared with the experimental. But, in the calculations the modulus of elasticity (E) value used was very small and varied for each storey from 0.26×10^6 to 0.12×10^6 lbf/in^2 for 1st to 4th floors, respectively. From the present investigation, this was found not to be the case, for the E value.

The longitudinal strain distribution was measured by electric gauges placed on the web of the bottom storey, at section Y-Y of wall A, and the results of the calculated stresses are given in Figure (4.14). In the figure, the stresses are compared with the results calculated by the theory presented by Kalita [37] and the theory proposed in this thesis. The approximate analysis of stress at section Y-Y due to twisting moment and direct loading, can be obtained from the principal of superposition. On comparison of theory and experimental, the stress calculated from the theory, including the slab effect, compared closely with the experimental, but without the slab effect, the stress was over estimated. The figure also shows that the stress calculated by Kalita's theory overestimates more than the proposed theory.

5 - DISCUSSION

The same general pattern of results has been obtained from analysis of the channel cross-section, as from the analysis of the test structure.

The measured values of strain are in close enough agreement with the pattern of strain distribution expected on the assumption of the walls acting independently to make this assumption feasible. The true behaviour of the walls lies somewhere between complete composite action and complete independent action, the true action being decided by the degree of coupling and stiffness of the floor slabs [63].

In both structures it appears that the stiffness of the floor slabs considerably increases the strength and stiffness of the whole structure. The analytical results, including the slab effect were gross underestimates of rotation compared with the experimental results and when the slab effect was neglected there was close agreement, but still a slight underestimate. The experimentally observed behaviour of the structures should be between the theoretical predictions. The discrepancy may be due to various reasons, one being rotation at the base of the structure. The base deformations are probably very small but they may change the entire behaviour of the structure because the shear wall and diaphragm distortions are so small. Additionally, each structure will not behave as idealized in the theory due to interaction between the various structural elements, non-homogeneity of the material, shrinkage cracks and workmanship in masonry construction.

A structure can be classified as warpable or warpless, depending upon the shape of the wall elements. From the analytical and experimental data presented for the warpable symmetrical channel structure, it can be seen that the warping stiffness was of little importance. Neglect of warping stiffness of slabs and wall elements would appear not to have a profound effect but should be included where practicable for better accuracy. The proposed theory, not including the slab effect, seems to be suitable for analysis of both warpable and warpless structures.

6 - GENERAL CONCLUSION

In this thesis, the problem of a shear wall system with openings and coupled by floor slabs has been analyzed for bending and torsion. As a result of the study, the following conclusions can be made.

1 - The wide column frame analogy and finite element methods give about the same underestimated values for deflection when compared with the experiment data, although finite element gives a satisfactory prediction of stresses. Better agreement with the experimental results for bending deformation is provided by the equivalent frame analogy which usually gives tolerably overestimated values. Also this method, as well as the wide column frame analogy is much more efficient computationally than finite element.

2 - The calculated results obtained from the proposed theory outlined in Chapter II are in close agreement with the experimental values measured from a one-third scale model.

3 - The results calculated by the theory modified for a different plan form are in agreement with the results from tests on a one-sixth

scale model, taken from Kalita [37].

4 - From comparison of both structures, it has been shown that analytical results for rotation are improved if stiffness of the slabs is neglected. Warping is of negligible effect.

5 - Shear forces associated with the bending of the shear walls are not negligible and cause serious error when neglected.

6 - Comparison between results calculated by the proposed theory and the theories of other workers, given in Table 4.1, shows that the proposed theory compares favourably with these other theories and is simpler to apply.

7 - SUGGESTION FOR FUTURE WORK

A large number of problems connected with shear wall structures still remain to be considered. Some suggestions for future research which are relevant to the present thesis, have been outlined below.

1 - In the present study a three dimensional 1/3rd scale model was tested under lateral point loading at the top of the structure. Further experimental work should be carried out on the model when distributed lateral loadings are applied. A comparison may then be made between the experimental results and those obtained using the method of analysis presented in this thesis. Also, special attention should be paid to the measurement of the movement and rotation at the base of the structure.

2 - Another type of warpable structure should be tested to find the magnitude of any additional warping stiffness and stresses, over that calculated on the assumption that the walls act independently in torsion.

3 - A range of structures of different magnitudes and plan form should be analysed using the proposed theory and the results compared with the experimental values measured on actual structures (or models).

4 - Since rotation at base of structure greatly affects the calculated results, an attempt should be made to calculate the degree of fixity at the base of real structures.

REFERENCES

[1] Amaratunga, M.M. "AN INVESTIGATION INTO THE LINEAR ELASTIC BEHAVIOUR OF STRUCTURAL WALLS CONTAINING OPENINGS", Ph.D. Thesis University of Southampton, 1962.

[2] Beck, H. "CONTRIBUTION OF THE ANALYSIS OF COUPLED SHEAR WALLS" Journal of A.C.I., Vol. 59 Aug. 1962, pp. 1055-69.

[3] Benjamin, J.R. "STATICALLY INDETERMINATE STRUCTURES" McGraw-Hill Book Co., Inc., London, 1959.

[4] British Standards Institution: "SPECIFICATION FOR PRECAST CONCRETE BLOCKS" B.S. 2028 1364 AMD 411 Jan. 1970.

[5] British Standards Institution: "SPECIFICATION FOR BUILDING SANDS" B.S. 1198 PD 4835 March 1963.

[6] British Standards Institution: "FORTLAND CEMENT, ORDINARY AND RAPID HARDENING" B.S. 12 Part -2- 1971.

[7] British Standards Institution: "SPECIFICATION FOR BUILDING LIMES" B.S. 890, 1972.

[8] British Standards Institution: "CODE OF BASIC DATA OF THE DESIGN OF BUILDINGS' CP 3 Chapter V: Loading part 2 1972

[9] British Standards Institution: "STRUCTURAL RECCOMENDATION FOR LOAD-BEARING WALLS" CP 111 part 2 AMD 744 June 1971.

[10] Blume, J.A., Newmark, M.N. and Corning, L.H. "DESIGN OF MULTISTOREY REINFORCED CONCRETE BUILDINGS FOR EARTHQUAKE MOTIONS" Portland Cement Association 1961.

[11] Biswas, J.K. and Tso, W.K. DISCUSSION OF "LATERAL-LOAD ANALYSIS OF ASYMMETRIC MULTISTOREY STRUCTURES", by Jacob Gluck, Journal of the Structural Division, A.S.C.E. Vol. 96, No ST11, Nov. 1970 pp. 2540-44.

[12] Burns, R. "AN APPROXIMATE METHOD OF ANALYSIS OF COUPLED SHEAR WALL SUBJECTED TO TRIANGULAR LOADINGS" proc. third world conference on Earthquake Engineering. New-Zealand, 1965.

[13] Clough, W., King, I.P. and Wilson, E.L. "STRUCTURAL ANALYSIS OF MULTISTOREY BUILDINGS" Journal of the Structural Division, A.S.C.E. No. ST3, June, 1964.

[14] Chitty, L. "ON THE CANTILEVER COMPOSED OF A NUMBER OF PARALLEL BEAMS INTERCONNECTED BY CROSS-BARS", Phil. Mag., Series 7, Vol. 38, 1947 pp. 685-99.

[15] Chitty, L. and Wan, Wen-Juh. "TALL BUILDING STRUCTURES UNDER WIND LOAD" Proc. Int. Conf. for Appl. Mech. Vol. 1 paper 22 1948 pp.254-68.

[16] Coull, A. and Chaudhury, J.R. "STRESSES AND DEFLECTIONS IN COUPLED SHEAR WALLS". Journal of A.C.I. March 1967, pp. 05-72.

[17] Coull, A. and Puri, R.D. "ANALYSIS OF PIERCED SHEAR WALLS" Journal of the Structural Division, A.S.C.E., Vol. 94, No. ST1 Proc. Paper 5710, January, 1968, pp. 71-82.

[18] Coull, A. "INTERACTIONS BETWEEN COUPLED SHEAR WALLS AND CANTILEVERED CORES IN THREE-DIMENSIONAL REGULAR SYMMETRICAL CROSS-WALL STRUCTURES" Proceedings the instituion of civil engineers, part 2, Vol. 55, December 1973, pp. 827-40.

[19] Coull, A. and Irwin, A.W. "LOAD DISTRIBUTION IN MULTISTOREY SHEAR WALL STRUCTURES" Proc. 8th Congress of I.A.B.S.E. New York, Sept. 1968 pp. 994-1004.

[20] Coull, A. and Irwin, A.W. "ANALYSIS OF LOAD DISTRIBUTION IN MULTI-STOREY SHEAR WALL STRUCTURES" The Structural Engineer, Vol. 48, No. 8 August 1970, pp. 301-307.

[21] Coull, A. and Irwin, A.W. "TORSIONAL ANALYSIS OF MULTISTOREY SHEAR WALL STRUCTURES" To be published in Journal of A.C.I. 1974.

[22] Coull, A. and Stafford Smith, B. "TORSION ANALYSIS OF SYMMETRIC BUILDING STRUCTURES" Journal of the Structural Division A.S.C.E. Vol. 99 No. ST1 1973.

[23] Galambos, T.V. "STRUCTURAL MEMBERS AND FRAMES" Prentice-Hall Inc., Englewood Cliffs, N.J. 1968.

[24] Gluck, J. "LATERAL-LOAD ANALYSIS OF ASYMMETRIC MULTISTOREY STRUCTURES" Journal of the Structural Division A.S.C.E. Vol. 96, No. ST2 Proc. Paper 7089, Feb. 1970, pp. 317-33.

[25] Gluck, J., Gellert, M., and Danay, A. "DYNAMICS OF ASYMMETRIC MULTISTOREY STRUCTURES" I.A.B.S.E. Vol. 32-1 1972 pp. 72-90.

[26] Gluck, J., Gellert, M., and Danay, A. "DYNAMICS OF ASYMMETRIC MULTISTOREY STRUCTURES" I.A.B.S.E. Vol. 32-1 1972 pp. 91-107.

[27] Gluck, J. and Winokur, A. "STATICAL ANALYSIS OF MULTISTOREY STRUCTURES" Publication No. 075, Faculty of Civil Eng. Tecknion Israel Inst. of Tech. Halfa 1965.

[28] Gluck, J., Gellert, M., and Danay, A. "THE AXIAL STRAIN EFFECTS ON LOAD DISTRIBUTI IN NONSYMMETRIC TIER BUILDINGS", Buildings S Vol. 9 Pergamon Press, 1974. pp. 29,38.

[29] Green, N.B. "BRACING WALLS FOR MULTISTOREY BUILDINGS" Journal of A.C.I. Vol. 49 1952. pp. 233-45.

[30] HARRISON, T. "THE ELASTIC BEHAVIOUR OF STRUCTURES COMPOSED OF INTERCONNECTED THIN-WALLED MEMBERS" Ph.D Thesis, Univ. of Bradfrod 197

[31] Heidebrecht, C. and Stafford Smith, B. "APPROXIMATE ANALYSIS OF OPEN SECTION SHEAR WALLS SUBJECT TO TORSIONAL LOADING". Journal of the Structural Division, A.S.C.E. No. ST12 December, 1973. pp. 2355-73.

[32] Heidebrecht, C. and Swift, R.D. "ANALYSIS OF ASYMMETRICAL COUPLED SHEAR-WALLS" Journal of the Structural Division A.S.C.E., No. ST5 proc. paper 8100 pp. 1407-23, May, 1971.

[33] Irwin, A.W. "ANALYSIS OF SHEAR WALL STRUCTURES", Ph.D. Thesis, University of Strathclyde. June, 1970.

[34] Jaeger, L.G., Mufti, A.A. and Mamet, J.C. "THE STRUCTURAL ANALYSIS OF TALL BUILDINGS HAVING IRREGULARLY POSITIONED SHEAR WALLS", Building Sci. Vol. 0 Pergamon Press, 1972 pp. 1-12.

[35] Jenkins, W.M. and Harrison, T. "ANALYSIS OF TALL BUILDINGS WITH SHEAR WALLS UNDER BENDING AND TORSION" and DISCUSSION. Tall buildings (proc. symp. Tall Buildings) Pergamon, 1967, pp. 413-44.

[36] Jenkins, W.M. "MATRIX AND DIGITAL COMPUTER METHODS IN STRUCTURAL ANALYSIS" McGraw-hill 1968.

[37] Kalita, U.C. "EXPERIMENTAL AND THEORETICAL STUDIES OF THE STRUCTURAL BEHAVIOUR OF BRICKWORK CROSS-WALL SYSTEMS" Ph.D. Thesis, University of Edinburgh, May, 1970.

[38] Macleod, I.A. "LATERAL STIFFNESS OF SHEAR WALLS WITH OPENINGS" Ph.D. Thesis Glasgow University, 1966.

[39] Macleod, I.A. "NEW RECTANGULAR FINITE ELEMENT FOR SHEAR-WALL ANALYSIS" Journal of Structural Division A.S.C.E. March 1969. pp. 399-09.

[40] Macleod, I.A. and Green, D.R. "FRAME IDEALIZATION FOR SHEAR WALL SUPPORT SYSTEMS" The Structural Engineer, Vol. 51 No. 2 Feb. 1973. pp. 71-74.

[41] Maurenbrecher, A.H.P., Sinha, B.P. and Hendry, A.W. "MODEL AND FULL-SCALE TEST ON A FIVE-STOREY BRICK CROSS-WALL STRUCTURE UNDER LATERAL LOADING". S.I.B.M.A.C., Proceedings, April, 1970.

[42] Michael, D. "TORSION COUPLING OF CORE WALLS IN TALL BUILDINGS" The Structural Engineer Vol. 47, No. 2 Feb. 1959 pp. 87-91.

[43] Murthy, C.K. and Hendry, A.W. "INVESTIGATION OF THE BEHAVIOUR OF A THREE-STOREY CROSS-WALL STRUCTURE" SCRU - Publication No. CRM/3/4 1964.

[44] Rosman, R. "APPROXIMATE ANALYSIS OF SHEAR WALLS SUBJECT TO LATERAL LOADS" Journal of A.C.I., Vol. 61 No. 6 June, 1964 pp. 717-32.

[45] Rosman, R. "AN APPROXIMATE METHOD OF ANALYSIS OF WALLS OF MULTISTOREY BUILDINGS" Civil Engineering and Public Works Review (London) Vol. 59, 1964, pp. 67-69.

[46] Rosman, R. "TORSION OF PERFORATED CONCRETE SHAFTS" Journal of Structural Division, A.S.C.E., Vol. 95 No ST5 May 1969 pp. 991-1010.

[47] Rostampour, M. "ASPECTS OF THE DESIGN OF THE MULTI-STOREY BUILDINGS IN LIGHT-WEIGHT CONCRETE BLOCKWORK". Ph.D. Thesis University of Edinburgh, July 1973.

[48] Schwaighofer, J. and Microys, F.H. "ANALYSIS OF SHEAR WALL STRUCTURES USING STANDARD COMPUTER PROGRAMS". Journal of A.C.I., Vol. 66 No. 12, December 1969. pp. 1005.

[49] Seto, Y. "ANALYSIS OF SINGLE-STOREY SHEAR WALL STRUCTURES". Journal of A.C.I., June, 1967, pp. 191-196.

[50] Sinha, B.P. "MODEL STUDIES RELATED TO LOAD-BEARING BRICKWORK", Ph.D. Thesis University of Edinburgh, May, 1967.

[51] Sinha, B.P. and Hendry, A.W. "THE LATERAL LOAD ANALYSIS OF BRICK MULTI-STOREY SHEAR-WALL STRUCTURES". Third International Brick Masonry Conference, Essen. W.G. 1973.

[52] Stafford Smith, B. and Taranath, B.S. "THE ANALYSIS OF TALL CORE-SUPPORTED STRUCTURES SUBJECT TO TORSION" Proceedings of the Institution of Civil Engineerings part 2, Vol. 53, September, 1972. pp. 173-187.

[53] Taranath, B.S. "THE TORSIONAL BEHAVIOUR OF OPEN SECTION SHEAR WALL STRUCTURE" Ph.D. Thesis, University of Southampton, 1968.

[54] Timoshenko, S. and Young, D.H. "ELEMENTS OF STRENGTH OF MATERIALS" Fifth edition, D. Van Nostrand Company, Inc. 1968.

[55] Timoshenko, S. "STRENGTH OF MATERIALS" Part 2, Third Edition, June, 1970.

[56] Tso, W.K. and Biswas, J.K. "GENERAL ANALYSIS OF NONPLANAR COUPLED SHEAR WALLS" Journal of the Structural Division, A.S.C.E., No. ST3, March, 1973. pp. 365-81.

[57] Tso, W.K. and Biswas, J.K. "ANALYSIS OF CORE WALL STRUCTURE SUBJECTED TO APPLIED TORQUE" Building Sci. Vol. 8, 1973, pp. 251-257.

[58] Vlasov, V.Z. "THIN-WALLED ELASTIC BEAMS" Translated from the Russian by the Israel Program for Scientific Translations, Jerusalem, 1961.

[59] Vlasov, V.Z. "THIN-WALLED BEAMS FROM THEORY TO PRACTICE" By K. Zbirohowski-Koscia, Dip. Ing. London, 1966.

[60] Winokur, A. and Gluck, J. "LATERAL LOADS IN ASYMMETRIC MULTISTOREY STRUCTURES" Journal of the Structural Division A.S.C.E., Vol. 94, No ST3, March, 1968. pp. 645-53.

Additional References

[61] British Standards Institution — REINFORCED CONCRETE CP. 114 1958.

[62] Hendry, A.W. — "ELEMENTS OF EXPERIMENTAL STRESS ANALYSIS" Oxford, 1964.

[63] Coull, A. — "TEST ON A MODEL SHEAR WALL STRUCTURE" Civil Engineering and Public Works Review, September, 1966 pp. 1129-31.

[64] Macleod, I.A. — "LATERAL STIFFNESS OF SHEAR WALLS WITH OPENINGS" Tall Buildings (Proc. Symp. Tall Buildings) Pergamon 1967 pp. 223-244.

APPENDIX -I-

SECTORIAL PROPERTIES OF A SECTION

The sectorial properties of a section may be found using the theory of thin-walled beams [59]. In Figure (-I-) the sectorial co-ordinate of any point S_i is defined as the double area enclosed by straight lines PO and PS_i and curved line OS_i measured from the pole P and with initial radius PO. A sectorial co-ordinate is denoted by $\omega(s)_i$ and the units of measurement are in^2, ft^2, cm^2 or m^2. The sign of the sectorial co-ordinate is negative if the angle $\sphericalangle OPS_i$ is measured from the radius PO in an anticlockwise direction, and positive if the angle $\sphericalangle OPS_2$ is measured in a clockwise direction.

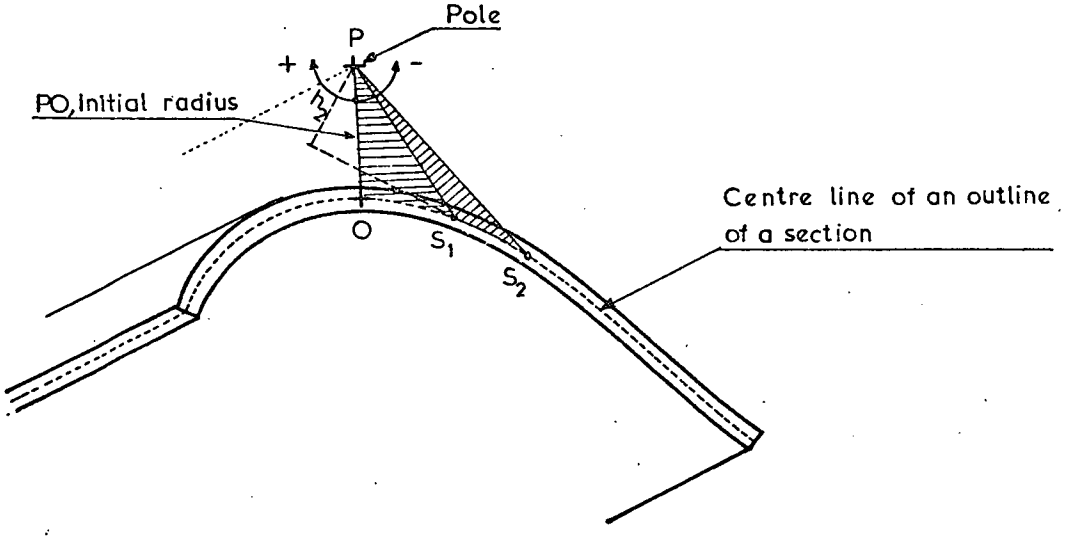

Figure -I-

a) In the example shown in Figure (-I-) the value of $\omega(s)_i$ is equal ($i = 1,2$) to the algebraic sum of twice the sum of area OPS_1 and S_1PS_2 or any point between O and S_i is as

$$\omega(s)_i = \int_0^{s_i} d\omega(s) = \int_0^{s_i} h_{(s)i}\, ds$$

where: S_i is the length of a centre line of the section measured from point O and $h_{(S)i}$ is the function of S representing the distance between the pole P and the line tangential to the outline of the point of the co-ordinate S.

For the calculation of internal stresses due to bimoment and flexural twist, additional properties built up from the sectorial co-ordinate $\omega_{(S)i}$ must be known.

b) The sectorial statical moment of inertia of a section in (in^4, ft^4, cm^4 or m^4) from a pole P and initial radius PO is given by

$$S_\omega = \int_A \omega \, dA$$

c) The sectorial moment of inertia of a section in (in^6, ft^6, cm^6, or m^6) from a pole P with an initial radius PO can be calculated as

$$I_\omega = \int_A \omega^2 \, dA$$

APPENDIX -II-

FLEXURAL STRAIN MEASUREMENT CORRECTION

When the vibrating wire gauge is fitted on the wall by the metal plate, the wire is a finite distance from the wall surface. If this distance is appreciable compared to the wall's depth the measured strain will be considerably higher than the true value. Therefore, a correction factor must be applied to the strain readings, as demonstrated in the figure.

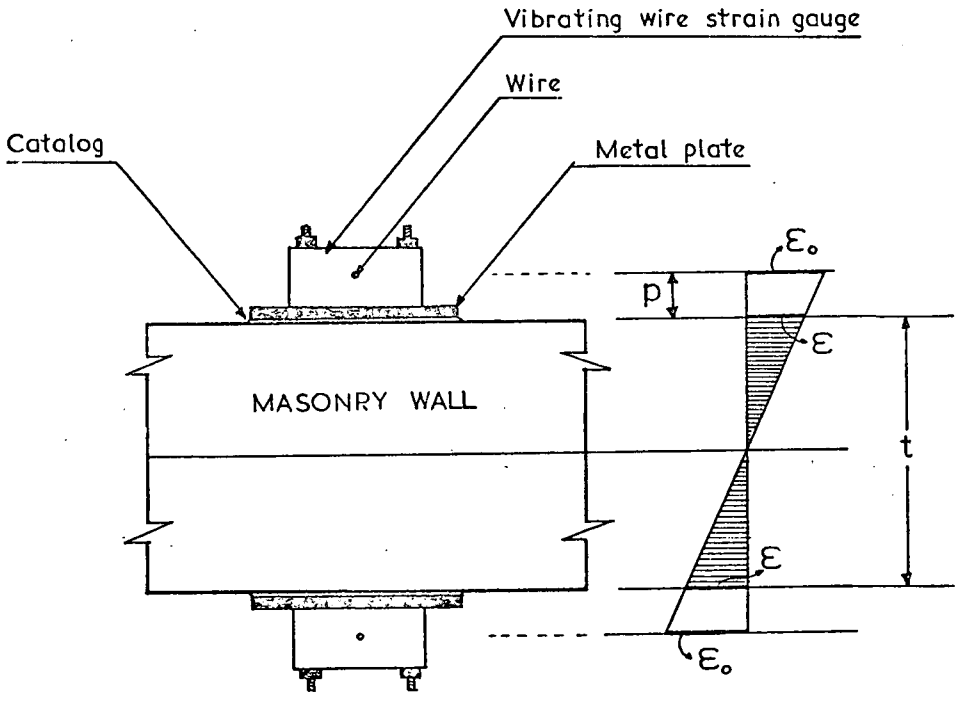

$$\varepsilon = \varepsilon_0 \beta$$

in which $\beta = \dfrac{t}{t + p}$

ε_0 = measured strain on the wire

ε = true strain on the wall

p = distance of vibrating wire from the wall surface

t = thickness of the wall

APPENDIX -III-

CALCULATION OF THE PRINCIPAL STRAIN

The direction of the principal strains are not normally known in advance and so the measurements must be made in many arbitrary directions. The arbitrary gauge lines, inclined at α_1, α_2 and α_3 to the x-x axis are sufficient to measure the strains. The calculations are simplified by having $\alpha_1 = 0^\circ$ $\alpha_2 = 45^\circ$ and $\alpha_3 = 90^\circ$ as shown in Figure.

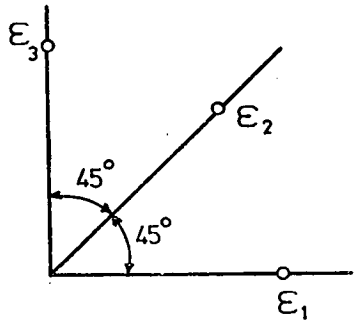

STPAIN ROSETTES

The principal strains and their directions are calculated by the formulae as suggested by Hendry [*].

$$\varepsilon_{p,q} = \frac{\varepsilon_1 \quad \varepsilon_3}{2} \pm \frac{\sqrt{2}}{2} \sqrt{\left[\varepsilon_1 - \varepsilon_2\right]^2 + \left[\varepsilon_2 - \varepsilon_3\right]^2}$$

$$\tan 2\alpha_{p,q} = \frac{2\varepsilon_2 - \left[\varepsilon_1 + \varepsilon_3\right]}{\varepsilon_1 - \varepsilon_3}$$

[*] A.W. Hendry "Elements of experimental stress analysis" Oxford 1964.